

**CRYOGENIC TECHNOLOGY RESEARCH AT MSFC**

**March 30, 1967**

**By**

**Raymond L. Gause  
Douglas A. Gilstad  
E. Haschal Hyde  
Clyde D. Nevins  
James M. Stuckey  
Charles C. Wood  
Iva C. Yates, Jr.**



ADVANCED REQUIREMENTS FOR CRYOGENIC INSULATION

by Douglas A. Gilstad . . . . .	1
---------------------------------	---

PRACTICAL INFLUENCES ON THERMAL DESIGN OF HIGH PERFORMANCE INSULATION

by E. Haschal Hyde

SUMMARY. . . . .	3
INTRODUCTION. . . . .	3
INSULATION PURGING . . . . .	5
Flight-Configuration Tank and Insulation System Design . . . . .	5
Purging Requirements . . . . .	7
Full-Scale Test Tank Purge Results . . . . .	7
INSULATION PERFORMANCE . . . . .	9
Calculated Insulation System Thermal Performance - Evacuated Condition. . . . .	9
Helium Purge Condition. . . . .	10
Predicted Versus Measured System Thermal Performance . . . . .	10
System Thermal Performance. . . . .	13
LONG-TERM CRYOGENIC STORAGE. . . . .	14
Insulation Purging, Venting and Evacuation. . . . .	14
Insulation Pressure Decay with Outgassing and Component Leakage. . . . .	16
Penetration Heat Transfer Prediction. . . . .	20
Tank Sidewall Insulation System Design . . . . .	21
Testing of Multilayer Insulation Concepts . . . . .	23
CONCLUSIONS. . . . .	25
REFERENCES . . . . .	26
BIBLIOGRAPHY . . . . .	26
APPENDIX A. SYMBOLS FOR EQUATION IN FIGURE 27. . . . .	27

LIST OF TABLES

Table	Title	Page
I.	Estimated and Calculated Heat Transfer Rates for the 2.67-m (105-in.) Diameter Test Tank . . . . .	9

## LIST OF ILLUSTRATIONS

Figure	Title	Page
1.	Thermal Conductivity of Insulation Material as a Function of Helium Gas Pressure . . . . .	4
2.	MSFC and Contractor Basic Insulation Systems . . . . .	5
3.	Apparent Thermal Conductivity Trend for Tests on Different Type Vessels . . . . .	6
4.	2.67-m (105-in.) Cryogenic Test Tank Assembly . . . . .	6
5.	2.67-m (105-in.) Diameter Tank With He Purged Insulation System . . . . .	7
6.	Section of Insulation Overlap Design Used for Computer Thermal Model . . . . .	8
7.	Estimated Pressure Versus Time and Temperature for Outgassing of NRC-2 Multilayer Insulation. . . . .	8
8.	Boiloff Rate Versus Insulation Thickness for a 2.67-m (105-in.) Diameter Tank (Including Heat Leak Caused by Penetrations). . . . .	10
9.	Temperature Profile Through a Penetration as a Function of Insulation Thermal Conductivity. . . . .	11
10.	Thermocouple Location for Calorimeter Test No. 2 (NASA Design, NRC-2 Shingle Insulation) . . . . .	11
11.	Heat Flux Versus Time for Scale Model Tank, Preliminary Thermal Test No. 1 (NASA Design, NRC-2 Shingle Insulation). . . . .	12
12.	Boiloff Rates for the 2.67-m (105-in.) Diameter Test Tank with Different Insulation Preconditioning . . . . .	12
13.	Boiloff Rate as a Function of Tank Diameter . . . . .	14
14.	Typical Vehicle Insulation Considerations. . . . .	14
15.	Allowable Pressure Drop Across 6.35 $\mu$ (1/4 mil) Mylar During Boost Flight . . . . .	15
16.	Effect of Perforations on the Heat Flux Through Multilayer Insulations . . . . .	16
17.	Evacuation of Hot Helium Preconditioned and Perforated NRC-2 at LH <sub>2</sub> Temperature . . . . .	16
18.	Thermal Conductivity of Insulation Materials as a Function of Helium Gas Pressure . . . . .	17
19.	Effects of Leaks and Outgassing on Pressure at Closed End of 6.35 $\mu$ (1/4 mil) Aluminized Mylar Insulation Batten. . . . .	18
20.	Leakage Characteristics of Cryogenic Electrical Feedthru Connectors . . . . .	18
21.	Valves for Cryogenic Tank Application. . . . .	19

CONTENTS (Continued) . . .

Figure	Title	Page
22.	Duct Joint Attachment Concepts for Dissimilar Metallic Joints . . . . .	19
23.	Cryogenic Seals for Large Flanges . . . . .	20
24.	Potential Penetration Heat Leak Error. . . . .	21
25.	Heat Transfer Through Insulated Penetration with Different Insulation Conductivities . . . . .	22
26.	Comparison of Different Insulation System Designs . . . . .	22
27.	Estimated Insulation Thermal Conductivity Errors Using 2.67-m (105-in.) Diameter Test Tank. . . . .	23
28.	The Error in Superinsulation Thermal Conductivity Versus Tank Radius . . . . .	24

DESIGNING FOR CRYOGENIC INSULATION

by Clyde D. Nevins

	Page
SUMMARY . . . . .	29
INTRODUCTION. . . . .	29
BASIC PRESSURE VESSEL . . . . .	29
OPENINGS AND APPENDAGES. . . . .	31
INSULATION ATTACHMENT METHODS. . . . .	36
INSULATION COVERING . . . . .	38
CONCLUSIONS. . . . .	41
REFERENCES. . . . .	42
BIBLIOGRAPHY. . . . .	42

LIST OF TABLES

Table	Title	Page
I.	Comparison of Structural Support Materials . . . . .	34
II.	Evaluation of Insulation Attachment Methods . . . . .	38

LIST OF ILLUSTRATIONS

Figure	Title	Page
1.	A Typical Cryogenic Stage . . . . .	30
2.	Integral and Nonintegral Tanks . . . . .	30
3.	A Welded Manhole Cover Seal . . . . .	31
4.	A Vented Manhole Cover Seal . . . . .	32
5.	Bimetallic Joint Vibration Test . . . . .	32
6.	Support Structure for the Liquid Hydrogen Tanks of the S-VI Stage . . . . .	33
7.	Structural Support of the Spherical Liquid Hydrogen Tank of a Cryogenic Spacecraft Module . . . . .	33
8.	Structural Support of the Cryogenic Propellant Storage Experiment Tank for Project THERMO . . . . .	34
9.	A Nonmetallic Structural Support . . . . .	35
10.	Detail of Fiber Glass Strut Components . . . . .	35
11.	Attachment Methods for Pre-evacuated Insulation Systems . . . . .	36
12.	Attachment Methods for Purged Insulation Systems . . . . .	36
13.	Vibration and Acoustic Test of an Insulated Test Tank . . . . .	37
14.	Insulated Test Tank During Centrifuge Test . . . . .	37
15.	Insulated Test Tank Mounted in Vacuum Chamber . . . . .	37
16.	Rocket Sled for Testing Full-Scale Insulation Systems . . . . .	39
17.	Test Specimen for Screening Materials for Flexible Vacuum Jacket . . . . .	39
18.	Flexible Vacuum Jacket for the 2.67-m (105-in.) Diameter Tank . . . . .	40
19.	Purge Jacket for the 2.67-m (105-in.) Diameter Tank . . . . .	41

CRYOGENIC INSULATION MANUFACTURING TECHNOLOGY

by Iva C. Yates, Jr.	Page
SUMMARY . . . . .	43
INTRODUCTION . . . . .	43
INITIAL PRODUCIBILITY STUDY . . . . .	43

	Page
APPLICATION OF HELIUM PURGED CONCEPT . . . . .	44
PRE-EVACUATED INSULATION CONCEPT. . . . .	48
CONCLUSIONS . . . . .	52
BIBLIOGRAPHY . . . . .	53

LIST OF ILLUSTRATIONS

Figure	Title	Page
1.	1. 78-m (70-in.) Diameter Cryogenic Test Tank . . . . .	43
2.	Manufacturing Plan, Helium Purged NRC-2 Concept . . . . .	45
3.	Typical Batten Step-Down . . . . .	45
4.	Installation of Cryogenic Test Tank in Assembly Fixture . . . . .	46
5.	Removal of Cryogenic Test Tank from Assembly Fixture . . . . .	46
6.	Installation of Purge Jacket. . . . .	47
7.	Piping Penetration Before Insulation. . . . .	47
8.	Piping Penetration After Insulation. . . . .	47
9.	Completed Helium Purged Insulation Concept . . . . .	48
10.	Wrapping of Linde SI-62 Insulation . . . . .	49
11.	Band Tension Machines . . . . .	49
12.	Completed Cylindrical Wrap . . . . .	50
13.	Completed Insulation on Lower Bulkhead . . . . .	50
14.	Interleaving Opacified Paper Around Piping Penetration. . . . .	51
15.	Helically Wrapped Insulation on Piping Penetration . . . . .	51
16.	Completed Pre-Evacuated Insulation Concept . . . . .	51

**DEVELOPMENT OF A COMBINED HIGH PERFORMANCE MULTILAYER INSULATION AND MICROMETEOROID PROTECTION SYSTEM**

by James M. Stuckey

	Page
SUMMARY . . . . .	55
INTRODUCTION. . . . .	55

	Page
MULTILAYER INSULATION SYSTEMS . . . . .	56
Combined System Design and Material Selection . . . . .	56
Insulation Concepts Investigated . . . . .	57
Application of Insulation Concepts to Test Tank . . . . .	58
TESTS ON INSULATION SYSTEMS . . . . .	61
Test Procedure and Facilities . . . . .	61
Ground-Hold Tests . . . . .	62
Temperature, Pressure and Boiloff during Simulated Ascent Cycle . . . . .	62
Insulation Performance under High Vacuum Conditions . . . . .	64
Effect of Combined Vibration, Acceleration and Rapid Evacuation . . . . .	66
Hypervelocity Impact Tests . . . . .	66
FUTURE PLANS . . . . .	66

## LIST OF TABLES

Table	Title	Page
I.	Thermal Performance of Helium Purged Insulation Concepts . . . . .	63
II.	Thermal Performance Under High Vacuum - Insulation Concepts GAC-1, GAC-2, and GAC-3 . . . . .	65
III.	Thermal Performance Under High Vacuum - Insulation Concept GAC-4 . . . . .	65

## LIST OF ILLUSTRATIONS

Figure	Title	Page
1.	Foam Screening on Flat Plate Calorimeter . . . . .	56
2.	Insulation Concepts Evaluated on 76.2-cm Diameter End-Guarded Calorimeter . . . . .	57
3.	Composite Insulation System GAC-1 . . . . .	57
4.	Composite Insulation System GAC-2 . . . . .	58
5.	76.2-cm Diameter Cylindrical Calorimeter . . . . .	58
6.	Installation of Foam Spacer on 76.2-cm Diameter Calorimeter . . . . .	59
7.	Wrap of Aluminized Mylar Over Foam Spacer on 76.2-cm Diameter Calorimeter . . . . .	59
8.	Second Insulation Concept: Subpanel on Calorimeter . . . . .	60
9.	Preformed Outer GAC-4 Insulation Panel . . . . .	61
10.	Insulation System GAC-4 Completely Installed on Calorimeter . . . . .	61

CONTENTS (Continued) . . .

Figure	Title	Page
11.	Liquid Hydrogen Test Facility . . . . .	62
12.	Temperature Profiles for Simulated Ascent Cycle . . . . .	63
13.	Boiloff Profiles for Simulated Ascent Cycle . . . . .	64
14.	Vacuum Pump-Down Profiles for Simulated Ascent Cycle . . . . .	64
15.	GAC-4 Panels Employed to Insulate 73.7-cm Diameter Tank . . . . .	66
16.	GAC-4 Insulation Installed on 73.7-cm Diameter Tank . . . . .	67
17.	Sample for Hypervelocity Impact Test . . . . .	67
18.	Hypervelocity Impact Test on Insulation Concepts GAC-1 and GAC-2 . . . . .	68
19.	Hypervelocity Impact Test on Sample Without Multilayer Insulation . . . . .	68

NUCLEAR GROUND TEST MODULE INSULATION DEVELOPMENT

by Raymond L. Gause	Page
SUMMARY . . . . .	69
INTRODUCTION . . . . .	69
INSULATION SYSTEM DESIGN CRITERIA . . . . .	69
THE NGTM ENVIRONMENT . . . . .	70
INSULATION DEVELOPMENT CONSIDERATIONS . . . . .	71
SELECTION OF CANDIDATE INSULATION MATERIALS . . . . .	72
SELECTION OF CANDIDATE ADHESIVE MATERIALS . . . . .	74
SELECTION OF CANDIDATE VAPOR BARRIER MATERIALS . . . . .	74
THE TEST PROGRAM . . . . .	75
CONCLUSION . . . . .	77
REFERENCES . . . . .	79

LIST OF TABLES

Table	Title	Page
I.	Insulation System Design Criteria . . . . .	69
II.	Insulation Development Considerations . . . . .	72

CONTENTS (Continued) . . .

Table	Title	Page
III.	Candidate Adhesive Materials . . . . .	74
IV.	Material Evaluation Tests, Specimens, and Environments . . . . .	75

LIST OF ILLUSTRATIONS

Figure	Title	Page
1.	The NERVA Engine . . . . .	70
2.	Radiation Profiles for the 5 000 MW NERVA . . . . .	71
3.	NGTM Radiation Environment . . . . .	71
4.	NGTM Cold-Flow LH <sub>2</sub> Boiloff vs. Insulation Performance . . . . .	72
5.	Laminated Corkboard Insulation System . . . . .	73
6.	Polyurethane Spray Foam Insulation . . . . .	74
7.	Typical Lap Shear Adhesive Specimen . . . . .	76
8.	Composite Double Lap Shear Test Specimen . . . . .	76
9.	Typical Composite Flatwise Tensile Specimens . . . . .	76
10.	Cryogenic Insulation Test Dewar . . . . .	77
11.	Acoustic Noise Setup . . . . .	78
12.	Schematic of Model Tank Test Setup (Elevation) . . . . .	78

ASSESSMENT OF THE STATUS OF CRYOGENIC INSULATION DEVELOPMENT

by Charles C. Wood . . . . .	81
REFERENCE . . . . .	83

LIST OF ILLUSTRATIONS

Figure	Title	Page
1.	Modular Nuclear Vehicle Configuration . . . . .	81
2.	Estimation of Expended and Required Effort for High Performance Insulation Development for Space Flight Application . . . . .	82

CONTENTS ( Concluded) . .

Figure	Title	Page
3.	Solar Shield and Propellant State Influences on Propellant Storage Penalty for a Nuclear Manned Mars Braking Stage. . . . .	82
4.	Future Plans for High Performance Insulation Development . . . . .	82



# ADVANCED REQUIREMENTS FOR CRYOGENIC INSULATION

By

Douglas A. Gilstad

Extensive research has been conducted over the past several years directed toward the development of improved insulation systems for space vehicles employing liquid hydrogen. For earth-launch vehicle stages, the storage times are relatively brief and the tanks can be topped off shortly before launch so that nominal thermal performance can be tolerated without significant penalties. Research efforts have provided insulation systems of relative simplicity, reliability, and much greater efficiency than those currently in use on launch vehicles. These insulation system advances were developed extensively in MSFC programs for application to future vehicle development and improvement and have in large measure satisfied the foreseeable needs for booster insulation including the requirements for earth orbital storage of a few hours. Current space flight missions beyond earth orbital and lunar operations involve unmanned systems with no requirements for earth return or recovery. Consequently, these space propulsion needs can be met with available systems of nominal performance.

For manned planetary missions the necessity for high thermal efficiency is imperative for obtaining maximum vehicle thrust and payload. In view of the advantages of systems that use liquid hydrogen as the propellant, substantial research efforts are now devoted to upgrading present insulation systems. Thermal protection required for manned planetary vehicles must be orders of magnitude more effective than that for boost vehicles to minimize boiloff over prolonged storage periods in space. An obvious pacing factor in establishing research goals and approaches is the planning required to define a planetary mission and timetable. Although many studies have been and are continuing to be made of potential future manned planetary missions, the commitment to a manned planetary mission remains somewhat elusive. With a wide variety of system options involving such significant factors as propulsive versus aerobraking modes for planetary capture, nuclear versus storable or cryogenic chemical propulsion for various mission phases, and practical feasibility of large scale orbital assembly operations, to mention only a few, any straightforward direction at this time would require an arbitrary design decision. Even in the absence

of such a design decision, research to provide advances in cryogenic storage technology can intelligently proceed.

To provide guidance regarding when adequate technology should be available, it has recently been announced that NASA and AEC intend to proceed with the development of NERVA II, provided that Congressional authorization is forthcoming. The proposed schedule involves initiating preliminary design of a Nuclear Propulsion Module by midcalendar year 1969 with a potential flight test in 1975. Although no allocation of nuclear modules is being made now for any specific future missions, the prototype system should meet the requirements of advanced manned mission applications without requiring a major redesign. During this period, advanced cryogenic as well as space storable chemical rocket systems may also be expected to be candidates for these advanced missions. These expected propulsion system developments will require that cryogenic storage technology achieve a level of maturity by 1970 that will permit a reliable prediction of the thermal protection mass penalty for long-term storage (of at least 12 months) and provide the basis for design of optimum storage systems. This advance in technology should be possible if current and planned research efforts are sustained over this period.

The obvious importance of cryogenic insulation technology to these advanced missions is quite clear. Thermal protection systems to minimize the mass penalties that can result from liquid hydrogen boiloff during prolonged storage periods are readily appreciated. Some concern has been expressed that prolonged storage problems may seriously impede projected system developments. On the other hand, recent predictions indicate that very good thermal performance can be readily achieved. However, to actually fulfill such optimistic predictions will require highly efficient multilayer insulations and the minimization of heat leaks associated with tank supports and piping that must penetrate the basic insulation blanket. Experience to date has indicated that a number of serious problems must be solved to achieve the potential effectiveness of these thermal protection systems. Multilayer insulation is relatively flimsy and must be purged with non-

condensable gas or pre-evacuated before launch, be adequately supported during launch, be uniformly expanded in space to provide appropriate evacuated reflective layers, and must also thermally isolate insulation penetrations. Tank supports must have low conductivity and major supports required during launch may need to be retracted during low acceleration phases of space flight. Concepts for dealing with these problems are being developed, but extensive research remains before practical solutions can be made available.

Another potential problem area relates to the protection of insulation systems against damage by meteoroids. Unfortunately, only the near-earth meteoroid environment can be reasonably defined at this time. For planetary missions, particularly to Mars, a knowledge of the interplanetary environment is needed. Since initial statistical measurements cannot be expected for a number of years and a realistic definition of the meteoroid environment for spacecraft design appears to depend upon such measurements, appropriate criteria will not be available to directly influence insulation studies for some time. Perhaps the best approach in the meantime will be to incorporate such features that will aid in meteoroid protection without unduly compromising the performance of thermal protection systems.

Another major difficulty is that of adequately confirming the overall thermal performance of cryogenic storage systems and components prior to construction and launch of the full-scale hardware. The initial conditions of pre-launch purging followed by launch accelerations together with ambient pressure decay are difficult to simulate in ground tests even with small-scale specimens. Long-term vacuum tests can be conducted on systems of reasonable size, but reduced gravity effects can be simulated only for extremely short times. Size-scaling laws can be used to extrapolate certain elements of system thermal performance, but, in general, the overall insulation effectiveness is difficult to predict accurately, particularly in view of the effects of discontinuities associated with insulation penetrations or non-uniformities in system components. Accordingly, it is extremely important that the simulation and scaling techniques be examined with the objective of developing improvements that will enhance the reliability of thermal performance predictions. The pertinent environmental conditions can be provided in flight tests, but the limitations in scaling thermal performance can only be solved by

testing large-scale systems. It appears probable that flight testing will be necessary, but the timing, approach, and techniques involved should be very thoroughly evaluated to insure the maximum potential for positive results.

NASA research on thermal protection systems for cryogenic propellants in space propulsion systems is being conducted primarily at two Centers, Lewis Research Center and Marshall Space Flight Center. The primary research emphasis in the Marshall program is the development of large thermal protection systems required to store propellants for long durations, i. e., well beyond 30 days. Research at Lewis is concentrated upon developing smaller thermal protection systems pertinent to unmanned vehicles with relatively short storage times. Many problems involved in these systems are common, and adequate coordination of the research at the two Centers is obviously important.

The current cryogenic insulation research at Lewis consists primarily of contract studies. Development of prefabricated superinsulation panels by Linde is nearing completion; these CO<sub>2</sub>-filled panels, self-evacuated by cryopumping, simplify handling and installation problems and would be suitable for relatively short-term storage applications. At McGill University, the effects of meteoroid bumper debris on insulated liquid hydrogen tanks will be determined experimentally in light gas gun facilities during the next year. An evaluation of low heat leak tank support concepts is being initiated under contract, and the practical problems involved in the application of a shadow shielding concept will be the subject of another study. That shadow-shield concept was described during the Cryo-Propellant Storage Conference at MSFC in October, 1966. In past efforts sponsored by Lewis, important contributions have been made in studies of the basic performance of various superinsulation configurations. Also in the Lewis cryogenic storage program, extensive attention is directed toward other factors such as fracture mechanics of tank materials at cryogenic temperatures and the development of advanced tank materials.

In summary, the research program to advance the state of technology for prolonged storage of liquid hydrogen must be considered as extremely important. The following papers describe some of the major efforts at MSFC and how the current and planned program may be expected to provide solutions to the various problems and achieve the critical objectives in a timely manner.

# PRACTICAL INFLUENCES ON THERMAL DESIGN OF HIGH PERFORMANCE INSULATION

By

E. Haschal Hyde

## SUMMARY

High energy cryogenic propulsion systems offer high specific impulse for space vehicles. The cryogenic propellants for these systems must be protected from excessive boiloff. Multilayer insulation (MLI) offers a lightweight insulation system with excellent thermal qualities. However, development of a high performance insulation (HPI) system requires a balanced combination of (1) material selection, (2) structural design, (3) thermal analysis, (4) unique test equipment, (5) reproducible application procedures and fabrication methods, and (6) accurate test procedures. All environments of flight must be considered, such as prelaunch, ascent, and space conditions.

MSFC's first effort was toward development of a lightweight high performance insulation system for mission durations of 96 hours and up to 30 days. This effort was successful. However, current mission planning requires cryogenic stages for storage times over one year. Although the technology for multilayer insulation on flight-configuration vessels for long-term storage of cryogenics has not been demonstrated, MSFC has gained valuable experience through the inhouse and NASA sponsored HPI programs. From this effort MSFC was able to identify and define the remaining problems and to initiate programs to solve these problems in preparation for the application of multilayer insulation to large size, flight-configuration cryogenic storage tanks (up to and exceeding one year storage capability). This paper will discuss the thermal aspects of the helium-purged  $6.35\mu$  (1/4 mil) aluminized mylar insulation system applied to a 2.67-m (105-in.) diameter tank and future requirements and approaches.

## INTRODUCTION

Marshall Space Flight Center (MSFC) has been developing high performance insulation (HPI) technology for about five years. Significant inhouse and

support contractor effort has been directed toward developing a flight type high performance insulation system for long term storage of cryogenics in space. The initial objective of the HPI program at MSFC was development and application of HPI to flight configuration tanks to store cryogenics for mission durations up to 30 days. Stationary or roadable dewars have used HPI for several years with extremely small propellant losses. The HPI application concepts for insulating these dewars require that the insulations be evacuated to a very low pressure to avoid gas conduction and to reduce the primary mode of heat transfer to radiation and solid conduction. Hard metal shells protect the insulation and withstand the atmospheric pressure that would deteriorate the insulation thermal performance. High performance insulations for flight vehicles are similar; they depend on a vacuum environment for optimum performance.

MSFC has studied both ground and flight type evacuated insulation systems. The Linde insulation system (ground evacuated) is of aluminum foil with low-thermal-conductivity spacers between each reflective layer. Because of severe mass restraints, a flexible jacket replaced the rigid outer metal shell used on ground based storage equipment, permitting evacuation of the material before vehicle launch. The Linde insulation, alternate layers of  $6.35\mu$  (1/4-mil) aluminum foil and  $76.2\mu$  (3-mil) dexiglas paper, is evacuated before filling the tank with a cryogen. The outer jacket is flexible to help maintain a vacuum environment when ground evacuation of the insulation causes the insulation to compress to 25% of its original thickness. Although highly compressed, the insulation provides adequate ground-hold thermal protection. The HPI expands to 50 - 80% of its original thickness during launch and orbital flight; and incomplete physical recovery does not significantly hinder insulation performance (Fig. 1). Ground-hold evacuation of the compressible insulation makes the flexible plastic jacket crinkle and bend. The resulting pin hole leaks that appear will complicate obtaining and maintaining the required vacuum. Therefore, advanced material development has been required to alleviate this major difficulty with the compressible concept. This problem has

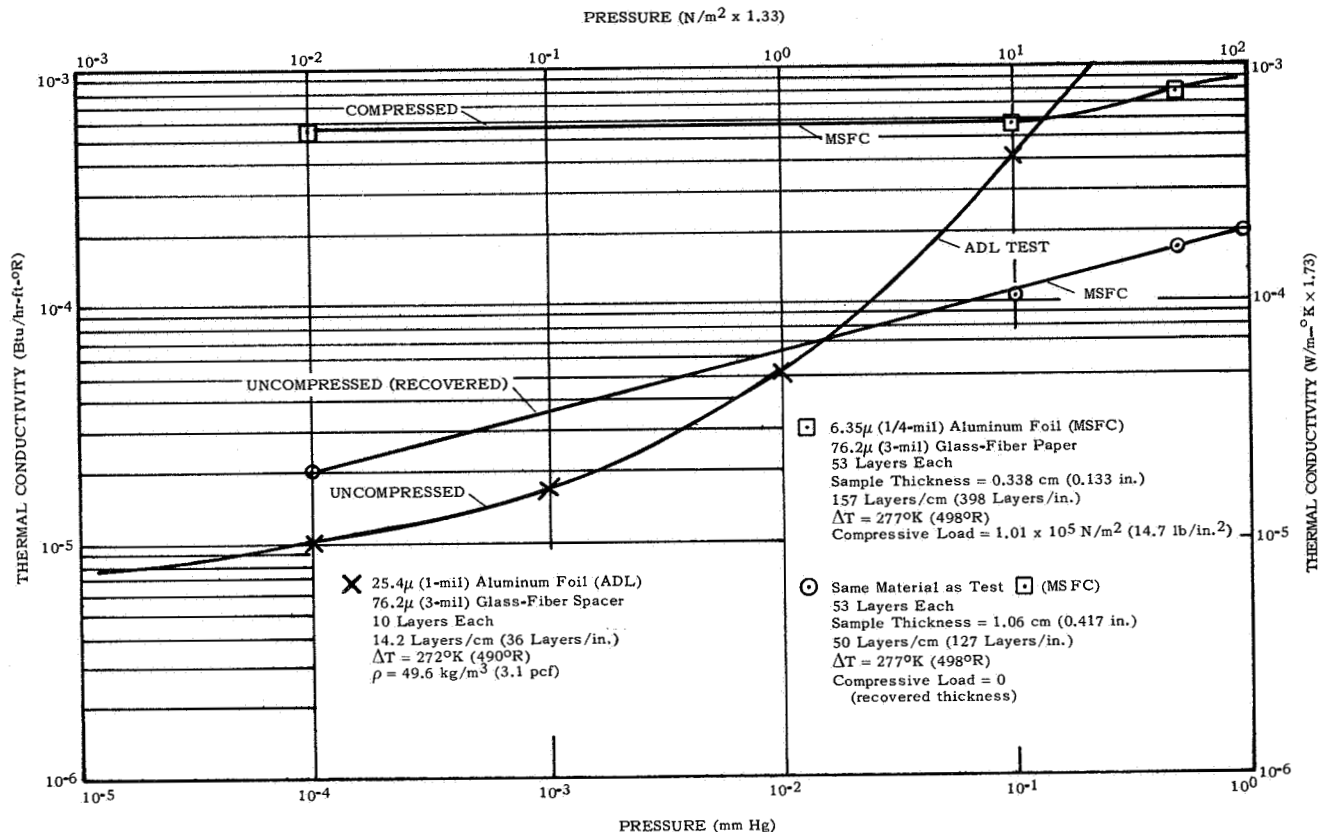


FIGURE 1. THERMAL CONDUCTIVITY OF INSULATION MATERIAL AS A FUNCTION OF HELIUM GAS PRESSURE

been significantly reduced by using a vacuum jacket of lead mylar laminate. A 2.67-m (105-in.) diameter tank has been insulated, evacuated, and is currently ready for testing with liquid hydrogen. This concept will not be discussed in this paper on thermal influences on design, but will be discussed in subsequent papers that deal with structural design and manufacturing procedures.

The other insulation system studied by MSFC was the NRC or crinkled aluminized mylar. This concept is ground purged and evacuation occurs during ascent. The system has layers of 6.35- $\mu$  (1/4-mil) aluminized mylar inside a lightweight purge jacket (Fig. 2, NRC). Although the ground-hold heat leak into the tank is much higher with the NRC system than with the Linde system, both systems do equally well if evacuated to less than  $0.0133 N/m^2$  ( $10^{-4}$  torr). The NRC insulation has an advantage of being about one-fourth

the mass of the Linde insulation. The major disadvantages of the NRC system are controlling insulation density, high ground-hold boiloff, and compressibility during and after application to a tank. The NRC system thermal performance is discussed extensively in this paper.

The third system now under study by MSFC has alternate layers of 6.35- $\mu$  (1/4-mil) aluminized mylar and thin sliced polyurethane foam (Fig. 2). This concept, too, is helium purged on the ground (to prevent air condensation) and the insulation is allowed to evacuate in flight. A 76.2-cm (30-in.) diameter calorimeter was insulated with this concept; the work will be discussed in a subsequent paper by Dr. J. M. Stuckey.

At the start of the MSFC HPI program, calorimeter thermal performance data existed for most of

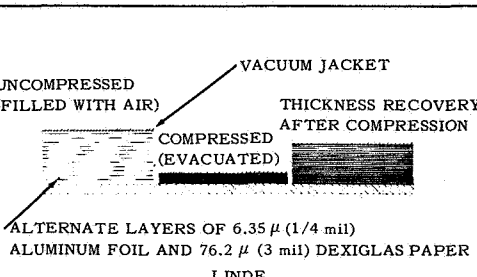
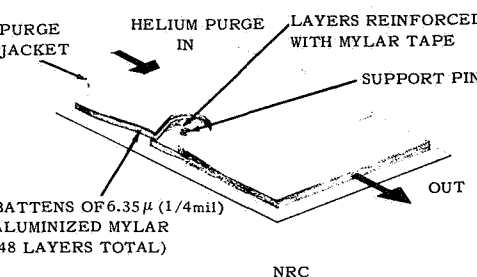
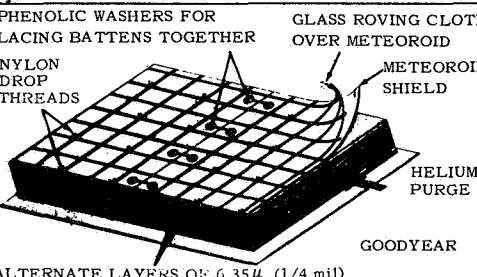
 <p>VACUUM JACKET UNCOMPRESSED (FILLED WITH AIR) THICKNESS RECOVERY AFTER COMPRESSION COMPRESSED (EVACUATED) ALTERNATE LAYERS OF 6.35 <math>\mu</math> (1/4 mil) ALUMINUM FOIL AND 76.2 <math>\mu</math> (3 mil) DEXIGLAS PAPER LINDE</p>	<p>APPROXIMATE DENSITY kg/m<sup>3</sup> (lb/ft<sup>3</sup>)</p>	<p>CALORIMETER THERMAL CONDUCTIVITY 289 - 20.6<sup>0</sup>K (520 - 37<sup>0</sup>R) W/m<sup>0</sup>K (Btu/hr-ft<sup>0</sup>F)</p>	APPROXIMATE LAYERS/cm (LAYERS/in.)	
			RADIATION SHIELDS	SPACERS
	88.1 (5.5)	3.46 X 10 <sup>-5</sup> (2 X 10 <sup>-5</sup> )	27.6 (70)	27.6 (70)
 <p>PURGE JACKET HELIUM PURGE IN LAYERS REINFORCED WITH MYLAR TAPE SUPPORT PIN OUT BATTENS OF 6.35 <math>\mu</math> (1/4 mil) ALUMINIZED MYLAR (48 LAYERS TOTAL) NRC</p>	32.0 (2.0)	5.19 X 10 <sup>-5</sup> (3 X 10 <sup>-5</sup> )	27.6 (70)	NONE
 <p>PHENOLIC WASHERS FOR LACING BATTENS TOGETHER GLASS ROVING CLOTH OVER METEOROID METEOROID SHIELD NYLON DROP THREADS HELIUM PURGE GOODYEAR ALTERNATE LAYERS OF 6.35 <math>\mu</math> (1/4 mil) DOUBLE ALUMINIZED MYLAR AND 0.102 cm (0.04 in.) SLICED POLYURETHANE FOAM</p>	38.5 (2.4)	6.05 X 10 <sup>-5</sup> (3.5 X 10 <sup>-5</sup> )	8.66 (22)	8.66 (22)

FIGURE 2. MSFC AND CONTRACTOR BASIC INSULATION SYSTEMS

the commercially available insulations. Since thermal conductivity is only one factor in an insulation system, it was decided to insulate a flight configuration tank to learn all facets of insulation application and performance. It was thought that the insulation thermal performance data from a system applied to a large tank would differ from data from small calorimeter tests for the same insulation application. Experimental results at MSFC and from NASA contractors show this is true. The apparent thermal conductivity of an insulation system compared with data from calorimeters seems to be degraded according to an increase in vessel size and complexity (Fig. 3). This degradation of insulation performance could result from (1) higher gas pressure within the insulation, resulting from longer pumping paths for entrapped residual gases, (2) local compression at penetrations and double contour surfaces, (3) inaccurate prediction of heat transfer rates through

ducting and structural support penetrations, and (4) residual gas conduction from leaking gaskets, electrical connectors, and valves.

Simulation of each of the above factors will yield reliable thermal performance data for an insulation system. To simulate the mechanical problems in flight type vessels, a 2.67-m (105-in.) diameter tank was chosen for insulation investigation at MSFC (Fig. 4).

## INSULATION PURGING

### FLIGHT-CONFIGURATION TANK AND INSULATION SYSTEM DESIGN

A sketch of the 3.18 m (125 in.) long, 2.67-m (105-in.) diameter tank is shown in Figure 4. It has

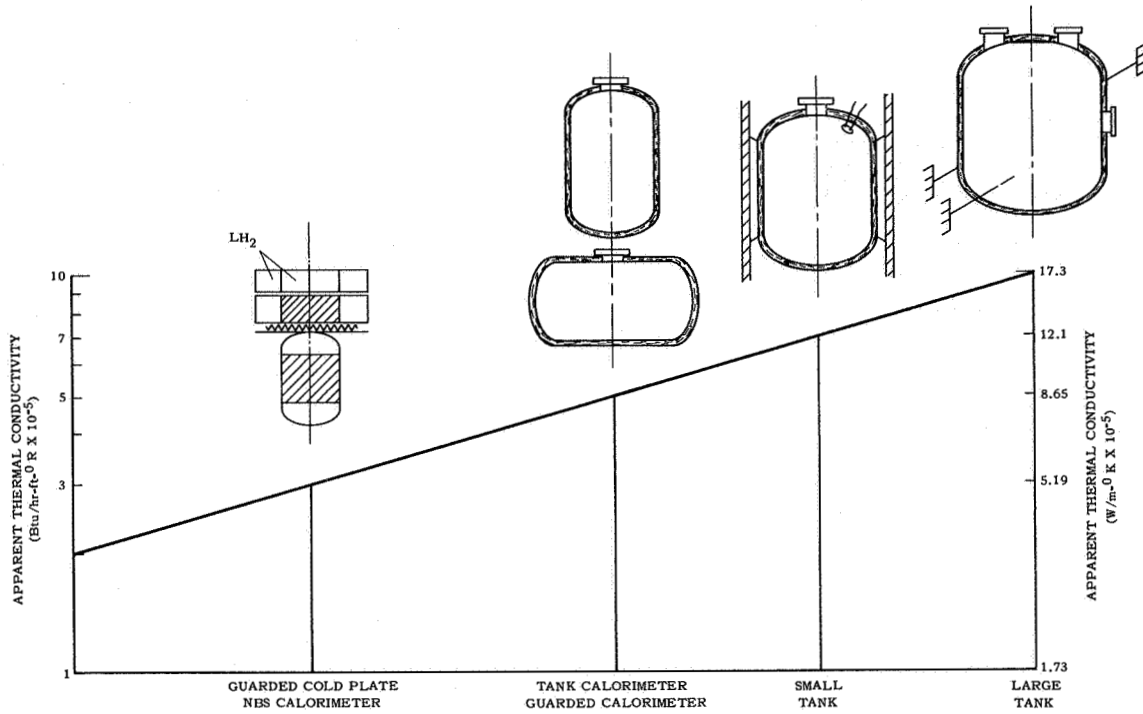


FIGURE 3. APPARENT THERMAL CONDUCTIVITY TREND FOR TESTS ON DIFFERENT TYPE VESSELS

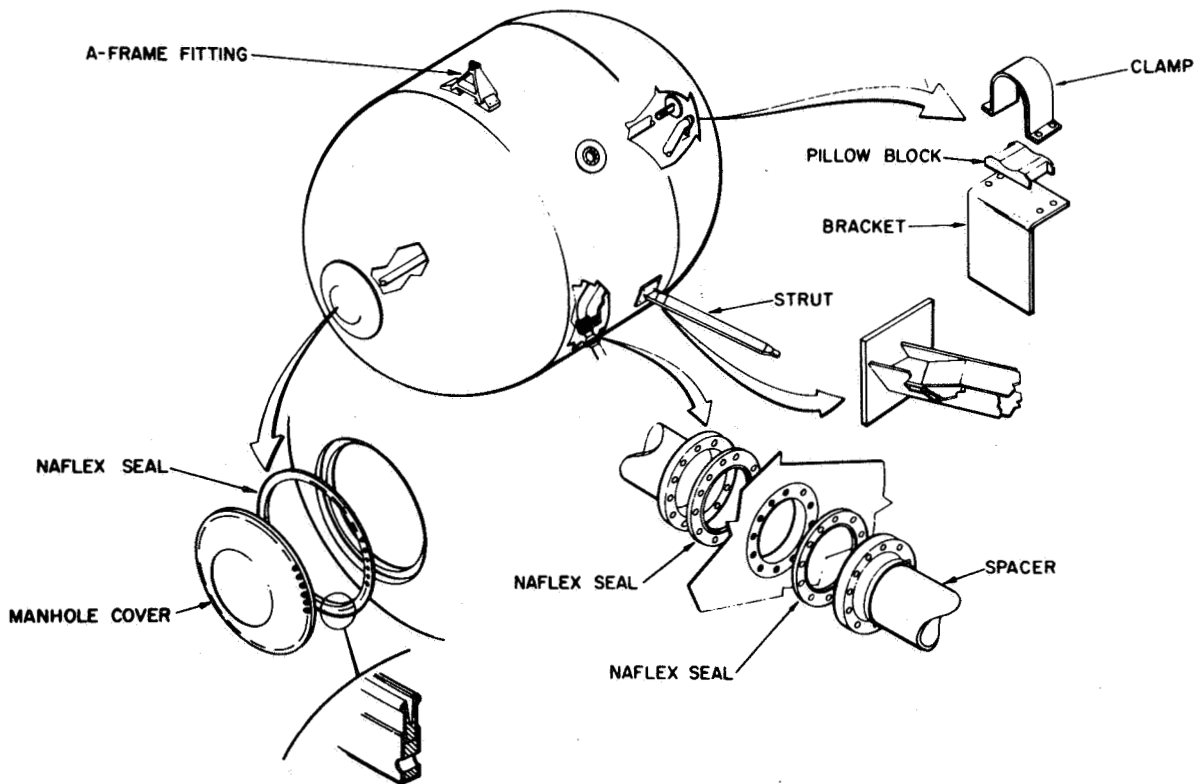


FIGURE 4. 2.67-m (105-in.) CRYOGENIC TEST TANK ASSEMBLY

a surface area of  $27.1 \text{ m}^2$  ( $292 \text{ ft}^2$ ), and a volume of approximately  $12.85 \text{ m}^3$  ( $454 \text{ ft}^3$ ). During testing the tank is loaded with approximately  $862 \text{ kg}$  ( $1900 \text{ lb}$ ) of hydrogen. The tank has a three-point support system, four  $7.62\text{-cm}$  ( $3.0\text{-in.}$ ) diameter ducting penetrations, an operational manhole cover, and a submersible fill valve. Forty-eight layers of crinkled  $6.35\text{-}\mu$  ( $1/4\text{-mil}$ ) aluminized mylar were applied to the tank (Fig. 5). The shingle arrangement for applying

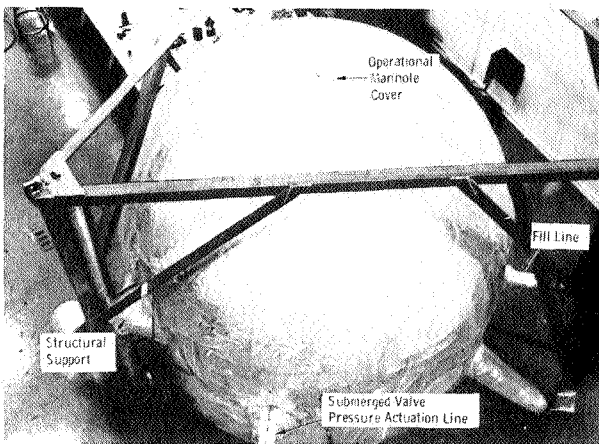


FIGURE 5. 2.67-m (105-in.) DIAMETER TANK WITH He PURGED INSULATION SYSTEM

insulation (Fig. 6) offers a positive attachment of the insulation to the tank sidewall. The shingles are held by  $0.635\text{-cm}$  ( $1/4\text{-in.}$ ) diameter aluminum pins. Overlapping shingles are used to help vent the helium purge gas within the layers during rapid ascent of the vehicle.

#### PURGING REQUIREMENTS

The assembled tank and insulation system are shown in Figure 5. To prevent condensation and solidification of either air or water vapor, a  $127\text{-}\mu$  ( $5\text{-mil}$ ) mylar purge jacket encloses the insulated tank. The entire insulation system is purged with dry helium gas through a purge collar at each of the support rods and ducting penetrations; purge gas exit ports were at the top and bottom of the purge jacket. A mathematical model of the sidewall insulation applied to the tank is in Figure 6. A one-dimensional gas flow analysis determined if outgassing and sublimation would affect the pressure level within the insulation layers. By ignoring outgassing, calculations showed the insulation system would evacuate

rapidly, with the pressure decay of the vacuum chamber. When considering insulation outgassing, the insulation pressure may be two orders of magnitude higher than the vacuum chamber pressure of  $0.0048 \text{ N/m}^2$  ( $3.6 \times 10^{-5} \text{ torr}$ ). Assumptions in this study were as follows:

1. Insulation outgassing coefficient =

$$1 \times 10^{-2} \frac{\mu\ell}{\text{sec-ft}^2} = 0.1076 \frac{\mu\ell}{\text{sec-m}^2}$$

2. Diffusion coefficient =  $0.1785 \frac{\text{m}^2}{\text{sec}}$  (Helium)
3. Flow length =  $54 \text{ in.} = 1.37 \text{ m}$

Figure 7 shows the study results. Two different cases with the one-dimensional mathematical model are described. In all cases, the vacuum chamber pressure was assumed to be  $0.0048 \text{ N/m}^2$  ( $3.6 \times 10^{-5} \text{ mm Hg}$ ). The first case assumed the pressure measured under the purge jacket was  $0.0133 \text{ N/m}^2$  ( $1 \times 10^{-4} \text{ mm Hg}$ ) and was the same as that at the end of the batten. Average gas temperatures for the two cases were selected as  $222^\circ\text{K}$  ( $400^\circ\text{R}$ ) and  $22.2^\circ\text{K}$  ( $40^\circ\text{R}$ ). As shown in Figure 7, the equilibrium insulation pressure did not vary significantly with temperature. The average gas temperature had even less effect on the pressure at the closed end of the batten when the pressure under the purge jacket was assumed to be  $0.133 \text{ N/m}^2$  ( $1 \times 10^{-3} \text{ mm Hg}$ ). With the insulation outgassing effect, however, the pressure at the end of the batten degraded approximately one order of magnitude. Another analysis determined if layer density was a significant factor in retarding insulation pressure decay with the insulation outgassing. The resulting pressure was approximately  $0.266 \text{ N/m}^2$  ( $2 \times 10^{-3} \text{ torr}$ ) for the  $15.7 \text{ layers/cm}$  ( $40 \text{ layers/in.}$ ),  $0.40 \text{ N/m}^2$  ( $3 \times 10^{-3} \text{ torr}$ ) for the  $27.6 \text{ layers/cm}$  ( $70 \text{ layers/in.}$ ) and  $0.80 \text{ N/m}^2$  ( $6 \times 10^{-3} \text{ torr}$ ) for the  $51.2 \text{ layers/cm}$  ( $130 \text{ layers/in.}$ ) case. All these studies assumed that the vacuum chamber pressure was  $0.0026 \text{ N/m}^2$  ( $2 \times 10^{-5} \text{ torr}$ ). Clearly, outgassing causes high equilibrium gas pressures within the insulation layers, and rapid insulation pressure decay is not significantly affected by residual gas temperature or layer density.

#### FULL-SCALE TEST TANK PURGE RESULTS

Tests were made to establish adequacy of the full-scale tank purge system in reducing the moisture content of the gas to 50 parts per million (ppm), while

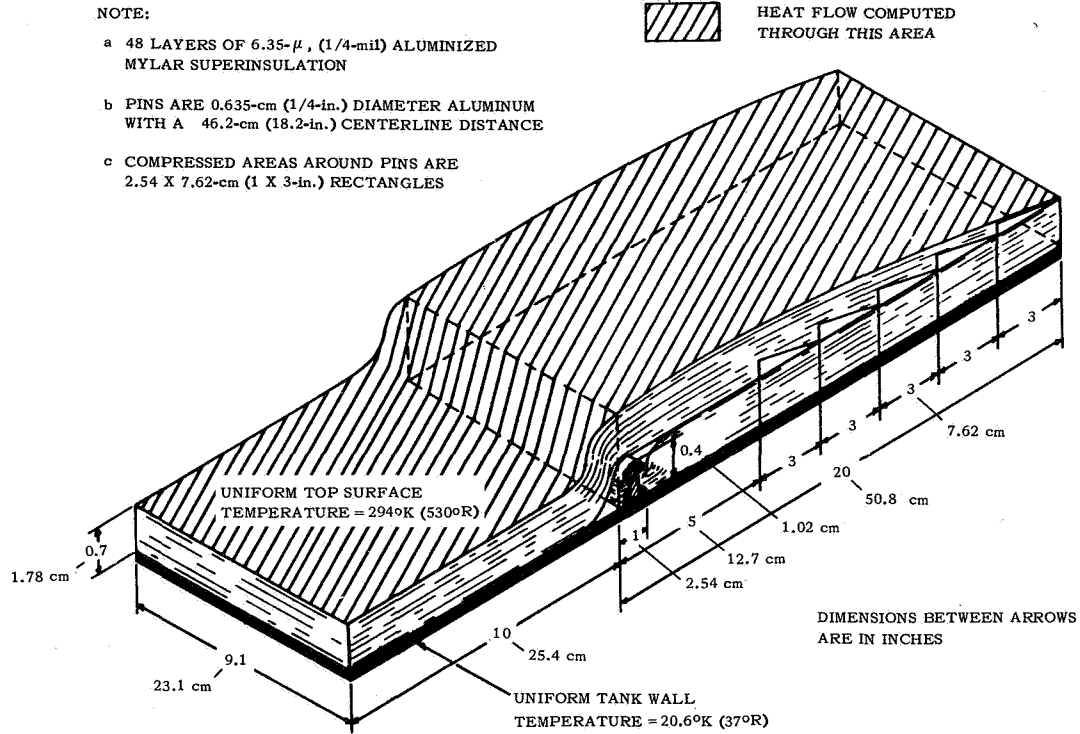


FIGURE 6. SECTION OF INSULATION OVERLAP DESIGN USED FOR COMPUTER THERMAL MODEL

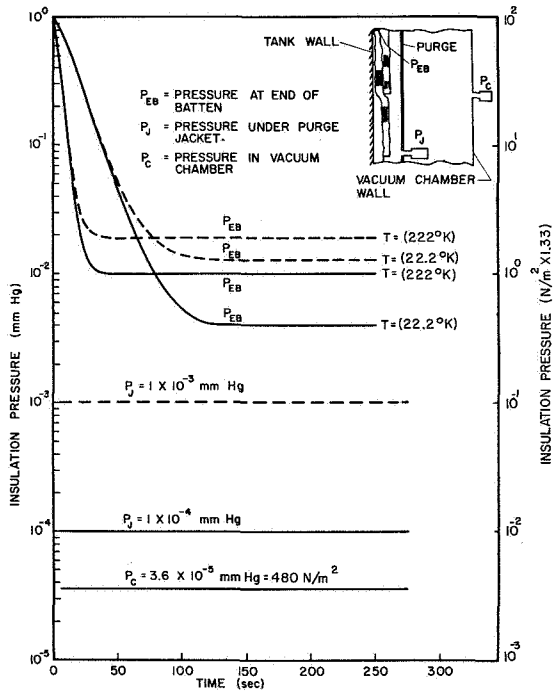


FIGURE 7. ESTIMATED PRESSURE VERSUS TIME AND TEMPERATURE FOR OUTGASSING OF NRC-2 MULTILAYER INSULATION

reducing the air concentration to less than 5%. Residual air content (in the purge gas) within the insulation layers was found before installation of the tank in the vacuum chamber. Equal quantities of helium purge gas (2.5 scfm total) were forced through each of the purge collars of the four piping penetrations, the titanium rod of the A-Frame and the titanium box supports (Fig. 5). Purge gas was vented through the exit ports at the upper and lower bulkheads. The differential pressure across the purge jacket was held at 344 N/m<sup>2</sup> (0.05 psi). A moisture monitor attached to the exit vent ports showed that the moisture content of the gas within the insulation was cut to less than 50 ppm. Calculations indicated that purging the system at a flow-rate of 0.00118 m<sup>3</sup>/sec (2.5 scfm) would reduce the air concentration to less than 5%. Purge gas samples during purging operations were taken by a hypodermic needle attached to an evacuated metal bottle. The laboratory gas analysis showed that the original test objectives were reached.

## INSULATION PERFORMANCE

## CALCULATED INSULATION SYSTEM THERMAL PERFORMANCE - EVACUATED CONDITION

Multilayer insulations are highly anisotropic. That is, the lateral thermal conductivity is much higher than the normal thermal conductivity of the material. For the aluminized mylar system the lateral thermal conductivity is 1 000 times larger than the perpendicular thermal conductivity. Due to its anisotropic nature and irregular configuration after the insulation was applied to the tank sidewall, a computer analysis was made to predict heat transfer rates through the insulated sidewall of the 2.67-m (105-in.) diameter tank. A sketch of the insulation overlap, for the mathematical model to predict the sidewall heat transfer rate, is in Figure 6. For overlap areas, normal and lateral conductivities in both the compressed and uncompressed areas away from the pin, and the compressed areas near the pin, were part of the mathematical model. A thermal conductivity normal to the insulation layers of  $8.65 \times 10^{-5}$  W/m-°K ( $5 \times 10^{-5}$  Btu/hr-ft-°R) was used in the computer analysis. Thermal conductivity of  $2.08 \times 10^{-2}$  W/m-°K ( $1.2 \times 10^{-2}$  Btu/hr-ft-°R) was assumed

parallel to the insulation layers. The parallel thermal conductivity value was calculated for a density of 27.6 layers/cm (70 layers/in.) using the thermal conductivity for solid mylar and aluminum. A normal and parallel conductivity of  $0.121$  W/m-°K ( $7 \times 10^{-2}$  Btu/hr-ft-°R) was used for the compressed areas around the pins [1].

The heat transfer rate of the tank sidewall was calculated by multiplying the heat leak (through a single overlap area) by the 77 overlap areas on the tank. The heat transfer rate through the structural supports and ducting penetrations was found by three-dimensional computer analyses [2]. The simultaneous effects of radiation and conduction down the ducting penetrations were considered. The radiation effect was negligible compared with overall heat transfer rate through the duct connection. Thermal conductivity as a function of temperature was used to calculate heat transfer rates for the titanium structural supports and the stainless steel piping penetrations [3]. Heat transfer rates to the cryogen through the tank sidewall were calculated with and without outgassing of the insulation material. The results are in Table I. With no insulation outgassing, approximately 70% of the total heat input came through the tank sidewall. A boiloff rate of 0.34 kg/hr (0.75 lb/hr) is expected from both sidewall and penetration

TABLE I. ESTIMATED AND CALCULATED HEAT TRANSFER RATES FOR THE 2.67-m (105-in.) DIAMETER TEST TANK

ITEM	GROUNDHOLD HEAT TRANSFER RATES <sup>a</sup>		ESTIMATED VACUUM CHAMBER ENVIRONMENT HEAT TRANSFER RATES <sup>b</sup>		EXPERIMENTAL VACUUM ENVIRONMENT HEAT TRANSFER RATES <sup>c</sup>	
	ESTIMATED	EXPERIMENTAL		INCLUDING OUTGASSING EFFECTS	W (Btu/hr)	
TANK SIDEWALL*	20 500 (70 000)		29.9 (102)			
BOX SECTION SUPPORT STRUTS (2)	58.6 (200)		3.52 (12)			
FILL LINE	70.3 (240)		0.88 (3)			
INSTRUMENTATION LINES (2)	141 (480)		5.86 (20)			
VENT LINE CONTINUOUS VENTING	0		0			
A-FRAME SUPPORT (TITANIUM ALLOY ROD)	87.9 (300)		0.88 (3)			
TOTAL	20 900 (71 220)	10 140 (34 600)	42.5 (145)	62.1 (212)	141 (480**)	130 (442***)

\*LH<sub>2</sub> TEMPERATURE

\*\*C-012-10

\*\*\*C-012-12

<sup>a</sup> 6.35 μ (1/4-mil) crinkled aluminized mylar insulation system

heat inputs. With insulation outgassing, approximately 82% of the total heat transfer into the cryogen came through the tank sidewall, resulting in a boil-off rate of 0.499 kg/hr (1.1 lb/hr).

HELIUM PURGE CONDITION

Assuming helium-purged conditions, the rate of heat transfer into the cryogen was calculated as an evacuated condition, with the thermal conductivity of helium gas being substituted for the normal insulation thermal conductivity. The same assumptions were used for the purged case as for the evacuated case, except as noted below, and the equilibrium hydrogen boiloff rate was predicted by hand calculations. An insulation thickness of 1.78 cm (0.7 in.) was used (except in overlap areas where the thickness was doubled). Overlap areas were estimated to cover approximately 30% of the tank surface area. In Table I, nearly all of the total heat was calculated as flowing through the tank sidewall for the purged condition.

PREDICTED VERSUS MEASURED SYSTEM THERMAL PERFORMANCE

Under simulated orbital conditions, a steady-state boiloff of about 1.04 - 1.13 kg/hr (2.3 - 2.5 lb/hr) was measured (Fig. 8). This value represents an insulation performance factor of about  $2.77 \times 10^{-4}$  W/m<sup>2</sup>-°K ( $1.6 \times 10^{-4}$  Btu/hr-ft<sup>2</sup>-°R). From Figure 8 and a boiloff rate of about 2% per day, the amount of stored hydrogen lost for a four day mission is about 10%. Therefore, by the addition of more insulation layers, the test tank could be used for mission duration up to 30 days.

The difference between the predicted heat leak and the experimental value obtained from the 2.67-m (105-in.) diameter tank equipped with aluminized mylar insulation (see Table I) was investigated. Indicated reasons for the difference were factors such as (1) inaccurate prediction of penetration heat transfer rates, (2) increased heat conduction from compression of the insulation layers during fabrication and assembly, (3) inaccurate prediction of heat transfer rate through batten overlays, and (4) increased thermal conductivity from gas leakage through the tank wall combined with leakage into the insulation layers from the seals at structural and piping penetrations.

The first and second factors above were eliminated by the following: thermocouples placed at

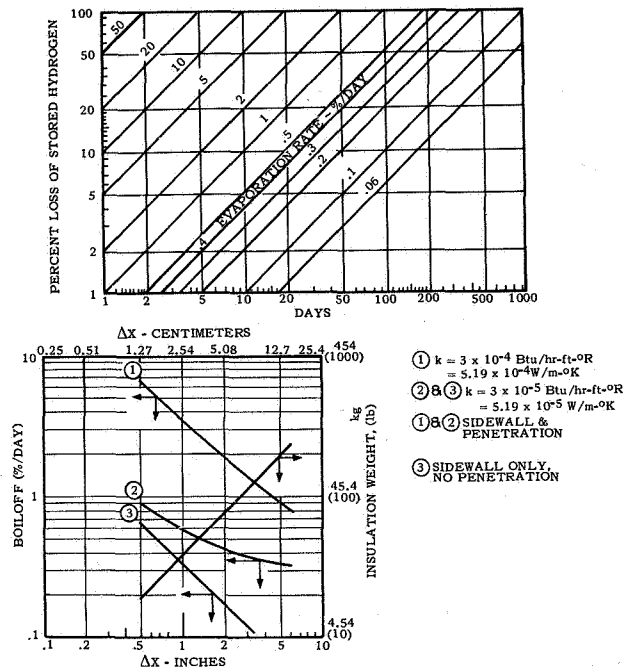


FIGURE 8. BOILOFF RATE VERSUS INSULATION THICKNESS FOR A 2.67-m (105-in.) DIAMETER TANK (INCLUDING HEAT LEAK CAUSED BY PENETRATIONS)

structural heat leak penetrations showed good agreement between measured and predicted values for a steady-state temperature gradient (Fig. 9); calorimeter tests showed that thermal degradation from slight insulation compression did not have a major effect on insulation performance [4].

To eliminate the third factor, the accuracy of the computed heat transfer rate through the insulation batten overlap area on the 2.67-m (105-in.) diameter tank was verified. A 24.2 cm (9.5 in.) modified National Bureau of Standards type calorimeter was used to determine the basic insulation configuration thermal performance factor (Fig. 10) [5]. The insulation was applied to the calorimeter with the insulation overlaps in a vertical plane. Equilibrium heat flux value for this test was 0.536 W/m<sup>2</sup> (0.17 Btu/hr-ft<sup>2</sup>), verifying that the computed heat transfer rate (Table I) for the insulation overlaps on the 2.67-m (105-in.) diameter tank was correct.

An insulation system similar to that on the 2.67-m (105-in.) diameter tank was put on a 73.6-cm (29-in.) diameter model of the larger tank. The insulation applied to the sub-scale tank had a much

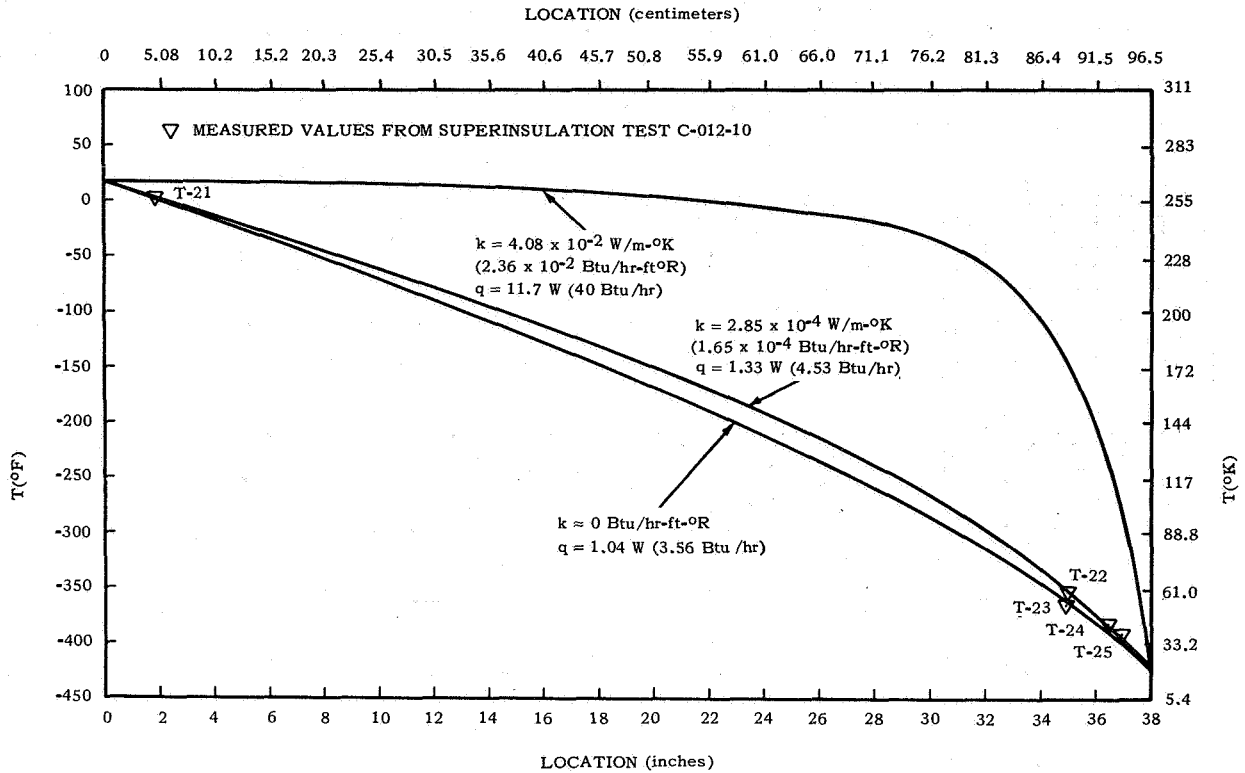


FIGURE 9. TEMPERATURE PROFILE THROUGH A PENETRATION AS A FUNCTION OF INSULATION THERMAL CONDUCTIVITY

higher overall layer density (100 - 125 layers/in.) than the larger tank, and the overlap was reduced to 17.8 cm (7.0 in.) for structural scaling purposes. A thermal test on this sub-scale insulation system gave a heat flux value of  $1.17 \text{ W/m}^2$  ( $0.37 \text{ Btu/hr-ft}^2$ ) (Fig. 11) [6]. This value was about 25% of that obtained on the 2.67-m (105-in.) diameter test tank during Tests C-012-10 and C-012-12 (Fig. 12) [7]. These two test results proved that the predicted heat transfer rate through the insulation overlaps was accurate. Thus, the difference between the predicted and experimental thermal performance for the 2.67-m (105-in.) diameter tank was obviously due to other causes.

Gas leakage or outgassing seemed to be the major reason for the higher than expected heat transfer rate. Accordingly, calculations were made to find the pressure distribution in the insulation batten as a function of batten length, and the thermal conductivity as a function of average batten pressure. An apparent thermal conductivity of  $1.9 \times 10^{-4} \text{ W/m-}^\circ\text{K}$  ( $1.1 \times 10^{-4} \text{ Btu/hr-ft-}^\circ\text{R}$ ) was calculated as the average conductivity of the batten with outgassing present (outgassing rates were obtained from Niedorf [8]).

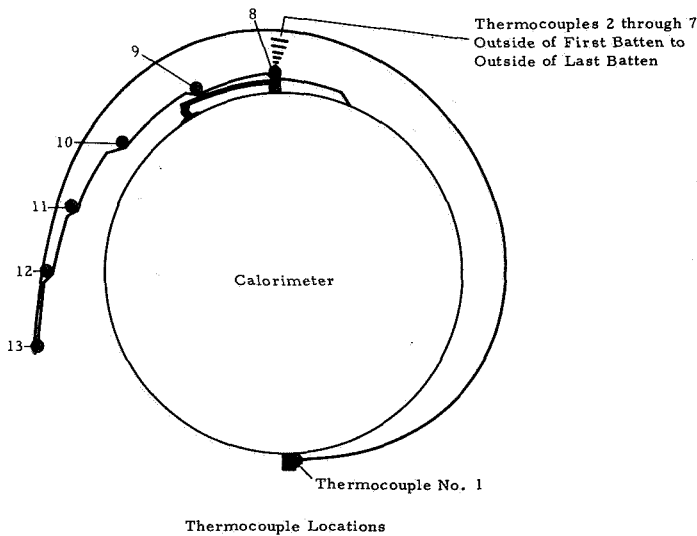


FIGURE 10. THERMOCOUPLE LOCATION FOR CALORIMETER TEST NO. 2 (NASA DESIGN, NCR-2 SHINGLE INSULATION)

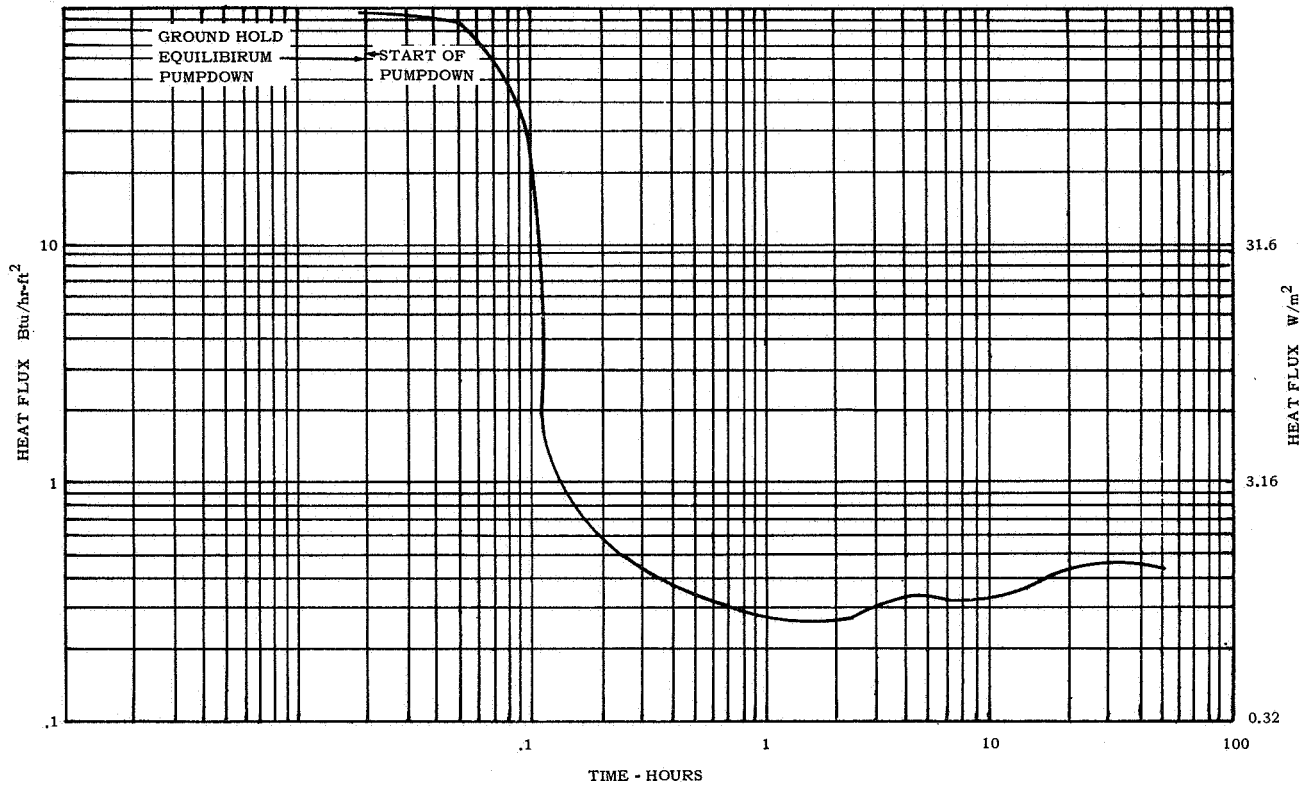


FIGURE 11. HEAT FLUX VERSUS TIME FOR SCALE MODEL TANK, PRELIMINARY THERMAL TEST NO. 1 (NASA DESIGN, NRC-2 SHINGLE INSULATION)

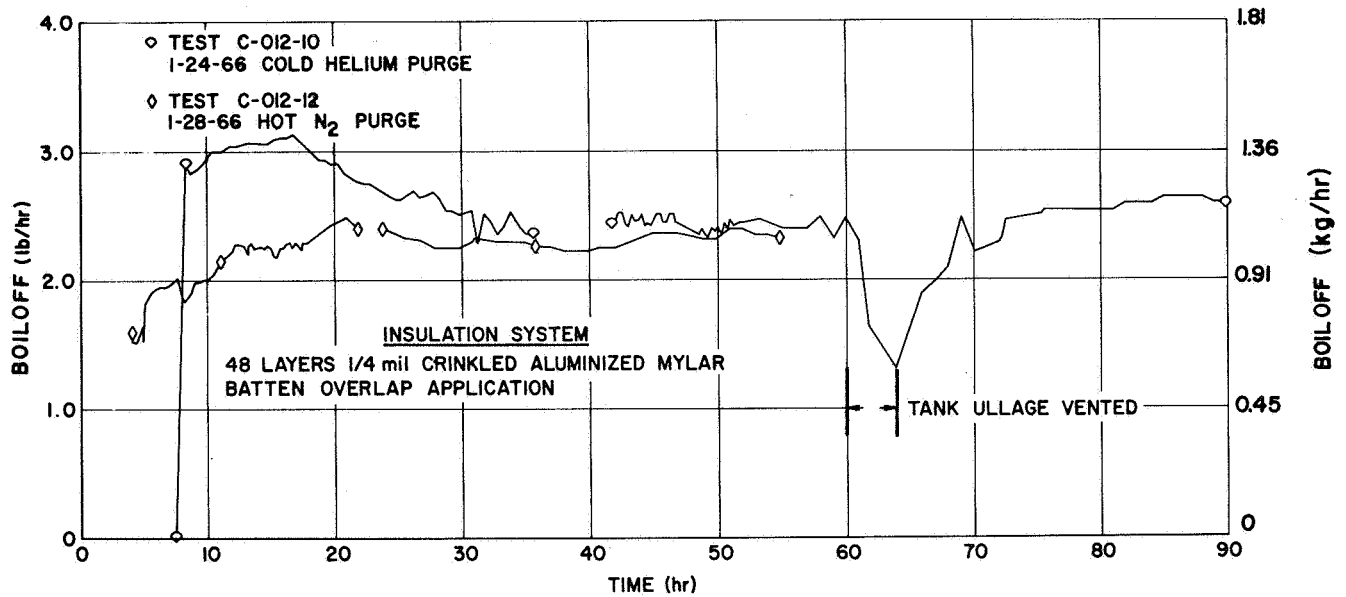


FIGURE 12. BOILOFF RATES FOR THE 2.67-m (105-in.) DIAMETER TEST TANK WITH DIFFERENT INSULATION PRECONDITIONING

The heat transfer rate through the tank sidewall was calculated at 62.1 W (212 Btu/hr) (Table I). This rate was one-half of the total measured heat leak. A gas analysis of the test tank, when filled with LH<sub>2</sub> and located in the vacuum chamber, showed no detectable amounts of GH<sub>2</sub> in the line to the insulation purge jacket. Yet, with the valve open to the purge jacket, the mass spectrometer measured 1.0% hydrogen gas concentration in the insulation system. This indicated a leak of unknown size at either the manhole cover or piping penetration seals. Therefore, with and without outgassing, the difference between computed heat transfer rates and test results on the 2.67-m (105-in.) diameter tank resulted from the increases in apparent thermal conductivity of the insulation caused by hydrogen gas leakage.

As reported by Crawford [9], a lenticular test tank, wrapped with 42 layers of 6.35- $\mu$  (1/4-mil) aluminized mylar insulation, was installed in a vacuum chamber. An equilibrium pressure level of 0.40 N/m<sup>2</sup> ( $3 \times 10^{-3}$  torr) was measured in the mylar layers when the vacuum chamber pressure was at  $1.33 \times 10^{-4}$  N/m<sup>2</sup> ( $10^{-6}$  torr). Because of testing problems and errors, the thermal conductivity of an insulation sample purged with helium gas and located on a lenticular type tank was estimated at  $1.95 \times 10^{-3}$  W/m<sup>2</sup>·K ( $1.13 \times 10^{-3}$  Btu/hr-ft<sup>2</sup>·°F). This value was higher than expected. Even though the estimated thermal conductivity value might have been incorrect, the measured pressure of 0.40 N/m<sup>2</sup> ( $3 \times 10^{-3}$  torr) under the insulation layers was thought to be accurate.

Since the higher than expected heat transfer rate through the lenticular tank sidewalls was apparently caused by high interstitial gas pressure, tests were made to find the cause for high pressure in the insulation layers. Water vapor at the 0.133 N/m<sup>2</sup> ( $10^{-3}$  mm Hg) level seemed to cause much delay in rapidly evacuating the insulation to the required pressure range of  $1.33 \times 10^{-2}$  to  $1.33 \times 10^{-3}$  N/m<sup>2</sup> ( $10^{-4}$  to  $10^{-5}$  mm Hg). But, nitrogen outgassing from the insulation was the delaying factor in the  $1.33 \times 10^{-2}$  N/m<sup>2</sup> ( $10^{-4}$  mm Hg) range. However, a 394°K (250° F) helium purge for one hour, before exposing the insulation sample to LH<sub>2</sub>, would remove the water vapor and decrease evacuation time significantly. Mass spectrometry work on samples of 6.35- $\mu$  (1/4-mil) aluminized mylar indicated no problems with helium sorption or desorption at ambient, LN<sub>2</sub> or LH<sub>2</sub> temperature. Next, a sample of 42 layers of 6.35- $\mu$  (1/4-mil) aluminized mylar with 0.5% open area [0.203-cm (0.080-in.) diameter holes on 2.54 cm (1.00 in.) centers] was perforated and applied to a lenticular test tank having a surface area of 2.43 m<sup>2</sup> (26.2 ft<sup>2</sup>).

The sample, preconditioned with hot helium gas before testing, yielded a thermal conductivity of  $8.21 \times 10^{-5}$  W/m<sup>2</sup>·K ( $4.75 \times 10^{-5}$  Btu/hr-ft<sup>2</sup>·°R) at a corresponding measured insulation pressure of  $2.4 \times 10^{-3}$  N/m<sup>2</sup> ( $1.8 \times 10^{-5}$  torr).

Consequently, optimum thermal performance of the insulation system on the 2.67-m (105-in.) diameter tank was precluded by insulation outgassing and hydrogen gas leakage in the insulation layers.

#### SYSTEM THERMAL PERFORMANCE

Measuring the boiloff rate of stored propellant is one way of evaluating how well an insulation system functions. For the 2.67-m (105-in.) diameter tank, curves 1, 2, and 3 of Figure 8 were plotted to show how this system would do with different thicknesses of insulation. Curve 1 was generated using a normal thermal conductivity of  $5.19 \times 10^{-4}$  W/m<sup>2</sup>·K ( $3 \times 10^{-4}$  Btu/hr-ft<sup>2</sup>·°R) and a constant penetration heat leak of 11.7 W (40 Btu/hr). Curve 1 shows that use of as much as 15.25 cm (6.0 in.) of insulation can significantly reduce the boiloff rate, even with the penetration heat leak of 11.7 W (40 Btu/hr) included. Curve 2, with normal insulation conductivity of  $5.19 \times 10^{-5}$  W/m<sup>2</sup>·K ( $3 \times 10^{-5}$  Btu/hr-ft<sup>2</sup>·°R) and constant penetration heat leak of 11.7 W (40 Btu/hr), shows that addition of more than 5.08 cm (2.0 in.) of insulation insignificantly lowers the boiloff rate. This results from the penetration heat leak rapidly becoming the principal heat source, so that the sidewall heat transfer rate contributes but a minor portion of the total. Curve 3 shows the importance of minimizing extraneous heat leaks, particularly with high performance insulation. Obviously, the theoretical boiloff rate continues to decrease as additional layers are used. An optimum insulation thickness occurs because the addition of more layers of insulation increases system mass.

Comparison of performance on a percent-per-day basis requires knowledge of tank size and shape, insulation thickness, and thermal conductivity factor. This is illustrated in Figure 13. In generating these curves, a cylindrical tank with hemispherical bulkheads, a length to diameter (L/D) ratio of 2, and no penetration heat leaks were assumed. Figure 13 shows that a propellant loss rate of 2% per day for the 2.67-m (105-in.) diameter tank would decrease to 0.5% boiloff per day for a vessel 10.06 m (33 ft) in diameter. Improving thermal conductivity to  $8.65 \times 10^{-5}$  W/m<sup>2</sup>·K ( $5 \times 10^{-5}$  Btu/hr-ft<sup>2</sup>·°R), would decrease the boiloff to 0.2% per day. An insulation

thermal conductivity of  $5.19 \times 10^{-5} \text{ W/m} \cdot ^\circ\text{K}$  ( $3 \times 10^{-5} \text{ Btu/hr-ft} \cdot ^\circ\text{F}$ ) and an insulation thickness of 7.62 cm (3.0 in.) would decrease boiloff to 0.025% per day.

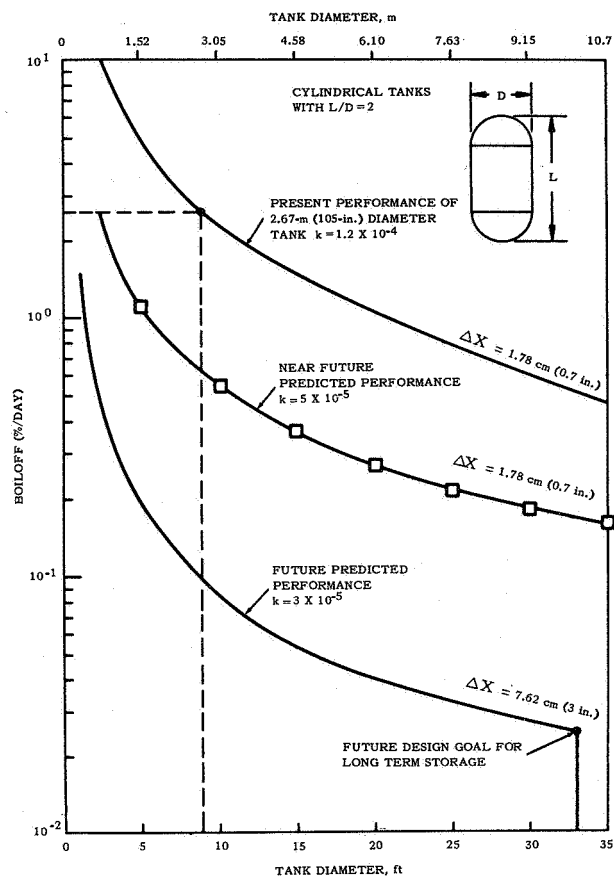


FIGURE 13. BOILOFF RATE AS A FUNCTION OF TANK DIAMETER

Figure 13 is illustrative only because penetration heat leaks have been neglected. To achieve this performance a program for improvement of multilayer insulation must be continued. The following discussion cites some of the parameters to be considered and the effort needed to exploit them.

### LONG-TERM CRYOGENIC STORAGE

The application of HPI for long-term storage of cryogenics to a flight stage (such as the modular nuclear vehicle) demands careful study and correlation of many factors that are not critical for short-term storage designs. Figure 14 outlines a typical stage showing the basic considerations for applying high performance insulation to a flight-configuration

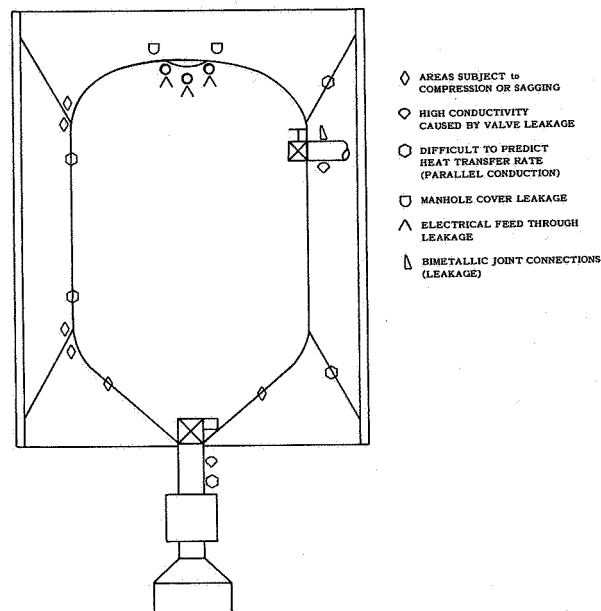


FIGURE 14. TYPICAL VEHICLE INSULATION CONSIDERATIONS

tank. These problems can be combined into five major groups as follows: (1) insulation purging, venting, and evacuation, (2) component leakage and outgassing effects, (3) heat transfer through penetrations, (4) sidewall insulation design and optimization, and (5) accurate insulation system thermal tests. Each of these areas is discussed in the following sections.

### INSULATION PURGING, VENTING AND EVACUATION

Rapid evacuation of insulation is necessary to maintain insulation structural integrity and to achieve desired thermal performance. As stated earlier, a purge system is used to remove air and moisture from within the insulation layers. The purge is maintained during ground hold and the insulation is allowed to vent during ascent. A large vent area for this escaping gas is required during ascent for a large flight stage. It is not practical, however, to have a huge exit pipe manifold on a large stage. A solution would be to develop a purge jacket that is gas tight for ground purging and would rupture during ascent. A purge jacket has been designed and fabricated with zipper inserts that will rupture at about  $3\,400 \text{ N/m}^2$  (0.5 psia) differential pressure and developmental testing will be completed in the immediate future.

Rapid evacuation of the insulation during ascent is important structurally. If the insulation is applied to a tank by a "continuous sheet" method, the purge gases must be vented through seams or holes caused by structural attachments. For thin layer applications, and small tank radii, venting of the purge gases without structural failure is possible. However, with large diameter tanks the insulation system becomes more susceptible to rupture during ascent (Fig. 15). Holes can be placed in the insulation for expediting evacuation and minimizing structural damage, but holes in the radiation shields decrease the insulation thermal performance (Fig. 16). These same perforations can be beneficial for minimizing insulation internal pressure resulting from material outgassing. Additional evacuation data as a function of perforated area and batten thickness are required to prevent overpressurization during ascent and yet provide adequate thermal performance in orbit.

Preliminary experiments using perforated, unperforated, and preconditioned aluminized mylar have been performed to determine the degree by which outgassing could be minimized or eliminated [10]. Results of three different tests are in Figure 17. An

unperforated sample of insulation, preconditioned with hot helium gas (about 394°K, or 250° F) and a perforated sample purged with room temperature helium failed to yield pressures below the acceptable level of 0.0133 N/m<sup>2</sup> (10<sup>-4</sup> torr). An insulation sample perforated with smaller diameter holes 0.318 cm (0.125 in.) on 5.08 cm (2 in.) centers and preconditioned with 394°K (250° F) helium gas yielded an acceptable level of 0.0133 N/m<sup>2</sup> (10<sup>-4</sup> torr) in a reasonable amount of time. This test data indicated that both perforations and preconditioning will be required for rapid evacuation of insulation. Test fixtures are being designed and evacuation tests are being planned for insulation samples 0.915 m (3.0 ft) square and up to 22.9 cm (9.0 in) thick to further define the effect of outgassing, perforation and preconditioning on equilibrium insulation pressure.

Most insulation materials without spacers evacuate more rapidly than those with spacers. Although the more dense insulations with spacers do not evacuate as quickly as the lighter insulations, they may have uses in spacecraft. For example, if the final equilibrium pressure is at the same level within an

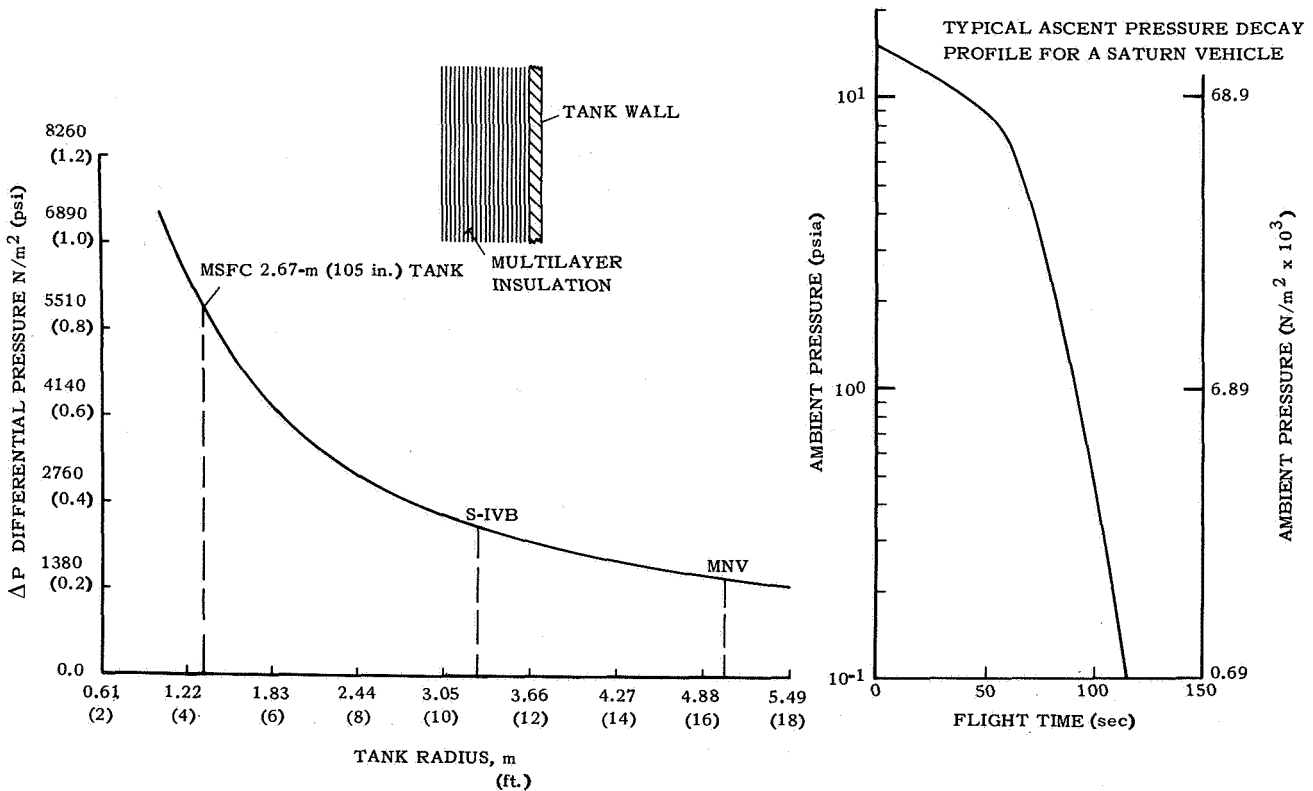


FIGURE 15. ALLOWABLE PRESSURE DROP ACROSS 6.35 μ (1/4 mil) MYLAR DURING BOOST FLIGHT

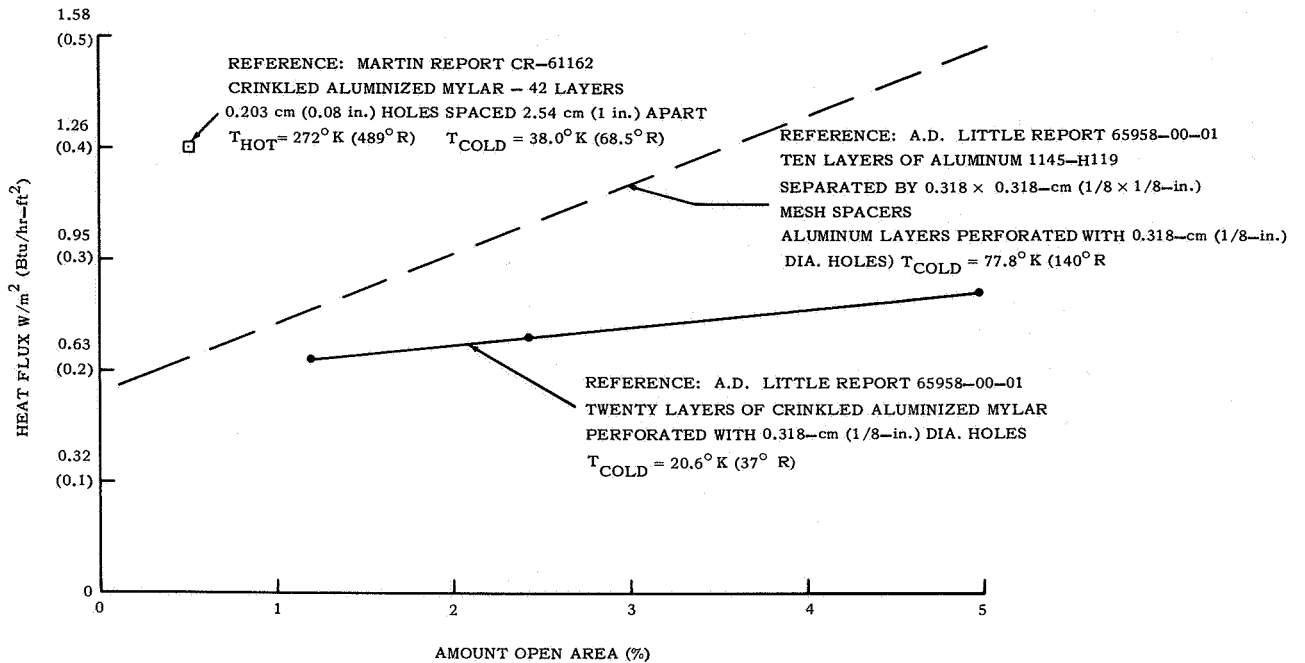


FIGURE 16. EFFECT OF PERFORATIONS ON THE HEAT FLUX THROUGH MULTILAYER INSULATIONS

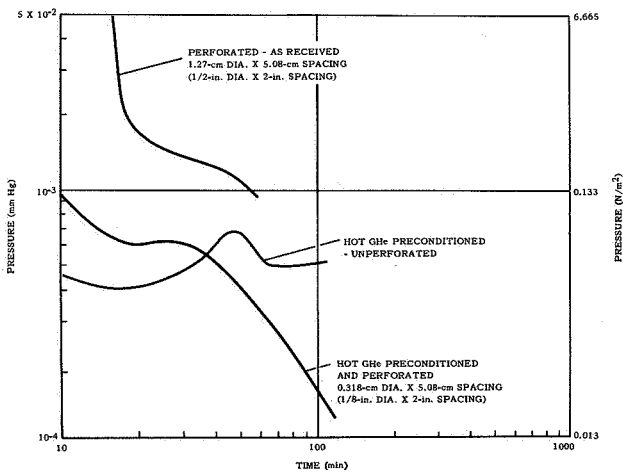


FIGURE 17. EVACUATION OF HOT HELIUM PRECONDITIONED AND PERFORATED NRC-2 AT LH<sub>2</sub> TEMPERATURE

insulation, and the pressure level is inadequate to reduce gas conduction, a significant difference in apparent thermal conductivity is noted for materials with and without spacers (Fig. 18). As shown throughout this paper, low insulation gas pressure is a must for good thermal performance. To accurately

assess thermal performance, knowledge of the insulation gas pressure is required. Currently, the apparent thermal conductivity as a function of pressure is found by assuming that the pressures within insulation layers are the same as the local chamber pressure. This is not necessarily an accurate assessment, but, unfortunately, commercial vacuum gauges do not exist which will operate at LH<sub>2</sub> temperatures. Gauges that do exist are also too heavy and cumbersome and impossible to mount within the insulation. A cryogenic vacuum gauge that can be mounted within the insulation layers is being developed. In conclusion, more effort is needed to determine HPI thermal performance as a function of thickness, evacuation rates, and equilibrium pressure level within the layers.

INSULATION PRESSURE DECAY WITH OUTGASSING AND COMPONENT LEAKAGE

Material outgassing and component leakage from hardware such as ducting connections, manhole covers, and electrical connectors have been shown to seriously affect insulation equilibrium pressure, and thus ultimately affect the steady-state thermal performance of the insulation system. A study was

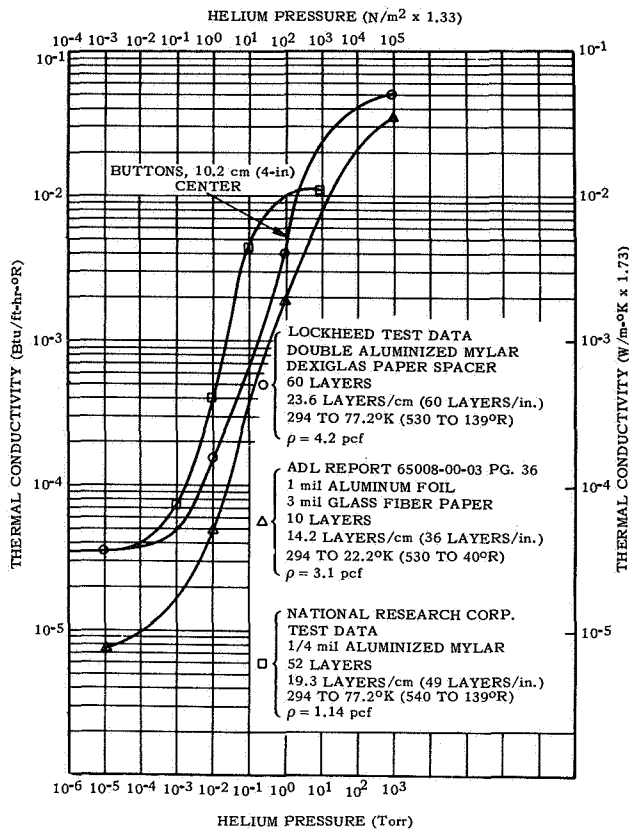


FIGURE 18. THERMAL CONDUCTIVITY OF INSULATION MATERIALS AS A FUNCTION OF HELIUM GAS PRESSURE

made to show the potential equilibrium pressure effect of leaking sources and outgassing within the insulation. Results are shown in Figure 19. The mathematical model chosen was a batten of insulation 137 cm (54 in.) long, 2.54 cm (1.0 in.) thick and infinitely wide. One end of the batten was assumed closed and all leakage or outgassing was assumed to flow through the batten (Fig. 19). Electrical connectors have a combined leakage rate large enough to possibly cause the pressure in the insulation layers to be more than four orders of magnitude higher than the local chamber pressure. Figure 20 shows typical cryogenic electrical connectors and their basic characteristics. The existing cryogenic electrical connector consists of a metal shell with a one piece molded glass insert and fused-in contacts. An important requirement of present electrical feedthrus is that the metal and glass of the feedthru must have matched expansion coefficients to prevent fluid leakage when subjected to required temperature variations. The glass-to-metal seal is also sensitive to mechanical shock and to temperature variations from welding during installation.

As a result of these environments, connectors leak worse than when they are tested under less severe static conditions. Cryogenic electrical connector vendors quote a leak rate as low as  $1 \times 10^{-8}$  scc/sec, but connector leak rates of  $1 \times 10^{-2}$  scc/sec, and in some cases 3 scc/sec, have occurred in practical application.

Other parameters, such as electrical insulation resistance and humidity, affect the connector fluid leakage. The optimum glass composition for minimizing the connector leakage has an electrical insulation resistance below the required value. To date, a glass material has not been found with both a low leak rate and a high electrical insulation resistance. A future cryogenic electrical connector required to satisfy both the electrical and low leakage requirements is shown conceptually in Figure 20. Research continues on a search to find an acceptable insert material.

Leakage through the valve seat and valve actuator of fill and drain valves can result in high heat leaks down the penetration because gas will accumulate in the duct. Leakage through the valve actuator can also cause an increase in insulation conductivity if the escaping gas passes through the insulation. The leakage problem through the actuator can be solved by submerging the valves in the cryogen. Valves have been recently developed that will operate while submerged in liquid hydrogen. This advance in valve design results from using bellows instead of dynamic seals in the valve actuator housing. With the bellows, the valve actuator can withstand liquid hydrogen temperatures, but leakage past the ball or the seal have not been eliminated. For short-term missions, this leakage can be tolerated. For longer missions, valve designs with a shear diaphragm of some type will be required and feasibility studies are underway (Fig. 21).

Gas leakage through separable ducting connectors degrades insulation thermal performance. Welding of aluminum ducting to aluminum tanks would eliminate gas leakage, but use of high conductivity aluminum would cause intolerable heat transfer rates. Presently, low thermal conductivity stainless steel ducts cannot be welded directly to aluminum tanks. Thus, a separable flanged type design is required. Likewise, the large manhole cover usually requires a similar type flange design. The recent development of the diffusion bonded joint (Fig. 22) represents a significant technological breakthrough. The leak rate for the diffusion bonded joint is so infinitesimal that it is virtually non-existent. However, the joint can be used only a few times because of a limited amount

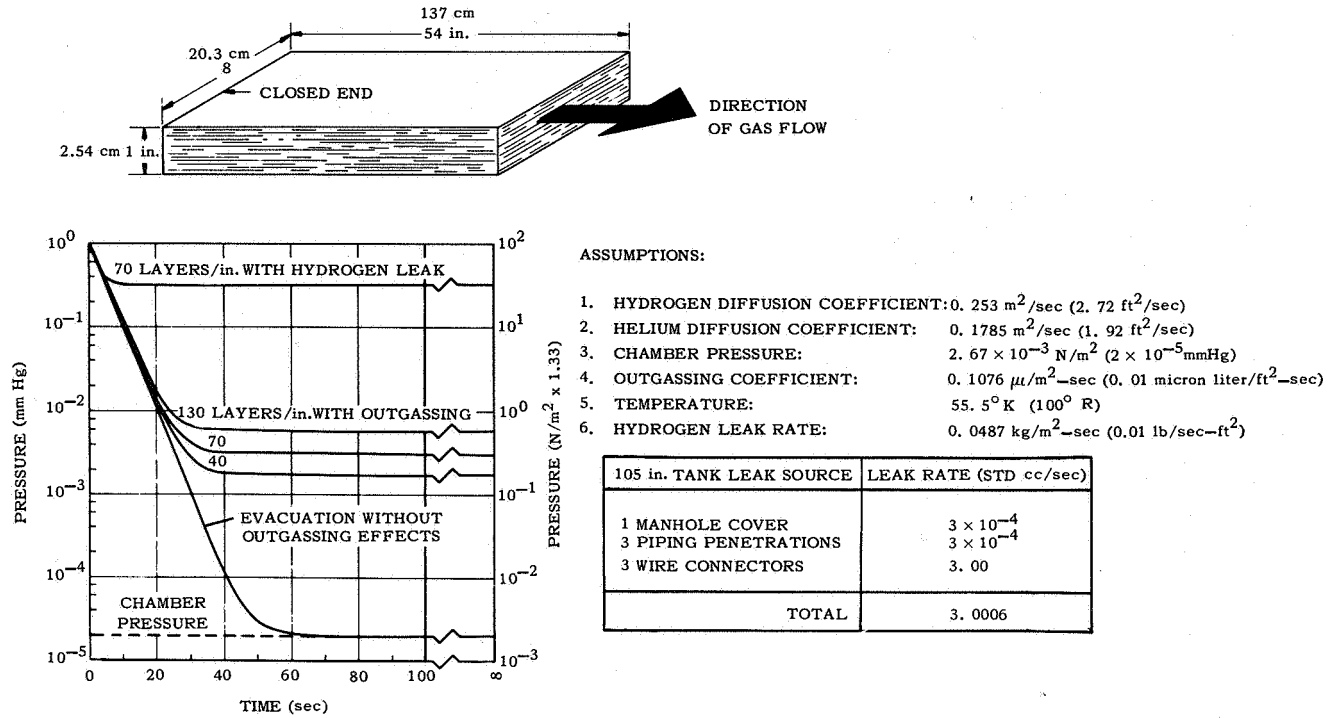


FIGURE 19. EFFECTS OF LEAKS AND OUTGASSING ON PRESSURE AT CLOSED END OF 6.35  $\mu$  (1/4 mil) ALUMINIZED MYLAR INSULATION BATTEN

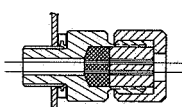
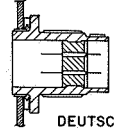
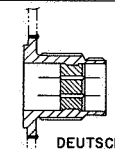
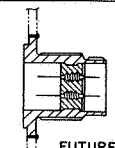
CRYOGENIC CONNECTOR	TEMPERATURE RANGE	PINS SUBJECT TO DAMAGE	SUSCEPTIBLE TO PIN CONTACT CHATTER	REUSABLE	APPROXIMATE TOTAL LEAK RATE STD cc/sec
 CONAX	WIDE RANGE (DEPENDS ON SEALING MATL.)	NO	YES	YES	$10^{-1}$ - 1.0 I.O MINIMUM AFTER VIBRATION
 DEUTSCH BOSS TYPE	WIDE RANGE (DEPENDS ON WIRE INSULATION)	YES	YES	YES	$10^{-2}$ - 1.0 DETERIORATES AFTER BEING SUBJECT TO VIBRATION
 DEUTSCH WELDED TYPE	WIDE RANGE (DEPENDS ON WIRE INSULATION)	YES	YES	NO	$10^{-3}$ - 3.0 DETERIORATES RAPIDLY AFTER BEING SUBJECT TO VIBRATION
 FUTURE	WIDE RANGE (DEPENDS ON WIRE INSULATION)	YES	NO	NO	$10^{-7}$ - LITTLE EFFECT FROM VIBRATION

FIGURE 20. LEAKAGE CHARACTERISTICS OF CRYOGENIC ELECTRICAL FEEDTHRU CONNECTORS

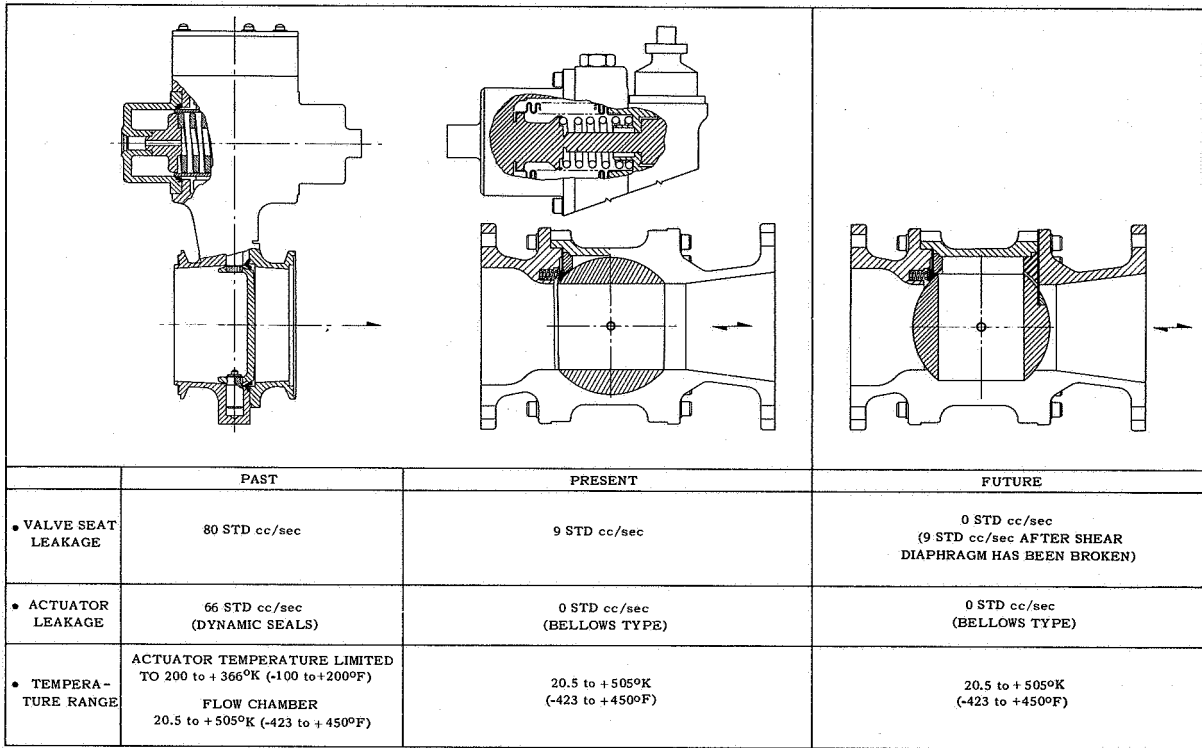


FIGURE 21. VALVES FOR CRYOGENIC TANK APPLICATION

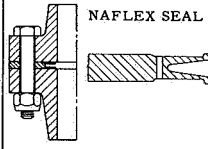
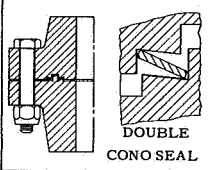
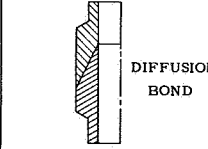
	WEIGHT kg (lb)	FLANGE O.D. DUCT O.D.	LEAKAGE RATE STD. cc/sec	ASSEMBLY PROBLEMS	SURFACE REQUIREMENTS	REUSABILITY	FLANGE COST	SEAL COST
 <p>NAFLEX SEAL</p>	2.50 (5.5)	1.7	10 <sup>-4</sup> PRIMARY, DRAIN OVERBOARD	SEAL HANDLING	FLATNESS 0.051 mm (0.002 in.)  SURFACE QUALITY 32	YES	LOW	HIGH
 <p>DOUBLE CONO SEAL</p>	3.23 (7.1)	1.8	10 <sup>-6</sup> PRIMARY, DRAIN OVERBOARD	SEAL HANDLING, CAREFUL INSTALLATION	SAME	CHANGE SEALS	HIGH	LOW
 <p>DIFFUSION BOND</p>	1.23 (2.7)	1.2	10 <sup>-12</sup>	PREFABRI- CATED JOINT, IN-PLACE WELD OF DUCT STUBS	CLEAN	CUT AND WELD	VERY LOW	DIFFUSION BONDING PROCESS (PLATING, BONDING) HIGH

FIGURE 22. DUCT JOINT ATTACHMENT CONCEPTS FOR DISSIMILAR METALLIC JOINTS

of metal available for rewelding. Tests are in progress to flight qualify the diffusion bonded joint as well as other recently developed bimetallic joints using different joining techniques.

Resulting gas leakage at ducting seals or manhole covers can be stopped under any environmental load by simply using a very heavy, rigid non-deforming flange. However, excessive flange mass and materials aspects will not permit such a simple solution for most spacecraft applications. Seals available for consideration for such applications can be separated into five different types (Fig. 23). Only types four and five, the conoseal and weld ring (omega seal) have acceptable leakage characteristics for HPI applications and each of these has disadvantages. The conoseal requires a high bolt loading, does not fit a standard flange, and cannot be reused, yet currently this is the best available gasket connection for use on tanks with multilayer insulation.

The welded ring (omega seal) is the most desirable for reducing leakage; still, it also has some undesirable mechanical features. In place welding of the ring requires two concentric welds of good quality, and a third weld in the center of the ring is required for sealing and must be ground off and rewelded after entry. Limited material for rewelding restricts reusability of this seal. Also, heat generated during the welding process can melt the insulation if it is not removed or thermally protected. In spite of these disadvantages, experimental development of this sealing method is continuing because of a demonstrated low leak rate.

PENETRATION HEAT TRANSFER PREDICTION

Heat transfer through cryogenic tank supports and penetrations is difficult to predict accurately.

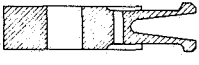
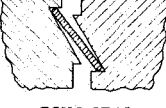
CRYOGENIC MANHOLE GASKETS	REUSABLE	FLANGE LOADING REQUIREMENTS	FITS STANDARD FLANGE	GROOVE SURFACE PROTECTED	SENSITIVE TO FLANGE DEFLECTION	SENSITIVE TO RADIAL SCRATCHES	LEAK RATE $\frac{STD. cc}{sec He}$
 TEFLON COATED "O" RING	YES	HIGH 35.8 - 500 kg/circ. cm (200 - 2800) (lb/circ. in.)	YES	YES	YES	YES	$1 \times 10^{-2}$
 GROOVE TYPE "K" SEALS	YES	LOW 5.36 - 10.7 kg/circ. cm (30 - 60) (lb/circ. in.)	YES	YES	YES	YES	$1 \times 10^{-4}$
 SPACER NAFLEX SEAL	YES	MEDIUM 12.5 - 17.9 kg/circ. cm (70 - 100) (lb/circ. in.)	YES	NO	YES	YES	$1 \times 10^{-4}$
 CONO SEAL	NO	HIGH 89.5 - 107 kg/circ. cm (500 - 600) (lb/circ. in.)	NO	YES	NO	NO	$1 \times 10^{-6}$
 FUTURE OMEGA SEALS	YES	LOW	YES	YES	NO	NO	$1 \times 10^{-12}$

FIGURE 23. CRYOGENIC SEALS FOR LARGE FLANGES

For irregular tank penetration geometries, a finite difference heat transfer program is essential to predict the heat transfer rate. A mathematical model of the penetration is broken up into nodes of finite length, depth, and width. A thermal resistance factor is then computed for each node, and data must be available on the apparent thermal conductivity of the insulation material as a function of temperature.

However, most thermal conductivity data for multilayer insulation material were obtained using either liquid hydrogen or nitrogen as the cold boundary temperature with the warm side boundary temperature varied between 111 and 333°K (200 and 600°R) (Fig. 24). A few data points were obtained using Freon 12 as a cold sink. The test data indicate that the apparent thermal conductivity of HPI is approximately a factor of three higher at the temperature of Freon 12 than at LH<sub>2</sub> or LN<sub>2</sub> temperatures.

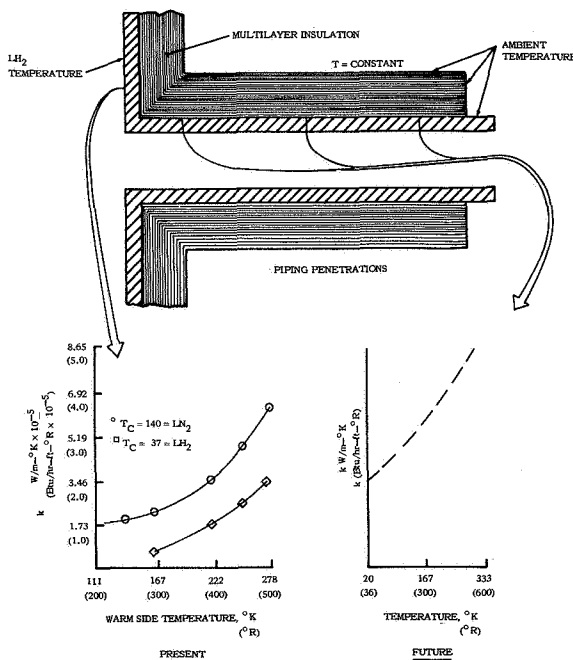


FIGURE 24. POTENTIAL PENETRATION HEAT LEAK ERROR

Unlike tank sidewall heat transfer problems, the penetration hot boundary temperature remains constant and the cold boundary temperature is the variable. Since most data are now input to computer programs as a function of warm side boundary temperature only, a more accurate appraisal of the heat

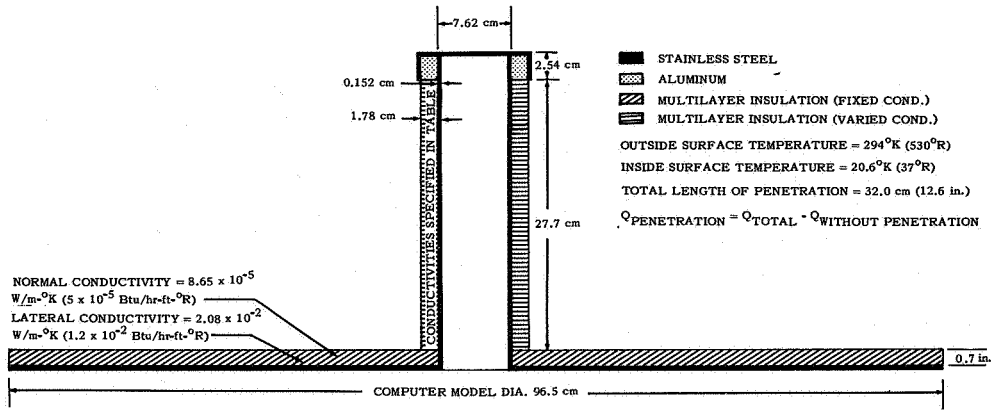
transfer through penetrations demands data input with the warm boundary temperature being a constant and the cold boundary temperature being a variable. Thus, for accuracy, the thermal conductivity data for the computer programs should be independent of the warm and cold boundary temperatures and large temperature differentials (Fig. 25). For the above reasons, a feasibility study has been performed, a calorimeter designed, and preliminary thermal conductivity data are being obtained for different multilayer insulation materials as a function of temperature. Detailed reports of this progress will be available in the near future.

#### TANK SIDEWALL INSULATION SYSTEM DESIGN

Insulation performance in the applied condition can be significantly affected by attachment methods. Figure 26 shows some different schemes that may be used to attach insulation to the tank sidewall. The results of the study (Fig. 26) were based on a theoretical application to the MSFC 2.67-m (105-in.) diameter tank. Column one in Figure 26 shows the difference in heat transfer rates for different pin materials used for structural attachments. Note the very small difference in computed heat transfer rates when either aluminum or nylon pins were used in concepts A, B, and C. For concept D, however, the uninsulated aluminum pin can cause a 10% increase over the computed heat transfer value for the nylon pin.

The second column, Figure 26, shows the equivalent conductivity of each concept: the product of the total heat flow into the tank and insulation thickness divided by the product of tank surface area and temperature difference through the insulation. This is essentially a systems performance index; in all cases, the equivalent thermal conductivity of the insulation is always greater than the basic thermal conductivity.

The third column in Figure 26 is an estimate of the number of equivalent layers in each concept. A performance-mass comparison can be made for the four concepts. The  $kN$  factor in the last column of Figure 26 is the product of the equivalent number of layers and the equivalent thermal conductivity. The lower the  $kN$  factor, the better the insulation system. From Figure 26, concept C was predicted to be the best system, with concept D almost as good. Because of manufacturing difficulties and the relatively close  $kN$  factors for concepts C and D, concept D would probably be chosen for further study. These concepts were studied for their thermal performance only. This study assumed that each system was fully



CASE	NORMAL CONDUCTIVITY W/m <sup>2</sup> K (Btu/hr-ft <sup>2</sup> -°R)	LATERAL CONDUCTIVITY W/m <sup>2</sup> K (Btu/hr-ft <sup>2</sup> -°R)	PENETRATION HEAT LEAK W (Btu/hr)	INCREASE IN HEAT LEAK (PERCENT)
1	8.65 x 10 <sup>-5</sup> (5 x 10 <sup>-5</sup> )	2.08 x 10 <sup>-2</sup> (1.2 x 10 <sup>-2</sup> )	3.33 (11.36)	0
2	8.65 x 10 <sup>-4</sup> (5 x 10 <sup>-4</sup> )	2.08 x 10 <sup>-2</sup> (1.2 x 10 <sup>-2</sup> )	3.50 (11.93)	5
3	8.65 x 10 <sup>-3</sup> (5 x 10 <sup>-3</sup> )	2.08 x 10 <sup>-2</sup> (1.2 x 10 <sup>-2</sup> )	4.70 (16.02)	41
4	8.65 x 10 <sup>-2</sup> (5 x 10 <sup>-2</sup> )	2.08 x 10 <sup>-2</sup> (1.2 x 10 <sup>-2</sup> )	7.66 (26.18)	130

FIGURE 25. HEAT TRANSFER THROUGH INSULATED PENETRATION WITH DIFFERENT INSULATION CONDUCTIVITIES

INSULATION SYSTEM DESIGN	Q <sub>DIST</sub> FOR 2.67-m (105-in.) TANK W (Btu/hr)	k <sub>EQUIV</sub> W/m <sup>2</sup> -°K (Btu/hr-ft <sup>2</sup> -°R)	AVERAGE NO. OF LAYERS DUE TO STRUCTURAL ATTACHMENTS	Q <sub>UNDIST</sub> 200 LAYERS W (Btu/hr)	PERCENT INCREASE IN Q DUE TO DISTURBANCE (%)	kN FACTOR W/m <sup>2</sup> -°K (Btu/hr-ft <sup>2</sup> -°R)
A	ALUMINUM PIN 16.8 (57.2)	11.93 x 10 <sup>-5</sup> (6.9 x 10 <sup>-5</sup> )	277	10.7 (37.86)	51.1	3.30 x 10 <sup>-2</sup> (1.91 x 10 <sup>-2</sup> )
	NYLON PIN 16.7 (57.0)	11.91 x 10 <sup>-5</sup> (6.89 x 10 <sup>-5</sup> )	277	10.7 (37.86)	50.6	3.30 x 10 <sup>-2</sup> (1.91 x 10 <sup>-2</sup> )
B	ALUMINUM PIN 18.3 (62.5)	15.32 x 10 <sup>-5</sup> (8.86 x 10 <sup>-5</sup> )	326	10.7 (37.86)	65.1	4.95 x 10 <sup>-2</sup> (2.86 x 10 <sup>-2</sup> )
	NYLON PIN 18.2 (62.2)	15.27 x 10 <sup>-5</sup> (8.82 x 10 <sup>-5</sup> )	326	10.7 (37.86)	64.3	4.95 x 10 <sup>-2</sup> (2.86 x 10 <sup>-2</sup> )
C	ALUMINUM PIN 20.7 (70.6)	9.70 x 10 <sup>-5</sup> (5.61 x 10 <sup>-5</sup> )	190	10.7 (37.86)	86.4	1.85 x 10 <sup>-2</sup> (1.07 x 10 <sup>-2</sup> )
	NYLON PIN 19.6 (66.9)	9.56 x 10 <sup>-5</sup> (5.53 x 10 <sup>-5</sup> )	190	10.7 (37.86)	76.8	1.82 x 10 <sup>-2</sup> (1.05 x 10 <sup>-2</sup> )
D	ALUMINUM PIN 21.9 (74.8)	11.25 x 10 <sup>-5</sup> (6.5 x 10 <sup>-5</sup> )	200	10.7 (37.86)	97.5	2.25 x 10 <sup>-2</sup> (1.30 x 10 <sup>-2</sup> )
	NYLON PIN 19.8 (67.6)	10.13 x 10 <sup>-5</sup> (5.86 x 10 <sup>-5</sup> )	200	10.7 (37.86)	78.5	2.02 x 10 <sup>-2</sup> (1.17 x 10 <sup>-2</sup> )
<b>GENERAL ASSUMPTIONS</b> 1. 1/8 mil SINGLE ALUMINIZED MYLAR 2. 200 LAYERS 3. 235 ANGSTROM ALUMINUM COATING 4. 133 LAYERS/in. 5. SURFACE TEMPERATURE 530°R & 37°R 6. UNCOMPRESSED AREAS K <sub>L</sub> = 5 x 10 <sup>-5</sup> Btu/hr-ft <sup>2</sup> -°R K <sub>II</sub> = 2 x 10 <sup>-2</sup> Btu/hr-ft <sup>2</sup> -°R		<b>SPECIFIC ASSUMPTIONS</b> 1. COMPRESSED AREAS: K <sub>L</sub> = 7 x 10 <sup>-2</sup> Btu/hr-ft <sup>2</sup> -°R K <sub>II</sub> = 7.5 x 10 <sup>-2</sup> Btu/hr-ft <sup>2</sup> -°R 2. PIN SIZE: LENGTH 0.400 in. O.D. 0.250 in. I.D. 0.125 in.		<b>SPECIFIC ASSUMPTIONS</b> 1. PIN AREA: K <sub>L</sub> = 2 x 10 <sup>-3</sup> Btu/hr-ft <sup>2</sup> -°R K <sub>II</sub> = 4.6 x 10 <sup>-2</sup> Btu/hr-ft <sup>2</sup> -°R 2. PIN SIZE: LENGTH 1.500 in. O.D. 0.250 in. I.D. 0.125 in.		

FIGURE 26. COMPARISON OF DIFFERENT INSULATION SYSTEM DESIGNS

evacuated and posed no venting problems during the boost phase of flight. The study showed that the same insulation, when applied in different system configurations, optimizes differently on a thermal conductivity-density basis, and that degrading factors should be used in optimization studies. Programs are now underway to obtain more realistic performance factors for insulation systems.

TESTING OF MULTILAYER INSULATION CONCEPTS

Large vessels at least 2.44 m (8 ft) in diameter are desirable for studies of thermal systems using high performance insulation. In most cases, this

size permits a reasonable simulation of the applied insulation concept to be used for a much larger tank. Application problems, such as structural supports, double contour surfaces, piping penetrations and areas subject to compression or sagging, can be simulated with this type of test tank. Also, sidewall insulation can be simulated because most proposed concepts have been applied in panels. In addition, the larger surface area of a large test tank allows better simulation of gas flow characteristics for all three phases of flight: prelaunch, ascent, and simulated space environments.

Figure 27 is an example of typical errors in thermal conductivity to be expected for vessels the size of the 2.67-m (105-in.) diameter tank. The

$$\frac{dk}{k} = \frac{d\dot{M}h_{r_0} + \dot{M}dh_{r_0} + [(dM_{L_1} - d\Delta M_{L_1})C_{pL}\Delta T_L + dC_{pL}\Delta T_L(M_{L_1} - \Delta M_{L_1}) + d(\Delta T_L)C_{pL}(M_{L_1} - \Delta M_{L_1}) + M_w C_{pw}d(\Delta T_L)]/\Delta\theta + d\dot{M}C_{p_0}\Delta T_0 + \dot{M}C_{p_0}d(\Delta T_0) + dQ_p}{\dot{M}h_{r_0} + [(M_{L_1} - \Delta M_{L_1})C_{pL}\Delta T_L + M_w C_{pw}\Delta T_L]/\Delta\theta + \dot{M}C_{p_0}\Delta T_0 - Q_p} + \frac{d\Delta x}{\Delta x}$$

ASSUMPTIONS

- |                                                              |                                                                      |
|--------------------------------------------------------------|----------------------------------------------------------------------|
| 1. ULLAGE PRESSURE CONTROL ( $\Delta P$ )                    | 3440 N/m <sup>2</sup> (0.50 psi)                                     |
| 2. ERROR IN PRESSURE MEASUREMENT (dP)                        | 826 N/m <sup>2</sup> (0.12 psi)                                      |
| 3. FLOWMETER ERROR                                           | 3.00%                                                                |
| 4. ERROR IN INSULATION THICKNESS MEASUREMENT (d $\Delta x$ ) | 0.254 cm (0.10 in.)                                                  |
| 5. ULLAGE HEATING ( $\Delta T_g$ )                           | 19.4° K (35.00° R)                                                   |
| 6. ERROR IN ULLAGE HEATING (d $\Delta T_g$ )                 | 0.167° K (0.30° R)                                                   |
| 7. LENGTH OF TEST ( $\Delta\theta$ )                         | 120.00 hr                                                            |
| 8. THERMAL CONDUCTIVITY (k)                                  | 8.65 x 10 <sup>-5</sup> W/m-° K (5 x 10 <sup>-5</sup> Btu/hr-ft-° R) |

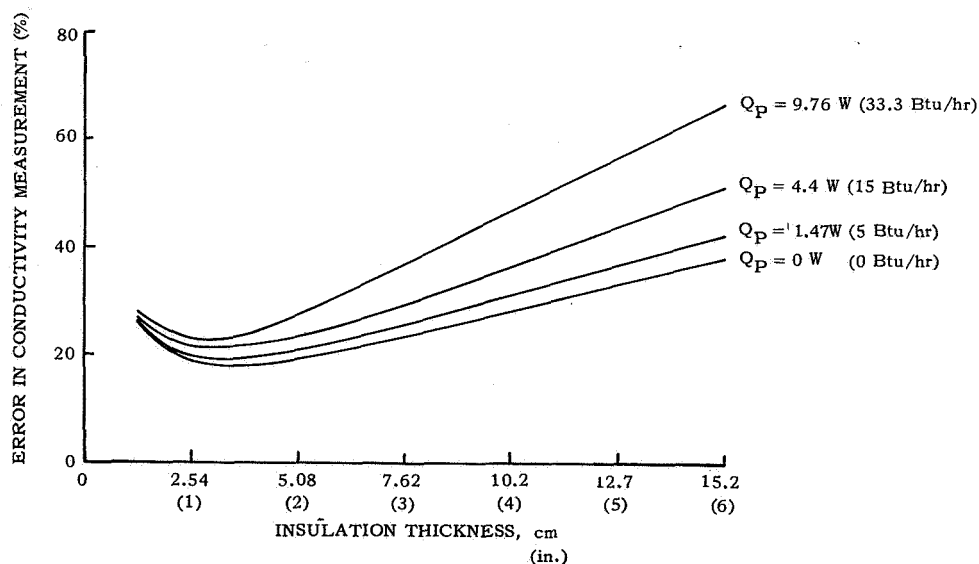


FIGURE 27. ESTIMATED INSULATION THERMAL CONDUCTIVITY ERRORS USING 2.67-m (105-in.) DIAMETER TEST TANK

error from measuring the performance of HPI concepts can be significant. To determine apparent thermal conductivity of an insulation system applied to a test vessel, the total heat flow must be established and extraneous heat leaks must be calculated and subtracted from the total heat input to the cryogen. To measure total heat flow, measurements such as temperature, pressures, insulation thickness, and boiloff rates are needed. Errors are inherent in each of these measuring instruments as well as in the recording system read-out devices. Many instrumentation measurements and fluid properties are also needed to reduce the boiloff data to an apparent thermal conductivity value as shown in the equation in Figure 27 (see Appendix A). These measured values, such as pressure and temperature, are also used in equations to find fluid properties (enthalpy, specific heat, internal energy, density and latent heat of vaporization). Each of these equations is a curve that has been obtained from experimental data; thus a tolerance is placed on the computed properties that introduces additional measured thermal conductivity error.

An equation for establishing the apparent thermal conductivity error has been programmed for computer

solution. Some results from such studies are as follows: (1) control of ullage pressure becomes more important as the penetration heat leak is reduced, (2) for thick insulation applications, it is important to minimize penetration heat leaks, (3) ullage pressure control becomes less critical as insulation thickness is decreased, and (4) accurate computation of penetration heat leaks is important.

An important parameter in the error analysis is the tank diameter. As tank size increases, the side-wall heat transfer rate increases and minimizes the effect of the penetration heat leak error. However, as the volume increases, the error in the computed stored energy of the test fluid increases, resulting in a practical limiting tank diameter. A tank diameter of about 2.44 to 3.05 m (8 to 10 ft) was the optimum size (Fig. 28). The slope of the thermal conductivity error versus tank diameter may take on a new shape, and a new optimum diameter may be found if other parameters (such as insulation thickness, tank shape, penetration heat leak, and instrumentation errors) are varied. Therefore, accuracy of the experimental data of an insulation system must be found after all variables in the equation in Figure 27 have been studied.

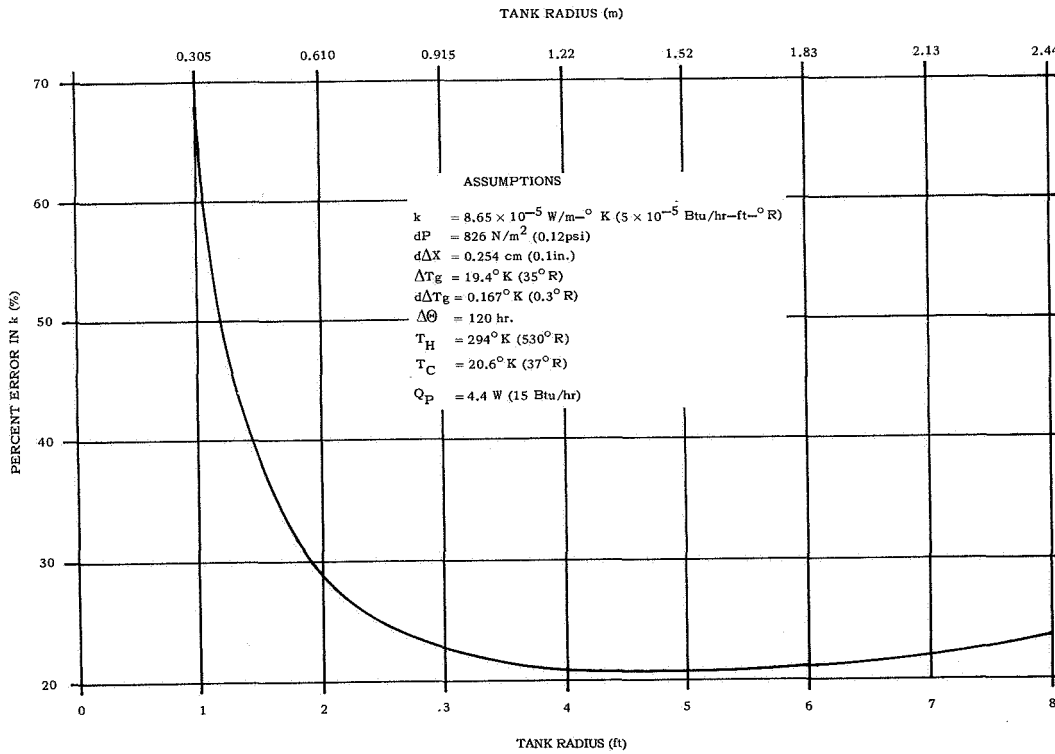


FIGURE 28. THE ERROR IN SUPERINSULATION THERMAL CONDUCTIVITY VERSUS TANK RADIUS

## CONCLUSIONS

Acceptable insulation system performance for short term missions was obtained from the shingle insulation concept applied on the 2.67-m (105-in.) diameter tank. The experience derived from the test tank program helped in identifying additional development problems requiring solutions before multilayer insulation can be used for long term storage.

Insulation evacuation can be improved by the use of preconditioning and perforation. A lightweight purge jacket has been designed to rupture during vehicle ascent to allow the insulation to expand and quickly obtain an equilibrium pressure within the insulation layers. Leakage into the insulation can be reduced by installing diffusion bonded joints at ducting connections, welded omega seals at manhole

covers, and submersible fill valves in fill and drain lines. The development of a low leak rate flight type electrical connector is in progress. Thermal conductivity measurements as a function of temperature are currently being generated, and techniques are being improved for computing penetration heat leaks through structural supports, ducting connections and insulation attachments. The development of a low temperature vacuum gage for use with multilayer insulation is in progress.

The design, fabrication, and application of multilayer insulation to flight configuration vessels has been successfully demonstrated. Research is continuing on problems now partially solved, and research programs have been initiated to solve those remaining problems. As a result of the above efforts, application of an insulation system to a large flight stage appears to be practical for long term storage of cryogenics.

## REFERENCES

1. Duggan, J. B. : Evacuation of Gases from Batten of Multi-Layer Insulation in a Vacuum Environment. Brown Engineering Co., Inc., Huntsville, Alabama TD-D1-PTE-011 Phase D, August 26, 1966.
2. Shea, D. C., ed. : 3-D Insulation Penetration Model Program Modification. Lockheed Missiles and Space Co., Huntsville, Alabama, Contract NAS8-20438, DCN 1-7-52-20060, Monthly Progress Report LMSC/HREC A784249, 10 May 1967.
3. Powell, R. L.; and Blandied, W. A. : Thermal Conductivity of Metals and Alloys at Low Temperatures. National Bureau of Standards, September 1, 1954.
4. Cody, J. C.; and Hyde, E. H. : Thermal Problems Associated with the Development of a Flight Configured Cryogenic Insulation System. Marshall Space Flight Center, Proceedings of the Conference on Long Term Cryo-Propellant Storage in Space, October 1966.
5. Getty, R. C. : Cryogenic Insulation Development. Monthly Progress Report for November, General Dynamics, Convair, Contract NAS8-18021, 10 December 1966.
6. Getty, R. C. : Cryogenic Insulation Development. Monthly Progress Report for March, General Dynamics, Convair, Contract NAS8-18021, 3 April 1967.
7. Harsh, M. George; and Humphries, William R., ed. : NRC-2 Super Insulation Groundhold and Altitude Tests C-012-4, 5, 7, 10, 11, 12, 13, 15, 16, 17 and 18. George C. Marshall Space Flight Center, Report R-TEST-CT-129-66, 15 December 1966.
8. Niedorf, L. R. : Investigation of a Lightweight Self-Evacuating Prefabricated Multi-Layer Insulation System for Cryogenic Space Propulsion Stages. Quarterly Progress Report Number 1, Linde Company, Contract NAS3-6289, December 16, 1965.
9. Crawford, R. F.; and Hannah, R. G. : Cryogenic Insulation Research, ER 14361, Martin Co., Baltimore Division, Contract NAS8-11397, Sept. 1966.
10. Crawford, R. F.; and Hannah, R. G. : Cryogenic Insulation Research. Final Report, Contract Number NAS8-11397, The Martin Company, CR-61162, January 23, 1967.

## BIBLIOGRAPHY

1. Arthur D. Little, Inc. : Basic Investigation of Multi-Layer Insulation Systems. Contract Number NAS3-4181, (ADL 65958-00-01), February 29, 1964.
2. Brogan, J. J. : Design of High Performance Insulation Systems. Summary Report, Lockheed/Sunnyvale, Contract NAS8-11347, August 20, 1965.
3. Cox, J. : The Effects of Temperature Dependent Insulation Thermal Conductivity of Penetration Heat Leak. Brown Engineering Co., Inc., Huntsville, Alabama, TE-D1-PTE-011 Phase 23, April 4, 1967.
4. Cox, J. : and Duggan, J. B. : An Analysis of the Errors Involved in Measuring the Thermal Conductivity of Multi-Layer Insulations by Cryogenic Calorimeter Techniques. Brown Engineering Co., Inc., Huntsville, Alabama, TD-D1-PTE-011, Phase 23, May 1, 1967.
5. Design Techniques for Structures - Cryogenic Insulation Integration. Final Report, Contract NAS8-5268, The Martin Company, NASA CR-61038, January 25, 1965.

## APPENDIX A

## SYMBOLS FOR EQUATION IN FIGURE 27

$k$	Conductivity of wall insulation, $\frac{W}{m \cdot ^\circ K} \left( \frac{Btu}{hr \cdot ft \cdot ^\circ R} \right)$
$\Delta x_{ave}$	The average tank wall insulation thickness, cm (in.)
$Q_P$	The heat leak through the penetration, W (Btu/hr)
$\dot{M}$	Mass flow rate of $GH_2$ out of tank, kg/hr (lb/hr)
$M_{L1}$	Mass of $LH_2$ in tank at start of test, kg (lb)
$\Delta M_L$	Mass of $H_2$ evaporated during the test, kg (lb)
$M_W$	Mass of tank wall, kg (lb)
$C_{PL}$	Specific heat of the $LH_2$ , $\frac{J}{kg \cdot ^\circ K} \left( \frac{Btu}{lb \cdot ^\circ R} \right)$
$C_{PW}$	Specific heat of the tank wall, $\frac{J}{kg \cdot ^\circ K} \left( \frac{Btu}{lb \cdot ^\circ R} \right)$
$C_{Pg}$	Specific heat of the ullage gas, $\frac{J}{kg \cdot ^\circ K} \left( \frac{Btu}{lb \cdot ^\circ R} \right)$
$\Delta \theta$	The length of time the test is run, hr
$\Delta T_L$	$T_{L2} - T_{L1}$ , $^\circ K$ ( $^\circ R$ ) {difference in $LH_2$ temperature at start and end of test}
$\Delta T_g$	$T_{gA} - T_{gL}$ , $^\circ K$ ( $^\circ R$ )
$h_{fg}$	Latent heat of vaporization for the $LH_2$ , $\frac{J}{kg} \left( \frac{Btu}{lb} \right)$
$dQ_P$	The estimated error in $Q_P$ , W (Btu/hr)
$d(\Delta x_{ave})$	The instrument error in measuring the thickness of the insulation, cm (in.)
$d\dot{M}$	The error in $\dot{M}$ as a result of measurement error, $\frac{kg}{hr} \left( \frac{lb}{hr} \right)$
$dM_{L1}$	The error in $M_{L1}$ caused by inaccuracy in calculating the density, kg (lb)
$d\Delta M_L$	The error in $\Delta M_L$ caused by inaccuracy in measuring $\dot{M}$ , kg (lb)
$dC_{PL}$	Error in $C_{PL}$ caused by inaccuracy of calculations, $\frac{J}{kg} \left( \frac{Btu}{lb} \right)$
$d(\Delta T_L)$	$dT_{L2} - dT_{L1}$ or to give the maximum error possible, change the - to +, $^\circ K$ ( $^\circ R$ )
$d(\Delta T_g)$	$dT_{gA} + dT_{gL}$ , $^\circ K$ ( $^\circ R$ )
$T_{gL}$	The temperature of the ullage gas just above the $LH_2$ surface, $^\circ K$ ( $^\circ R$ )
$T_{gA}$	The average temperature of the ullage gas as it vents over the length of the test, $^\circ K$ ( $^\circ R$ )



# DESIGNING FOR CRYOGENIC INSULATION

By

Clyde D. Nevins

## SUMMARY

Structural design studies at MSFC have shown that the type and means of application of high performance insulation will be a major influence on the design of spacecraft with cryogenic propellants. For long-term missions propellant tankage design requires new approaches, and concurrently, methods must be developed for insulation attachment and protection.

The basic pressure vessel may not require significant change of shape to be adapted for insulation application. However, the concept of an integral pressure vessel that also carries vehicle bending loads suggests a configuration in which the propellant tank is suspended within a load-carrying shroud. Openings into the tank and appendages to the tank use new techniques to minimize heat shorts.

MSFC and several contractors have investigated many insulation systems in thicknesses up to 2.5 cm (1.0 in.) for compatibility with the adverse environments of a rocket vehicle launch. Purged insulation systems now appear much better suited than pre-evacuated systems, both from the ease of attachment and reliability of the insulation covering.

## INTRODUCTION

The structural design of propellant tankage for long term cryogenic storage has brought many new and challenging problems to the designer. No longer can a propellant tank be designed solely for the structural loads and then released to the thermal engineers for application of the necessary insulation. Nor can a propellant tank be adapted efficiently to other missions by merely increasing the thickness of insulation. The thermal protection of cryogenics now requires consideration by the structural designer from the earliest stages of design.

There are four broad categories which essentially cover the range of considerations of structural engineers in this new technology. These categories are illustrated by the typical cryogenic stage shown

in Figure 1 and are: the basic pressure vessel; openings and appendages to the pressure vessel; insulation attachment methods; and the insulation covering, or jacket. The MSFC programs in each of these four categories are the major topics discussed in this paper.

## BASIC PRESSURE VESSEL

The general stage design for missions requiring long term storage of cryogenics will be considerably altered from the current configuration. Whereas the cryogenic stages of Saturn IB and Saturn V are "integral," i. e., where the propellant tank also forms the external contour of the stage, future stages will most likely be of the nonintegral type. The difference in the two approaches is shown in Figure 2.

The integral stage requires the propellant tank cylindrical walls to carry all the vehicle bending, shear, and axial loads. In this case, the tank skirts would introduce a severe heat short to the cryogenic propellant and excessive propellant boiloff results. In addition, the fragile insulation materials cannot withstand the aerodynamic heating and buffeting to which they would be subjected in this configuration.

The need to minimize the structural heat short and also to protect the insulation results in the non-integral configuration shown in Figure 2. The tank support structure need be sufficiently strong only to support the pressure vessel and the propellant it contains. The aerodynamic loads on the vehicle and the axial load resulting from an upper stage or payload are carried in the structural shroud surrounding the tank. For long duration missions this configuration also offers excellent protection from meteoroid damage.

Generally the shape of the basic pressure vessel should not be significantly altered by the requirement to store cryogenics for long periods of time. In theory, minimizing the surface area to volume ratio, i. e., approaching a spherical shape, is desirable for reducing the total heat flux through the insulation.

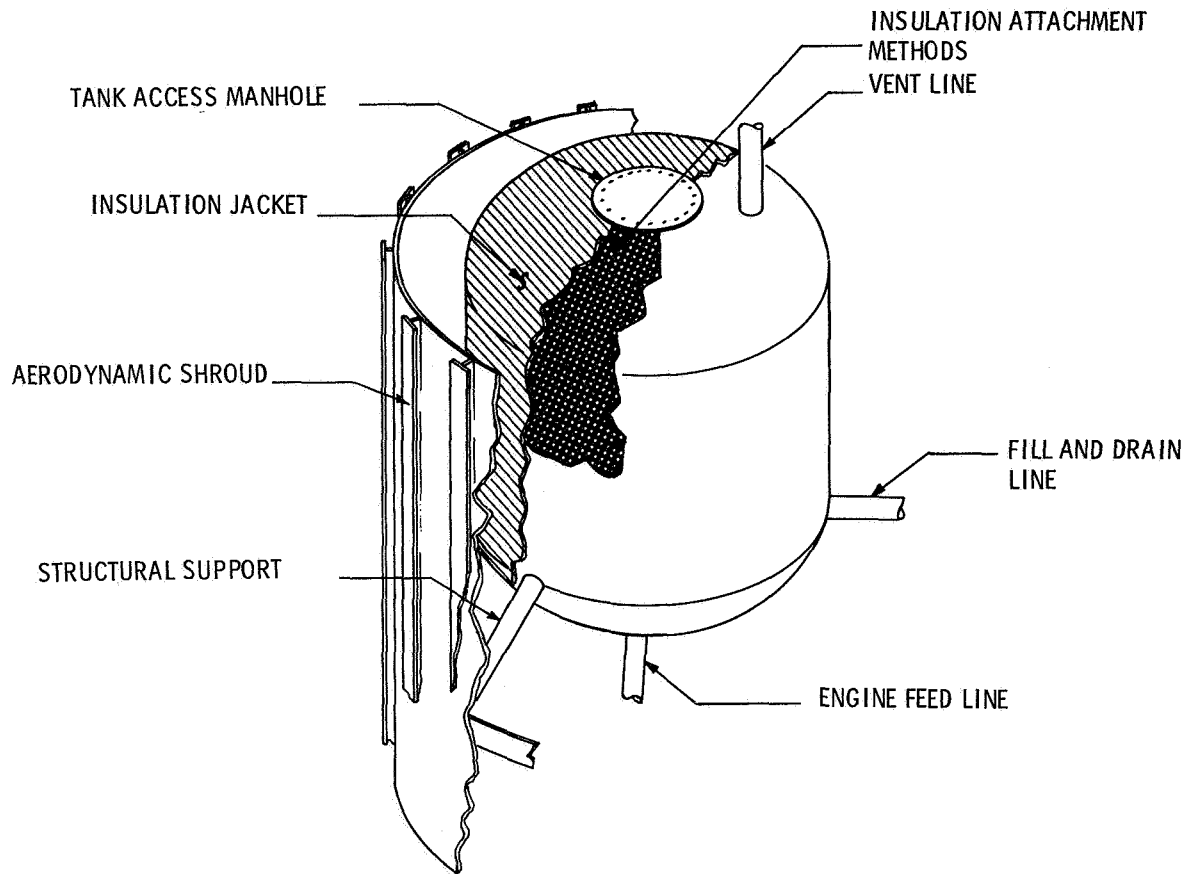


FIGURE 1. A TYPICAL CRYOGENIC STAGE

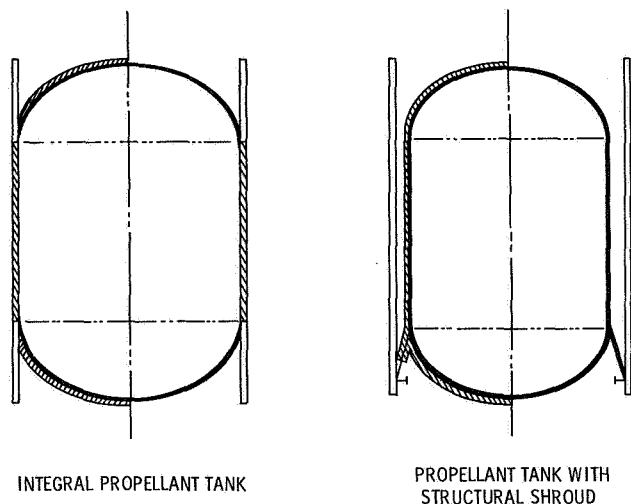


FIGURE 2. INTEGRAL AND NONINTEGRAL TANKS

In actuality, however, spheres are more difficult to insulate because of being composed entirely of a doubly-contoured surface, and insulation performance is degraded compared with that of a corresponding cylinder. Spheres are also very inefficient inhabitants of the cylindrical volume available in the stage contour and seldom look attractive from an overall structural mass standpoint. The conventional cylindrical tanks with elliptical or hemispherical domes that have evolved during a long history of pressure vessel design, strength analysis, and fabrication in the aerospace industry should still be most suitable.

Likewise, materials for tank structures are not significantly affected by the requirement to store cryogenics for long periods. The aluminum alloys selected for Saturn I and Saturn V propellant tanks, e. g. , 2219 aluminum alloy, will be quite satisfactory here as well. In some cases, titanium alloys may prove to be superior to aluminum. Titanium can offer a better strength-to-mass ratio for a pure pressure vessel and has the additional advantage of

permitting direct welding of low conductivity propellant lines.

## OPENINGS AND APPENDAGES

Both openings and appendages present formidable challenges when designing a structure compatible with long term storage requirements.

For large propellant tanks an access opening, or manhole, has proved to be indispensable during launch pad operations on Saturn stages; there is no reason to believe this requirement can be eliminated for stages requiring long term storage of cryogenes. Structural supports and propellant lines are mandatory, but their design now becomes a major factor in propellant storage capability.

Measurable leakage (in the order of  $10^{-9}$  cc/sec) of hydrogen into the insulation will seriously degrade the thermal performance of the insulation. Since current flange seal technology does not reliably limit leakage to this extent, this deficiency must be overcome by a design modification to either the sealing method or local insulation application.

One approach to reliably limit the hydrogen leakage is shown in Figure 3. An annular sealing

strip is welded to either side of the manhole cover joint, closing off any leakage through the mating surfaces or bolt holes. The disadvantage here is that access to the tank interior would require cutting the sealing strip and then rewelding (and leak checking) as a field operation.

Another approach is to allow for possible leakage through the seal and provide a leak-tight channel through the insulation blanket. By preventing hydrogen leakage into the insulation there will be no degradation other than a small local heat short. Figure 4 shows this latter approach.

Piping penetrations of the insulation can cause a significant heat leak. When aluminum alloys are to be used for construction of the tank, a method must be found to use low-conductivity materials such as corrosion resistant steels or perhaps titanium alloy for the penetrating lines. Until a reliable flange seal is found, the best approach appears to be using a bimetallic transition joint. For this approach the aluminum end of the joint is welded to the tank and the other end is butt welded to a low-conductivity pipe.

Several types of bimetallic transition joints are possible, and three different types have been tested by MSFC: (1) a threaded joint with a silver fusion-welded seal, (2) a commercially available brazed

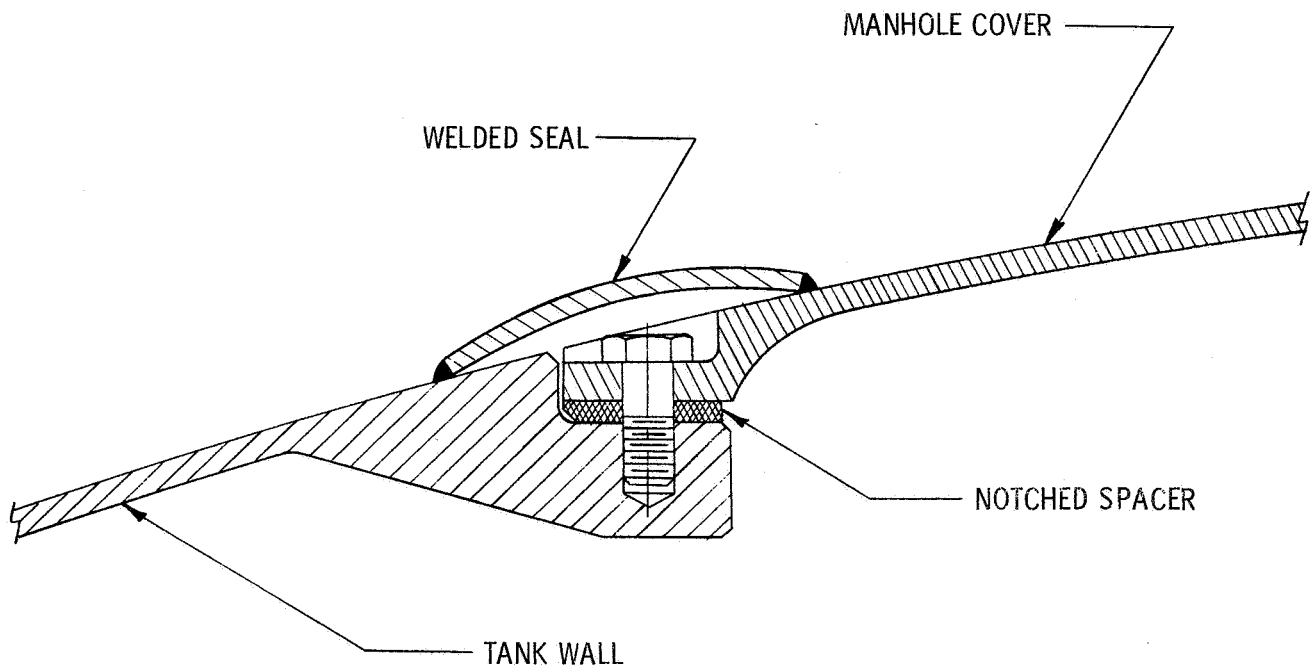


FIGURE 3. A WELDED MANHOLE COVER SEAL

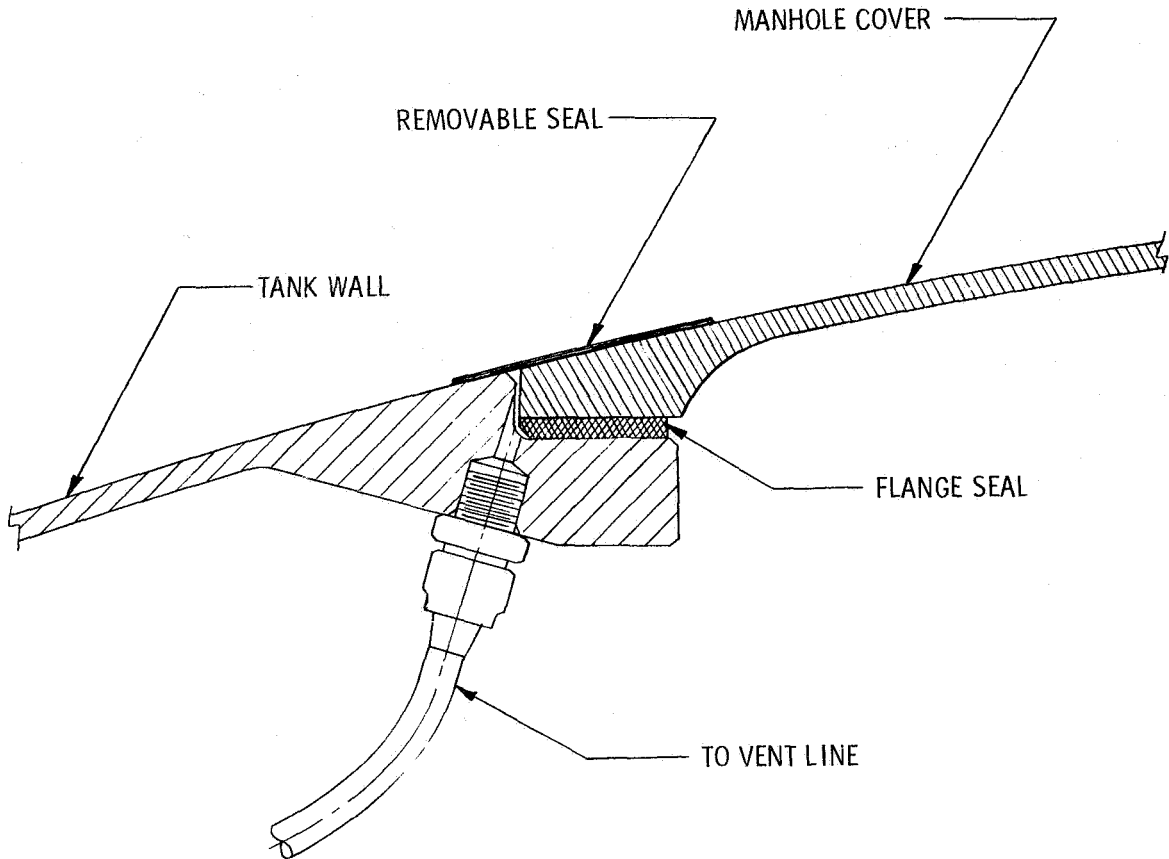


FIGURE 4. A VENTED MANHOLE COVER SEAL

joint, and (3) an explosively swaged joint. Each type of joint was subjected to the following series of tests: (a) preliminary leak check with helium mass spectrometer, (b) cold shock from 353°K (175° F) to LH<sub>2</sub> temperature for 15 cycles, (c) intermediate leak check with helium mass spectrometer, (d) pressurized to 0.38 MN/m<sup>2</sup> (55 psig) and vibrated longitudinally and laterally for 5 minutes each at the major resonant frequency with a 22.7 kg (50 lb) mass. (One of the test specimens is shown mounted in the vibration test fixture in Figure 5. ), and (e) final leak check with helium mass spectrometer.

Test results [ 1 ] indicated that the commercially available brazed joint was superior to the other types tested. The threaded joint seal failed during vibration testing and one sample of the explosively swaged joint failed to pass the preliminary leak check.

It is more difficult to generalize on the structural support members for cryogenic tankage because of the wide variety of support structures which may be

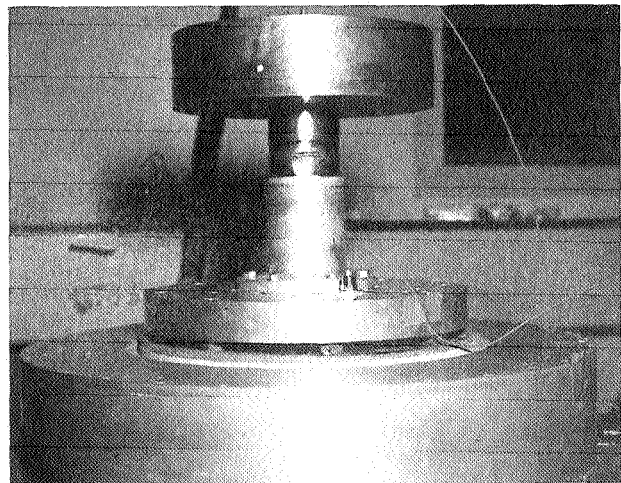


FIGURE 5. BIMETALLIC JOINT VIBRATION TEST

selected. As an illustration of this, the next three figures show the strong dependency of the structural supports on the configuration of the stage. Each of

the three structures shown has been carried through preliminary design and analysis, and each yields the lowest system mass penalty for the mission under consideration.

The first support structure was designed for the hydrogen propellant tanks for the S-VI stage (Fig. 6). This stage was studied in some detail by

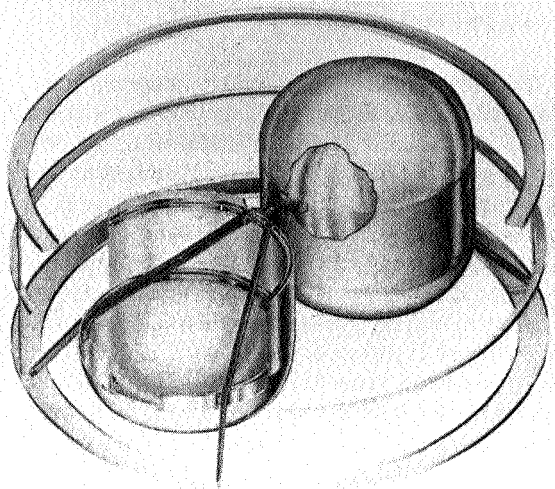


FIGURE 6. SUPPORT STRUCTURE FOR THE LIQUID HYDROGEN TANKS OF THE S-VI STAGE

MSFC for use as a "kick" stage and as the basic form of the Multi Mission Module for Lunar logistics missions. The two hydrogen tanks are mounted parallel in the stage. The support structure is comprised of four struts that form two A-frames and pierce the tanks to join at the center. This arrangement allows the two tanks to be supported by only four penetrations of the insulation blanket, the central support being completely insulated and thus offering no heat short into the system. Titanium was used for the penetrating members because high local bending stresses precluded the use of fiberglass.

Figure 7 shows a much different tankage arrangement, and consequently, a much different structural support. The spherical hydrogen tank is supported by a titanium conical frustum attached at the sphere's equator. This particular structural support configuration and material had the lightest overall mass for the eight day mission under consideration. It is interesting to note, however, that had the mission been eleven days or greater (rather than eight), a completely different support system configuration

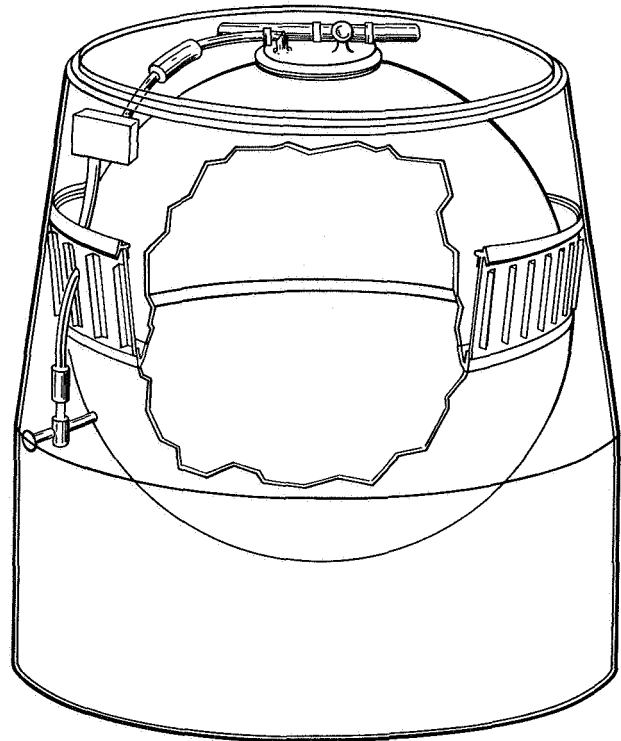


FIGURE 7. STRUCTURAL SUPPORT OF THE SPHERICAL LIQUID HYDROGEN TANK OF A CRYOGENIC SPACECRAFT MODULE

would have been selected. For the longer mission, the preferred system would have been comprised of three discreet attachments to the sphere, and although it would be some 46% heavier than the conical frustum because of the additional structure required within the sphere, only about 1/6 as much boiloff would occur [2].

Figure 8 illustrates the support system selected for the experiment tanks of project THERMO, which would include an orbital platform for cryogenic experiments. This system uses six struts which may carry either tension or compression loads. Achieving the objectives of the particular experiment required having not only a minimum heat short, but the minimum number of heat shorts as well. With the additional requirement to mate with a specified Rack structure, the configuration shown provided the minimum heat short with only four penetrations of the insulation. The struts in this case were of fiberglass.

As indicated previously, titanium and fiberglass are the preferred materials for structural supports. In Table I several materials used for aerospace structures are tabulated with their densities, thermal

CRYOGENIC PROPELLANT STORAGE EXPERIMENT

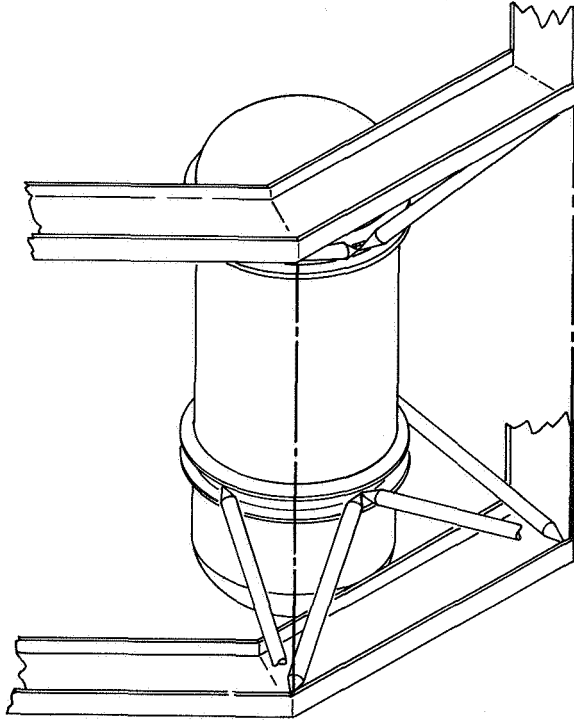


FIGURE 8. STRUCTURAL SUPPORT OF THE CRYOGENIC PROPELLANT STORAGE EXPERIMENT TANK FOR PROJECT THERMO

conductivities, and tensile strengths. At the right is the normalized efficiency index for each material; in this case a low index indicates the higher efficiency. The indices were run for minimizing boiloff for a specified inert mass fraction and assuming pure tension support members [3]. As shown, titanium alloys and filament wound fiberglass are far superior to the other materials. For support structures loaded in both tension and compression, or with superimposed bending loads, titanium supports are more competitive with the fiberglass than indicated by data in Table I.

The advantage of nonmetallic supports for cryogenic tankage is evident, however. Marshall Space Flight Center is now investigating the design problems associated with nonmetallic beams and struts for spacecraft structures [4]. Figure 9 shows a test strut recently completed under this contract and now undergoing structural tests. Figure 10 shows the strut's components and clearly shows the thickness of the nonmetallic cylindrical column. This cylinder is made of five layers of high strength glass filaments, three layers of longitudinal and an inner and outer circumferential wrap, in an epoxy resin. The total wall thickness is 0.084 cm (0.033 in.).

TABLE I. COMPARISON OF STRUCTURAL SUPPORT MATERIALS

	DENSITY kg/m <sup>3</sup> (lb/ft <sup>3</sup> )	THERMAL CONDUCTIVITY Joule/m-sec-°K (Btu/ft-hr-°R)	YIELD STRENGTH MN/m <sup>2</sup> (lb/in. <sup>2</sup> x 10 <sup>-3</sup> )	NORMALIZED EFFICIENCY
TITANIUM ALLOY 6 AL 4 VA	4570 (285)	4.8 (2.8)	828 (120)	0.093
ALUMINUM ALLOY 2014-T6	2760 (172)	156 (90.0)	413 (60)	1.000
BERYLLIUM	1780 (111)	151 (87.0)	448 (65)	0.714
STAINLESS STEEL 17-7 PH	7670 (479)	16.9 (9.75)	1034 (150)	0.198
FIBERGLASS S-994 GLASS UFW EPON 826 RESIN	1840 (115)	0.59 (0.34)	758 (110)	0.015

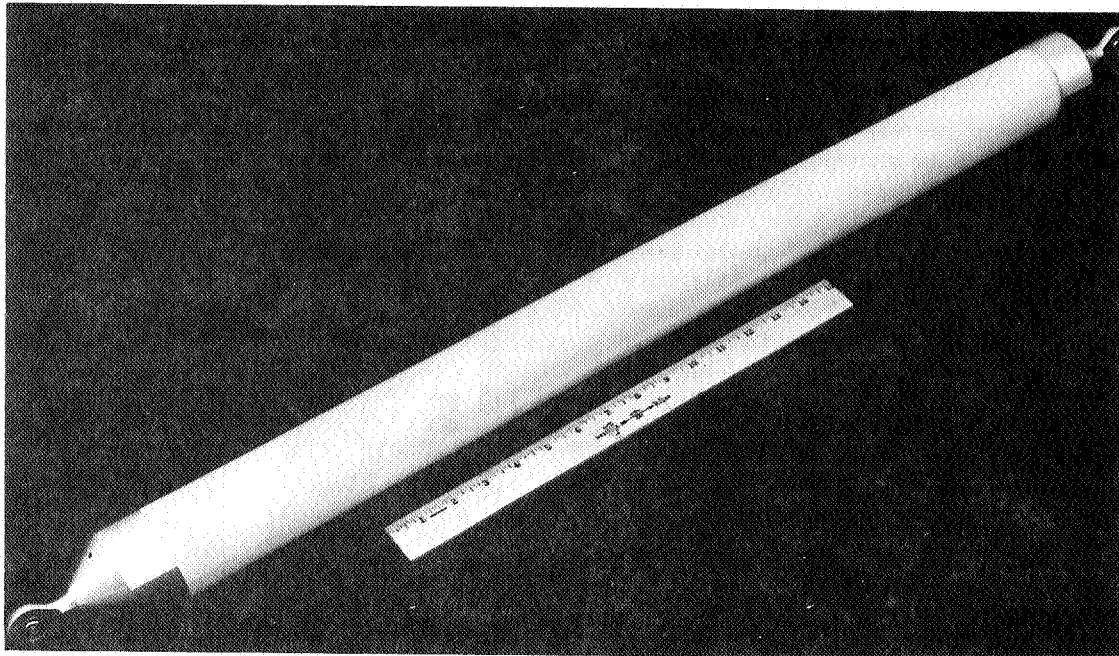


FIGURE 9. A NONMETALLIC STRUCTURAL SUPPORT

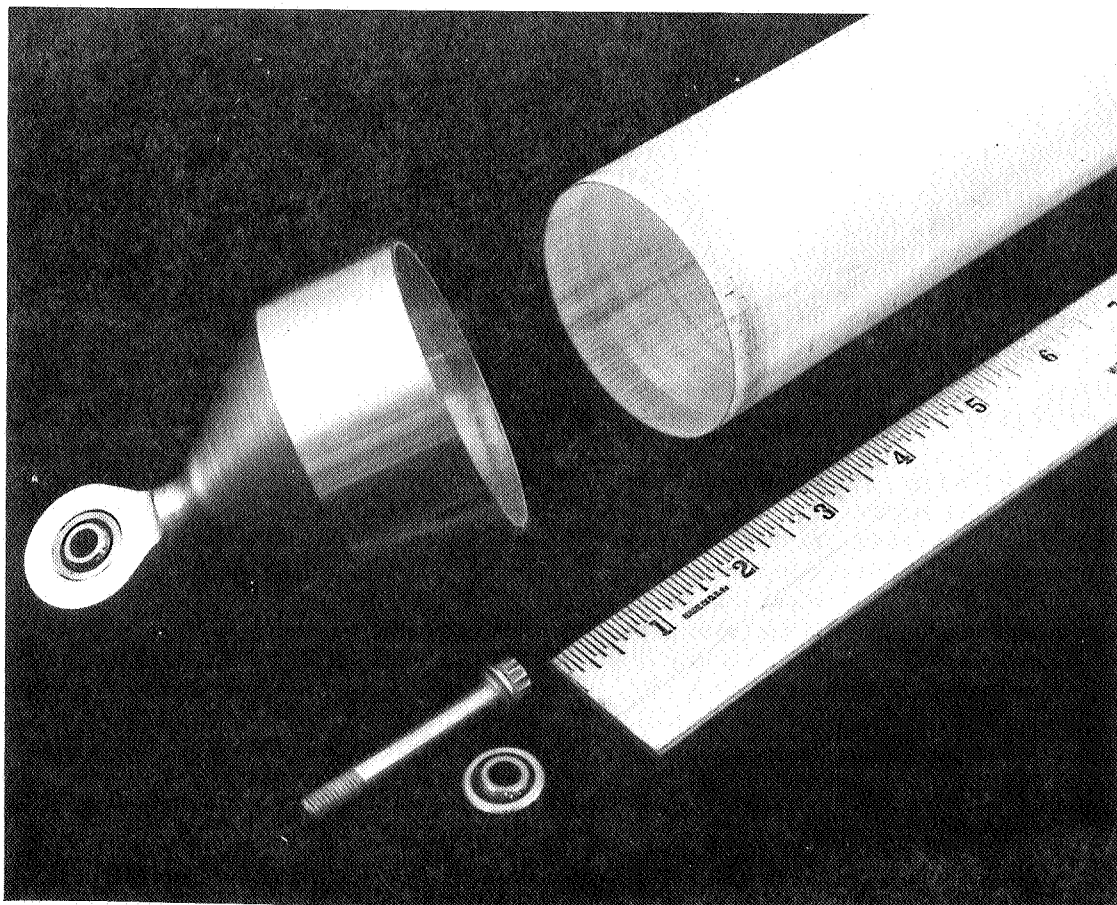


FIGURE 10. DETAIL OF FIBERGLASS STRUT COMPONENTS

## INSULATION ATTACHMENT METHODS

The third area of interest to structural engineers is the method of insulation attachment. This is undoubtedly the most challenging of the designer's problems, primarily as a result of the very fragile nature of materials used in high performance insulations. In addition, the insulation must be supported without significant penetration or compaction of the insulation, either of which would degrade the thermal performance of the insulation.

Figure 11 illustrates several types of attachment methods considered for pre-evacuated systems.

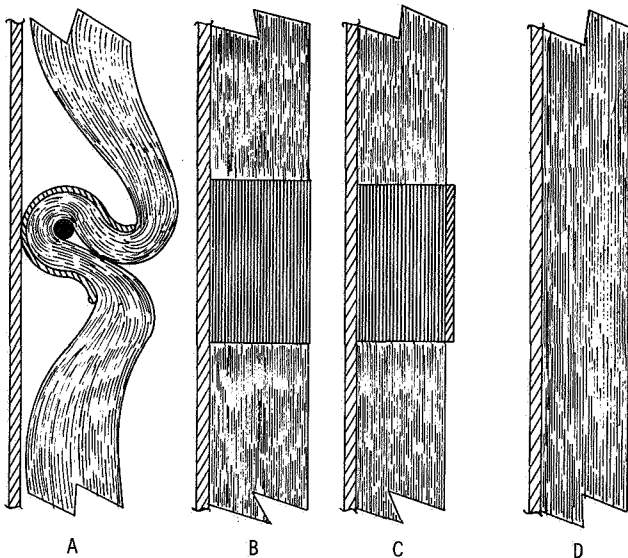


FIGURE 11. ATTACHMENT METHODS FOR PRE-EVACUATED INSULATION SYSTEMS

Method "A" uses nylon ropes placed around the tank and anchored to it. The insulation is clipped at intervals to the ropes as shown. Method "B" uses interwound tension bands. These thin aluminum straps are interwound on the tank along with the insulation. Proper tension control of the bands provides the frictional force necessary to hold the insulation in place. Method "C" is similar to Method "B" in that a tension band is used to provide friction. In this case, however, the band is placed externally and additional spacer material is wound within the insulation to prevent compaction. The band tension is maintained by spring loading. Method "D" is the so-called "envelope" method whereby each layer of insulation is a separate structural shell made by cutting, fitting, and taping

each layer individually during installation. Each envelope then supports only its own mass.

Figure 12 illustrates attachment methods suitable for purged insulation systems. Method "E" employs

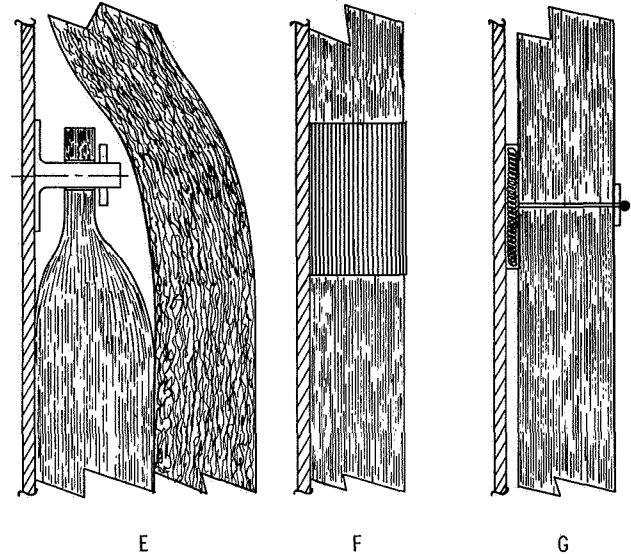


FIGURE 12. ATTACHMENT METHODS FOR PURGED INSULATION SYSTEMS

studs bonded to the tank surface, which pierce the insulation at areas where the insulation layers are compacted and bonded together. A hole is then punched through these areas to match the stud locations. This method requires a large overlap of insulation battens to prevent the studs from imposing a serious heat short through the insulation. Method "F" is the tension band method shown in the previous figure which is applicable to a purged system as well. Method "G" uses a pattern of dacron threads piercing the insulation and anchored by buttons at one end and to a Velcro fastener at the tank surface.

Each of these attachment methods must withstand the rigors of a rocket vehicle launch without damaging the insulation. In a rocket vehicle trajectory there are four periods that present adverse environments for the insulation and its attachments: first, the high acoustic environment at lift-off, next the rapid ascent and the associated rapid pressure drop (an adverse environment for purged systems only), then the maximum dynamic pressure point where there is the combination of severe vibration and moderately high acceleration, and finally, first stage burnout where the maximum acceleration level occurs.

The capability of each type of insulation attachment method to satisfactorily survive these environments has been assessed in a series of experiments on test tanks such as the one shown in Figure 13.

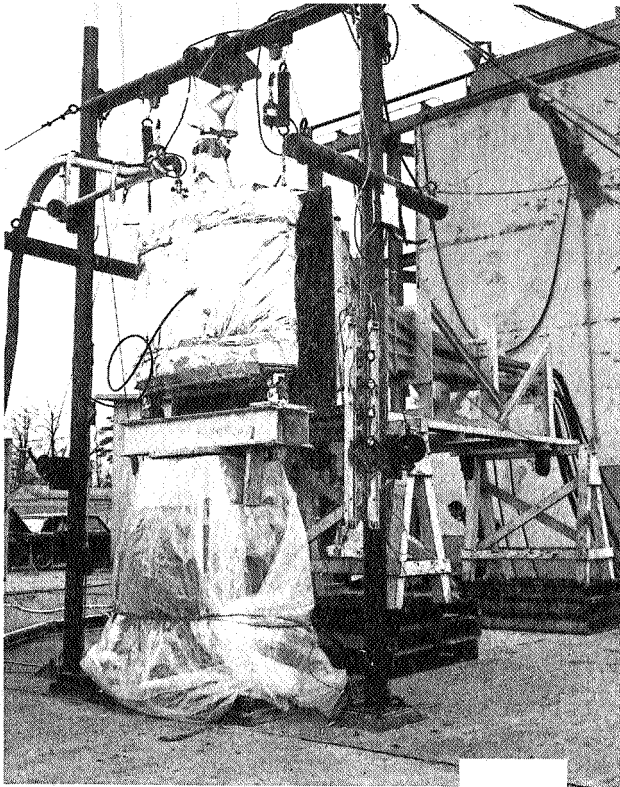


FIGURE 13. VIBRATION AND ACOUSTIC TEST OF AN INSULATED TEST TANK

This tank is a biconvex cylinder with radii of curvature equal to that of the 2.67-m (105-in.) diameter tank. The biconvex shape permits good representation of full scale parameters in a specimen small enough to use readily available test facilities.

In general, the test sequence followed the natural occurrence of environments in an operational mission. A ground-hold thermal performance test was performed initially to evaluate thermal characteristics of the system prior to launch. Next, a combined mechanical and acoustic vibration test was performed at liquid hydrogen temperature (Fig. 13). A steady acceleration test on a centrifuge followed with a 6.6 g acceleration applied in the direction of the tank's longitudinal axis for 5 minutes. Figure 14 shows an insulation system photographed during an acceleration test. After installation in a vacuum chamber (Fig. 15), a rapid evacuation test was performed to simulate the pressure-time history of

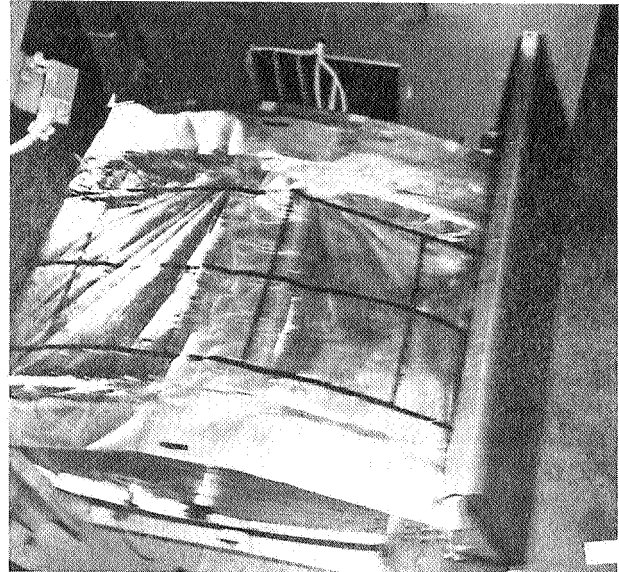


FIGURE 14. INSULATED TEST TANK DURING CENTRIFUGE TEST

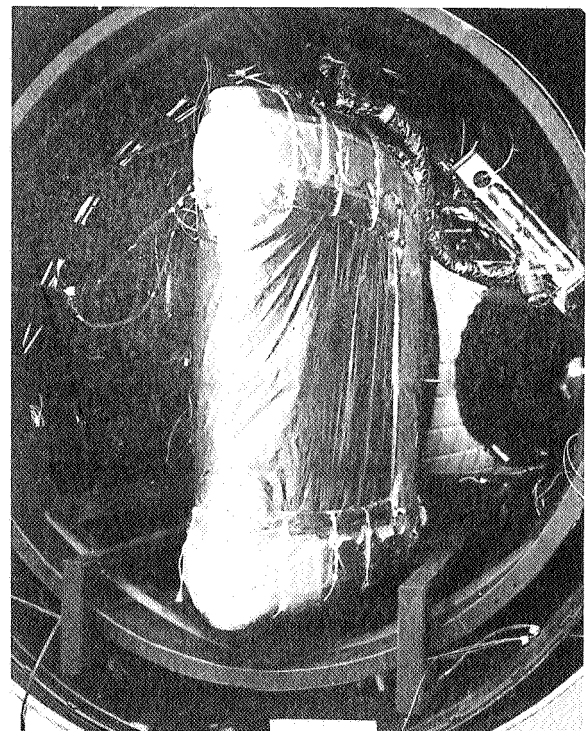


FIGURE 15. INSULATED TEST TANK MOUNTED IN VACUUM CHAMBER

a typical Saturn V boost. Finally, a space thermal performance test was performed to determine the heat transfer characteristics for each system in the space environment.

Results of experiments on test tanks of this general size and shape are summarized in Table II [5, 6]. The rope and clip method failed when metal clips were used, but passed when a nonmetallic clip was used. In the latter case, however, an additional attachment through the insulation had to be incorporated with each clip, thus adding a significant heat short. The tension band method proved to be acceptable if the insulation was not compressed prior to the dynamic environment; i. e., it is acceptable for purged systems but not for a pre-evacuated system. The external tension band satisfactorily solves the shortcoming of the interwound tension band for the pre-evacuated system, but still relies on friction, a somewhat unfaithful servant. The last two methods were developed primarily for purged insulation blankets approximately 2.5-cm (1.0-in.) thick and proved to be very satisfactory for that application. Their application to greater thicknesses has not been established, and is now being evaluated in the MSFC inhouse program.

Although much can be accomplished in small scale tests, it is seldom possible to simulate all the environments adequately in laboratory experiments. To produce the combination of environments coupled with the effects of cryogenic temperature acting on a full-scale insulation system, the rocket sled shown

in Figure 16 has been built and is now ready for the first test. The 7260-kg (16 000-lb) sled will be the largest rocket sled ever sent down a track. The insulated 2.67-m (105-in.) diameter tank will be mounted within the shrouded sled and accelerated to about 6 g's, the maximum level expected during a Saturn V launch. Along with the acceleration, there will be vibration induced by the track and a moderate level of acoustic energy.

## INSULATION COVERING

Finding a suitable covering for the insulation system is the final task of the structural engineer. The covering must not only protect the insulation system during handling, but also must provide for maintaining proper environmental control within the insulation layers during prelaunch operations.

The covering for a pre-evacuated system presents a particularly difficult set of requirements to meet. This "flexible vacuum jacket" must have low permeability, low moisture absorption, and a low outgassing rate in a vacuum environment. It also has to be flexible over a wide range of temperatures and be durable, i. e., resistant to formation of pin-hole leaks at wrinkles. It is desirable that the jacket can be stretch-formed to complex contours, and that it be compatible with LO<sub>2</sub>.

Figure 17 shows a jacket sample on a 61-cm (24-in.) diameter test fixture. Materials that

TABLE II. EVALUATION OF INSULATION ATTACHMENT METHODS

ATTACHMENT METHOD	SUITABILITY (INSULATION METHOD)	RESULTS OF DYNAMIC TESTS	REMARKS
ROPES & CLIPS	PURGED PRE-EVACUATED	ONE TYPE PASSED, ANOTHER FAILED	CAREFUL DESIGN REQUIRED
INTERWOUND TENSION BANDS	PURGED	PASSED ACOUSTIC & VIBRATION	FAILED FOR USE WITH PRE-EVACUATED
EXTERNAL TENSION BANDS	PRE-EVACUATED	PASSED ACOUSTIC & VIBRATION	RELIES ON FRICTION
ENVELOPE	PRE-EVACUATED	NOT TESTED	SENSITIVE TO LAY-UP DENSITY
PINS & SHINGLED BATTENS	PURGED	PASSED	FOR THIN INSULATION BLANKET
BUTTONS & STRINGS	PURGED PRE-EVACUATED	PASSED FOR PURGED SYSTEM	NOT TESTED FOR PRE-EVACUATED

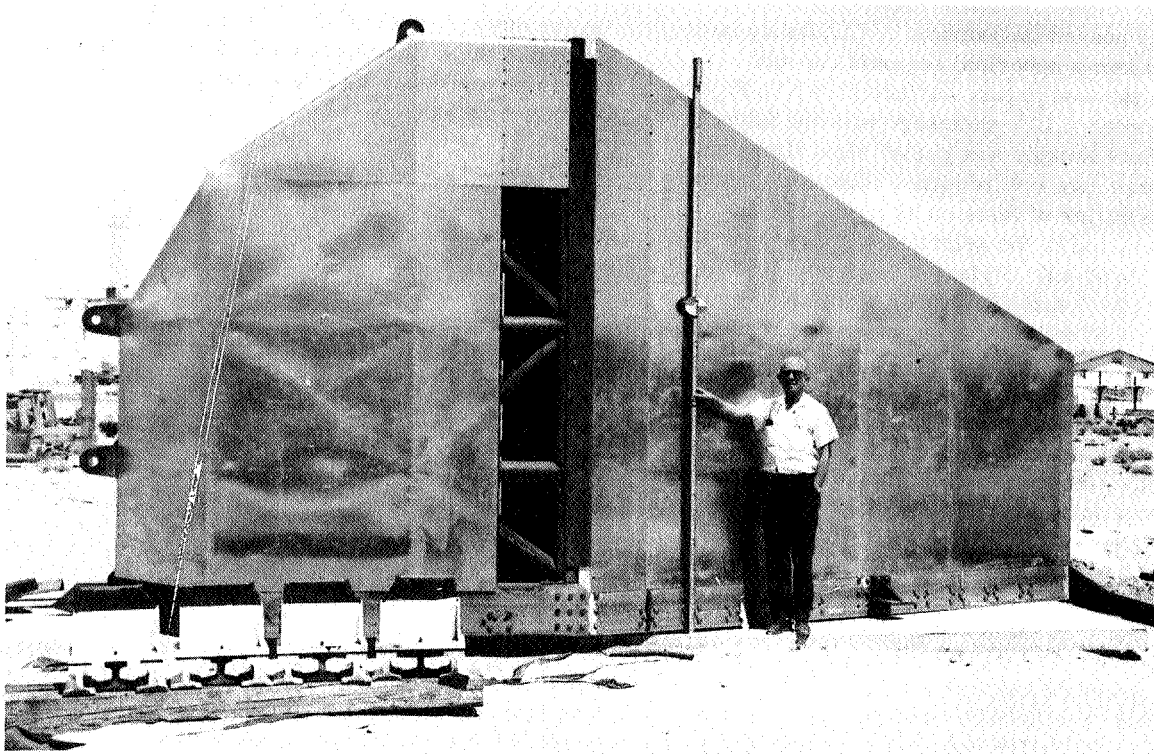


FIGURE 16. ROCKET SLED FOR TESTING FULL-SCALE INSULATION SYSTEMS

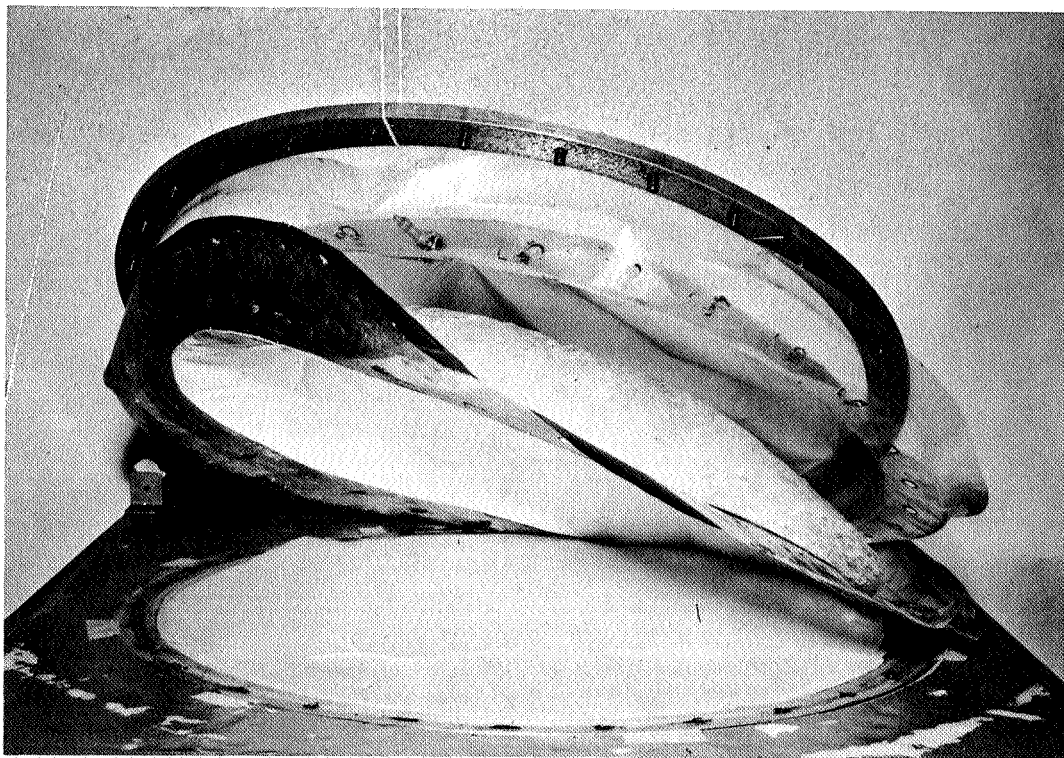


FIGURE 17. TEST SPECIMEN FOR SCREENING MATERIALS FOR FLEXIBLE VACUUM JACKET

satisfactorily passed flat-sample permeability tests were formed into a spherical segment cap and evacuated to the test fixture surface shown in Figure 17. This induced a 10% shrinkage with the attendant wrinkles. Each sample was cycled eight times and the helium leak rate was recorded after each cycle. An extensive series of tests on 30 metal-plastic laminates resulted in the selection of a laminate of 0.0127 mm (0.50 mil) Mylar, 0.0089 mm (0.35 mil) aluminum, 0.0089 mm (0.35 mil) aluminum, and 0.0127 mm (0.50 mil) Mylar as most nearly meeting the requirements of the jacket [7]. Springback data were also recorded on the fixture shown in Figure 17. The final springback test required the specimen to be evacuated for two weeks at which time the vacuum was released. The minimum acceptable springback time was three minutes.

The specimen shown in Figure 17 has two materials supplementing the basic laminated jacket material. Shown on the under side of the specimen is a layer of "two-way stretch" nylon. This layer of material prevents the formation of sharp creases when wrinkled, thus reducing the formation of pin-hole leaks and enhancing recovery characteristics.

On the outer surface of the jacket is a 5.1-cm (2.0-in.) thick fiberglass mat. This mat has the requisite resiliency to induce acceptable springback characteristics.

Figure 18 shows a nearly completed vacuum jacket for the 2.67-m (105-in.) diameter tank undergoing a pre-installation leak check. When the jacket is in place, the fiberglass mat material will be installed.

Unfortunately, the promise shown by jacket materials during specimen tests has not been realized in applications to test tanks. In general, these tests [5] show a lack of reliability in tank seams and a tendency for the development of tiny leaks that are very difficult to trace. For this reason, flexible vacuum jackets cannot now be considered sufficiently developed for application to a spacecraft.

Purge jackets are somewhat less demanding in their requirements. They must be relatively leak tight, capable of withstanding a small differential pressure, and have some means incorporated to allow the insulation to be evacuated by the vacuum of space. In addition, the jackets should be durable and easily installed.

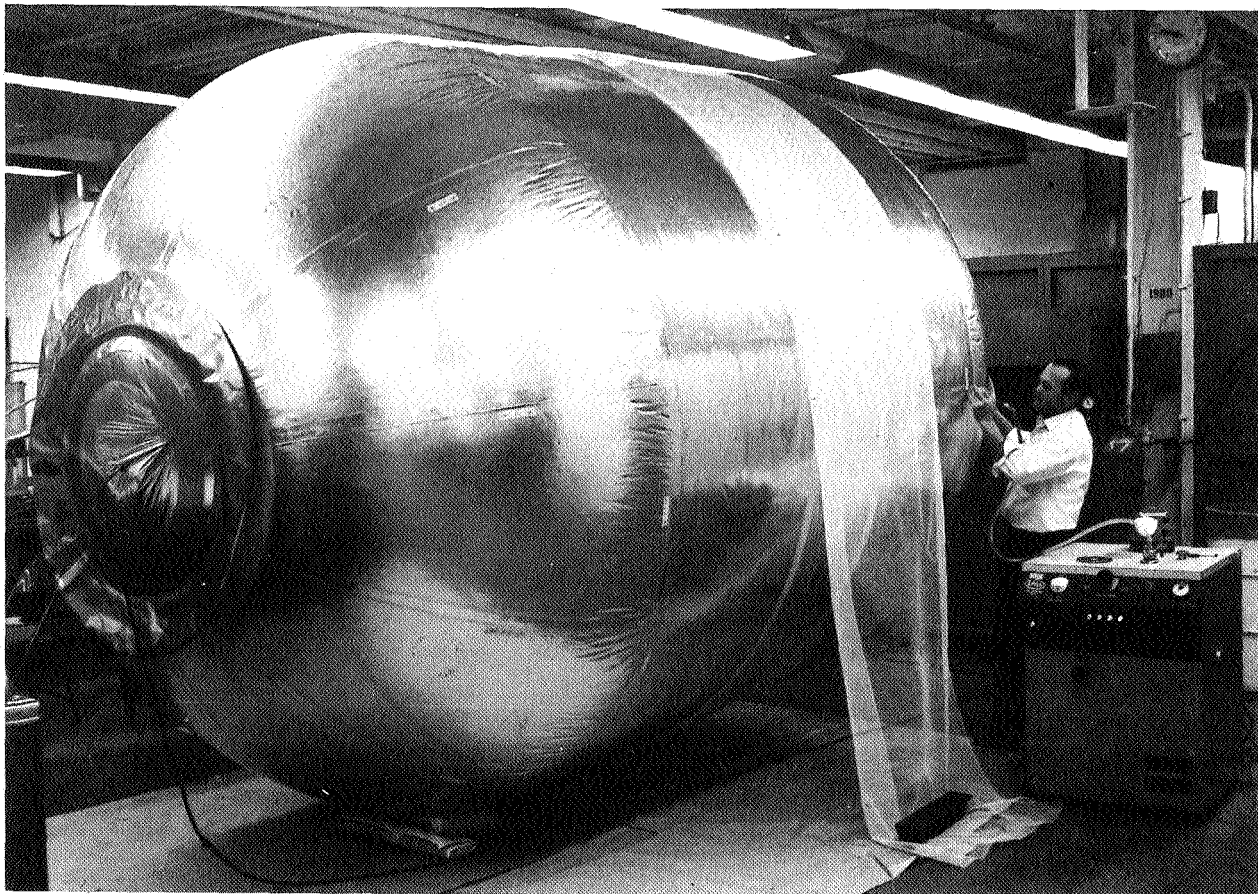


FIGURE 18. FLEXIBLE VACUUM JACKET FOR THE 2.67-m (105-in.) DIAMETER TANK

A purge jacket for the 2.67-m (105-in.) diameter tank is shown in Figure 19. This jacket, developed under contract to MSFC, is made of a polyurethane coated dacron cloth. It is installed by simply zipping it together along the seam shown in Figure 19. Incorporated in the zipper seam is a device which allows the jacket to unzip at a preset pressure differential of about  $3450 \text{ N/m}^2$  (0.5 psi).

## CONCLUSIONS

The need for high performance insulations on spacecraft cryogenic tanks has not affected the basic shape or materials of the tank to a significant

degree. Structural supports for cryogenic tanks, particularly for very long missions, need careful consideration and will use nonmetallic structures or possibly more sophisticated means such as retractable supports. The basic configuration approach for long missions will be the nonintegral tank.

The application of high performance insulation is a challenging but not insurmountable task. In general, purged systems are much easier to support than are comparable pre-evacuated systems; however, thicker insulations have not been investigated sufficiently. Jackets for purged systems are not considered a problem. On the other hand, jackets for pre-evacuated systems have been plagued with the development of leaks during tests and do not appear to have sufficient reliability to be flightworthy.

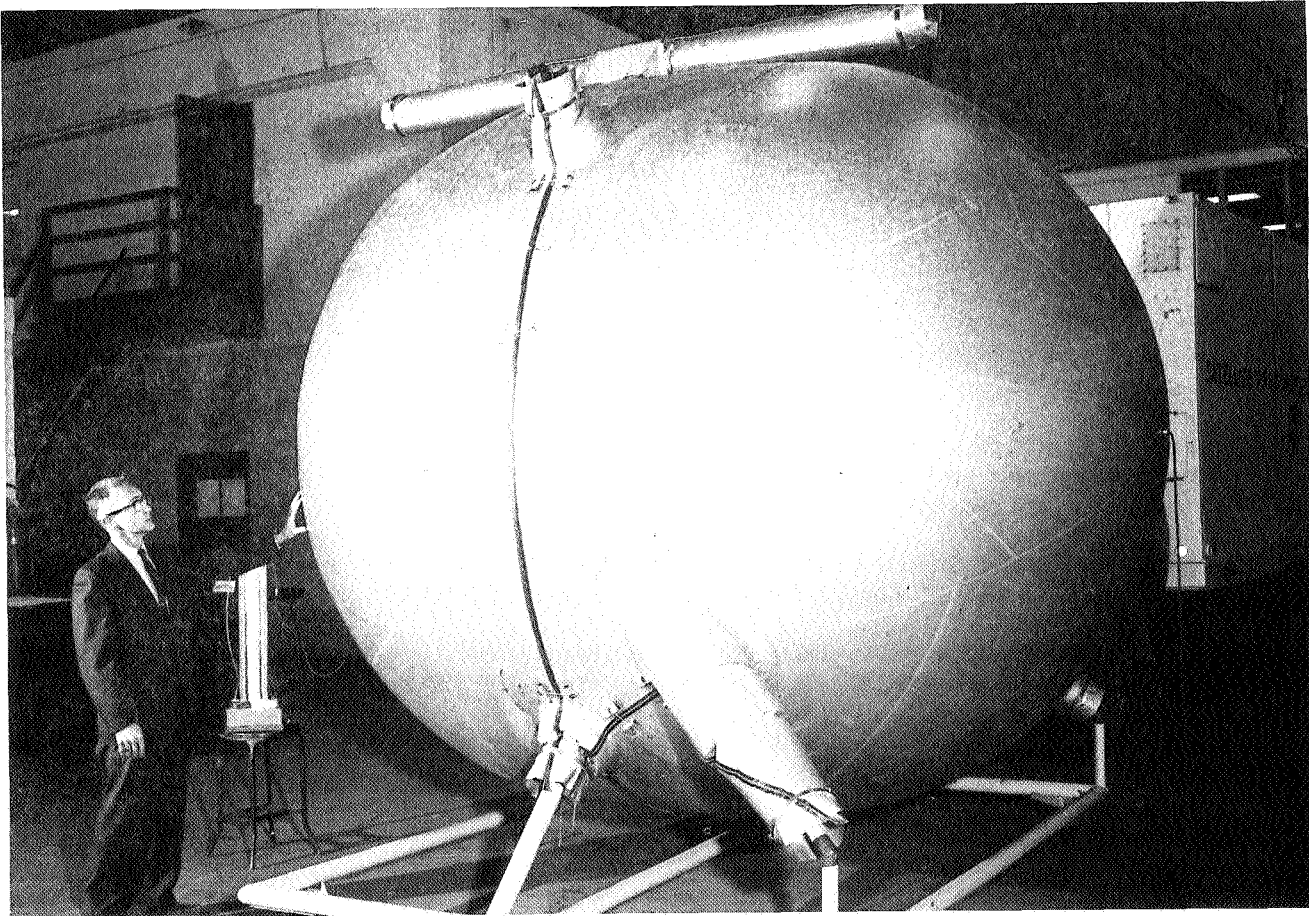


FIGURE 19. PURGE JACKET FOR THE 2.67-m (105-in.) DIAMETER TANK

## REFERENCES

1. Sturm, R. G.: Vibration Development Tests of Aluminum-to-Stainless Steel Couplings. Technical Memorandum R-3-65-5, Brown Engineering Company, Inc., March 31, 1965.
2. Sterbentz, W. H.; and Baxter, J. W.: Thermal Protection System for a Cryogenic Spacecraft Propulsion Module. Final Technical Report, Lockheed Missiles and Space Company LMSC-A794993, Volume II, November 15, 1966.
3. Design Techniques for Structure-Cryogenic Insulation Integration. Final Technical Report, Contract NAS8-5268, The Martin Company, ER 13502, October, 1964.
4. Analytical Study of Nonmetallic Parts for Launch Vehicles and Spacecraft Structures. Quarterly Progress Report Number 2, The Boeing Company, February 1967.
5. Crawford, R. F.; and Hannah, R. G.: Cryogenic Insulation Research. Final Report, Contract NAS8-11397, The Martin Company, ER 14361, September 1966.
6. Environmental Tests on Superinsulated Structural Specimens. Test Report, Contract NAS8-11414, Wyle Laboratories, ER 51401-06, October 1, 1964.
7. Shriver, C. B.: Flexible Vacuum Jacket Development. Progress Report No. 10, Contract NAS8-11376, Goodyear Aerospace Corp., GER 11706 S/9, May 5, 1965.

## BIBLIOGRAPHY

1. Swalley, F. E.; and Nevins, C. D.: Practical Problems in Design of High-Performance Multilayer Insulation System for Cryogenic Stages. Advances in Cryogenic Engineering, Volume 10, Plenum Press, 1965.
2. Cody, J. C.; and Hyde, E. H.: Thermal Problems Associated with the Development of a Flight Configured Cryogenic Insulation System. Proceedings of the Conference on Long-Term Cryo-Propellant Storage in Space, NASA/MSFC, October 1966.
3. Burge, G. W.: System Effects on Propellant Storability and Vehicle Performance. Final Technical Report AFRPL-TR-66-258, Douglas Aircraft Company, Inc., DAC-59314, October 1966.
4. Program for the Evaluation of Structural Reinforced Plastic Materials at Cryogenic Temperatures. Final Report, Contract NAS8-11070, Goodyear Aerospace Corp., GER 12792, August 31, 1966.
5. Cryogenic Storage System Study (AES Payloads) Program. Technical Final Report, Contract NAS8-20272, The Boeing Company, D2-113345-2, August 1966.
6. Getty, R. C.: Cryogenic Insulation Development. Monthly Progress Reports, Contract NAS8-18021, General Dynamics (Convair).

# CRYOGENIC INSULATION MANUFACTURING TECHNOLOGY

By

Iva C. Yates, Jr.

## SUMMARY

This paper describes manufacturing techniques and processes used to apply high performance multilayer insulation systems to flight type cryogenic tanks. The methods used in the application of a helium purged concept and a pre-evacuated concept are reported, and the problems associated with each concept are discussed.

It is concluded from these application studies that manufacturing technology is available for the application of high performance insulation systems to cryogenic tanks for short term space storage. Additional studies are needed to more completely assess the effect of manufacturing methods on thermal performance and to develop insulation systems for long term storage of cryogenics in space.

## INTRODUCTION

The producibility of high performance multilayer insulation systems is of primary concern to designers of advanced space vehicles requiring storage of cryogenic fluids. Even in the preliminary design phase the designer must have an evaluation of the availability and adequacy of manufacturing technology in order to proceed confidently with the design.

The inhouse program for the development of high performance cryogenic insulation was designed to provide a basis for the evaluation of proposed concepts for extended orbital, lunar, and planetary missions. The program has been carried out under the direction of a working group composed of structural, thermal, materials and manufacturing engineers. The procedure generally followed in evaluating a concept consists of a number of screening tests on calorimeters, test fixtures, and small-scale tanks to obtain preliminary data on the thermal and structural performance followed by application to a large-scale tank for complete thermal testing. Application methods and techniques are developed in the process to achieve the most workable solution that will meet the design objectives.

## INITIAL PRODUCIBILITY STUDY

At the beginning of the program in 1962, it was decided that a study of the practical problems associated with the application of an high performance insulation system should be carried out inhouse. A simplified cryogenic test tank, 1.78 m (70 in.) in diameter by 4.01 m (161 in.) long, was designed and fabricated to serve as a test article for the application of multilayer insulation systems. The tank shown in Figure 1 has fiberglass support rods, manhole cover, concentric fill, drain, and vent lines, and an instrumentation pole.

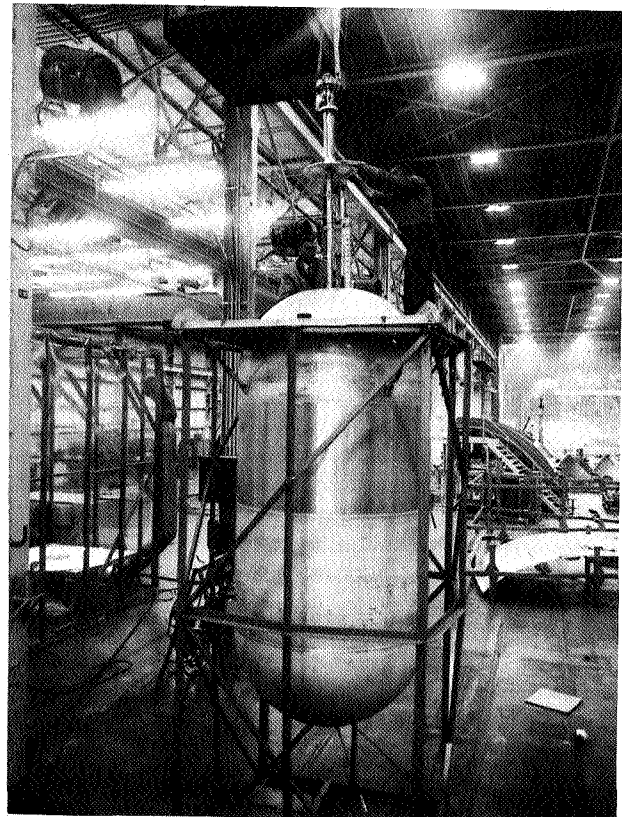


FIGURE 1. 1.78-m (70-in.) DIAMETER CRYOGENIC TEST TANK

Contracts were awarded to Linde Division of Union Carbide Corporation and National Research Corporation for the design of insulation systems to be applied to the tank at Marshall Space Flight Center by NASA personnel. The design concepts were synthesized from available technology developed primarily for application to storage vessels and transportable dewars. The insulation systems were designed for typical acceleration, vibration, acoustic, and thermal environments although the tank was not designed for dynamic testing.

The Linde SI-62 insulation system was selected for application to the tank. This insulation system consisted of alternate layers of aluminum foil, 0.006 mm (0.00025 in.) thick, and microglass-fiber paper, 0.05 mm (0.002 in.) thick, encased in a flexible vacuum jacket made of a laminate of mylar-aluminum-mylar. The insulation was applied to the cylindrical part of the tank using a wrapping technique, and the bulkheads, piping and structural supports were insulated by interleaving separate layers of glass-fiber paper and aluminum foil into the cylindrical insulation. The flexible vacuum jacket was partially pre-fabricated and then assembled on the insulated tank using contact adhesives. Major problem areas were: insulation of penetrations, fabrication of the flexible vacuum jacket, and evacuation of the insulation.

A ground hold test of the insulated tank was attempted using liquid hydrogen; however, because of a failure of the vacuum jacket around the vent line, the test was aborted before meaningful data could be obtained. Although the thermal test was a failure, the objective to evaluate available technology and identify areas requiring additional research and development was accomplished. Recommendations were made to do additional work on insulation application, to evaluate materials and adhesives, to develop improved techniques for fabricating flexible vacuum jackets, and to evaluate methods of improving the evacuation of the insulation and leak detection of the vacuum jacket. As a result, the inhouse program was greatly expanded to investigate these areas. Flight type cryogenic tanks, 2.67 m (105 in.) in diameter by 3.18 m (125 in.) long, were designed and fabricated and a program was initiated to develop high performance insulation systems for a 96 hour mission.

## APPLICATION OF HELIUM PURGED CONCEPT

The first system selected for application to one of the flight type 2.67-m (105-in.) diameter tanks

was a helium purged concept using NRC-2 [6.35- $\mu$  (1/4-mil) crinkled aluminized mylar] insulation. Preliminary concepts were applied to models of components such as piping penetrations and structural supports to evaluate attachment techniques and structural integrity when exposed to the acoustic and vibration environments. The final design consisted of battens of NRC-2 insulation wrapped around the tank and mechanically attached to aluminum support pins adhesively bonded to the tank.

The general manufacturing plan for application of the insulation is outlined in Figure 2 and details of the major steps are as follows:

### 1. Fabricate Major Battens.

Insulation battens were prefabricated from 8 sheets of aluminized mylar bonded together at intervals of about 0.48 m (19 in.) along one edge with a thermo plastic tape adhesive. A complete batten assembly consisted of 6 battens of 8 sheets making a total of 48 layers of insulation. Each of the 6 battens was cut to a different width so that when assembled on the tank, a shingled effect is achieved as shown in Figure 3. The 8 sheets of insulation in each batten were bonded together at the same interval forming a thin, tough area in which holes were punched for attachment to the support pins. The hole spacing was determined by actual measurement of the spacing of the pins bonded on the tank. The hole spacing was increased on successive battens to allow for the build-up in thickness.

### 2. Install Support Pins.

The location of the support pins was laid out on the tank and each location was etched and cleaned. The pins were bonded to the tank using the room temperature curing NARMCO 7343 adhesive. A vacuum bag was arranged over the pins so that atmospheric pressure provided the clamping force during the curing period.

### 3. Install Insulation Battens on Tank.

The tank was then installed in the assembly fixture as shown in Figure 4. The driving end was attached to the tank by bolting it to the manhole fitting and a rubber faced ring engaged the lower bulkhead for support. Arc measurements of the distance between pins were taken and transferred to the insulation battens. Holes were punched through the bonded area of the battens with a standard 0.635-cm (1/4-in.) diameter paper punch. The battens were rolled up, transferred to the tank, and installed over the pins. The battens,

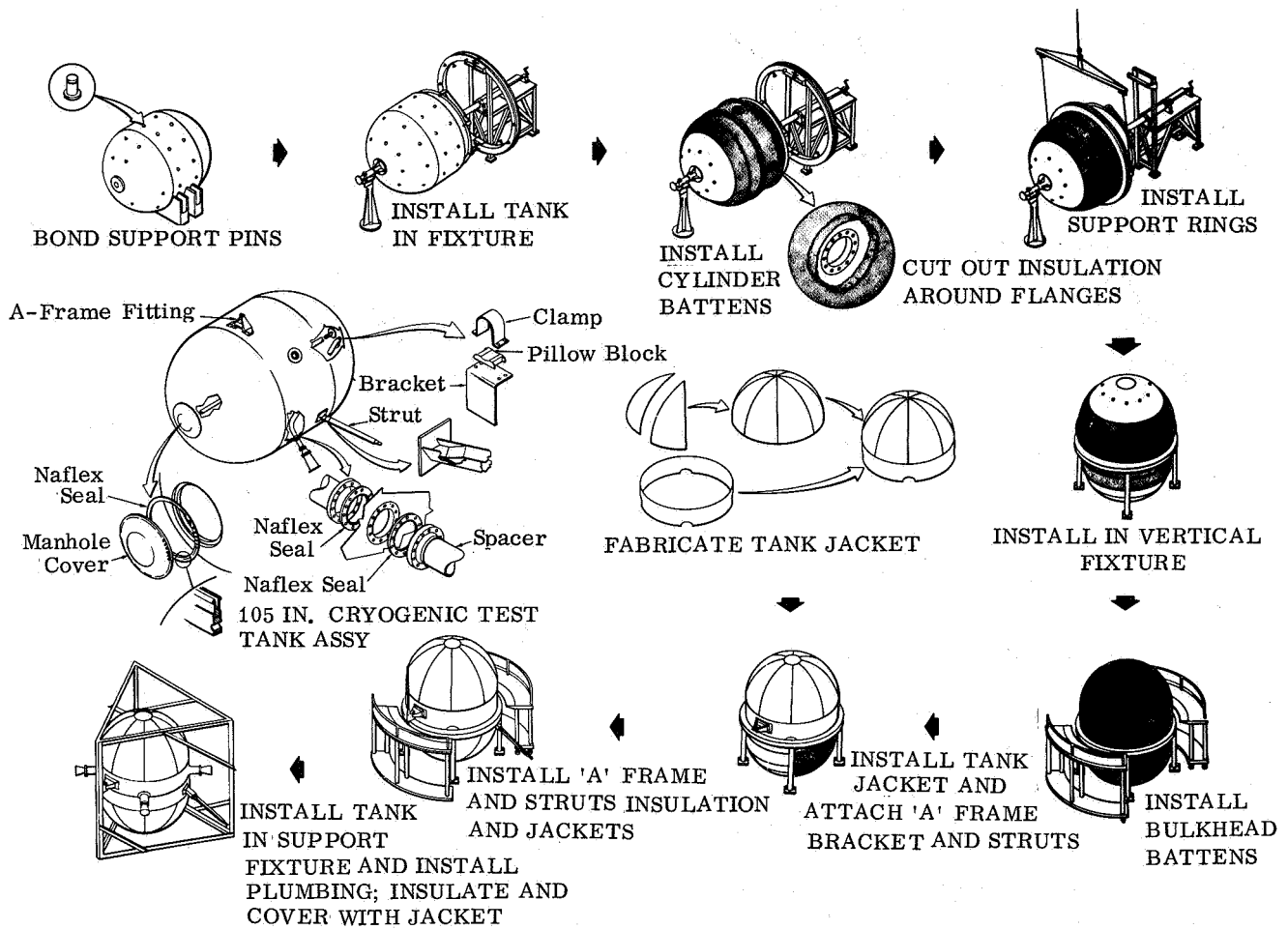


FIGURE 2. MANUFACTURING PLAN, HELIUM PURGED NRC-2 CONCEPT

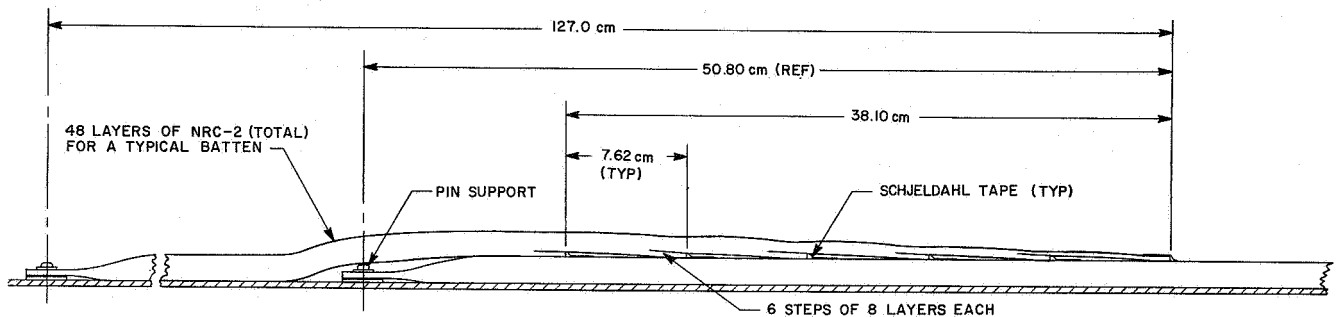


FIGURE 3. TYPICAL BATTEN STEP-DOWN

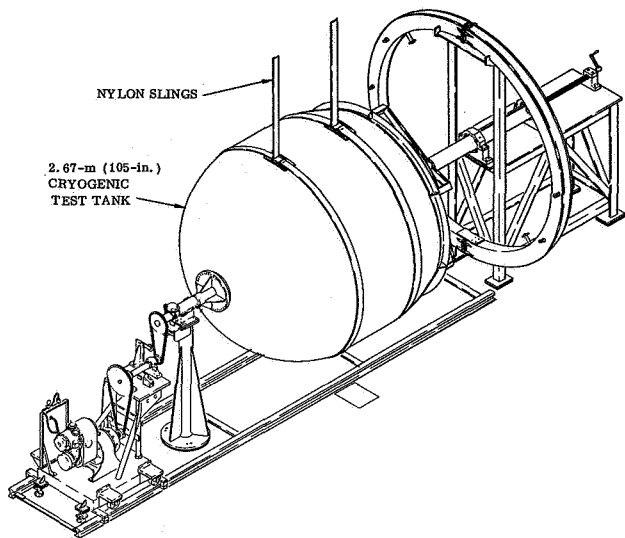


FIGURE 4. INSTALLATION OF CRYOGENIC TEST TANK IN ASSEMBLY FIXTURE

rectangular in shape, had excess material in the areas covering the bulkheads. The excess material was tucked, folded and taped. The location of each of the tucked and folded areas was staggered to control the build up as successive battens were installed. When the last batten was installed over a pin, an E-ring was used as a permanent fastener. Holes 90 degrees apart were cut in the insulation around the center of the cylindrical part of the tank to expose the fittings for the piping penetrations. The handling ring was attached to the tank at these points in order to remove the tank from the assembly fixture (Fig. 5). The tank was then installed in the vertical assembly fixture where the bulkhead insulation was installed.

4. Purge Jacket Fabrication and Installation.

The purge jacket was made of transparent mylar film  $127\mu$  (5 mils) thick. The bulkhead portions of the jacket were made of vacuum formed gore sections and assembled with a contact adhesive. A short cylindrical section was bonded to each bulkhead cap forming a complete jacket half. The two jacket halves were then installed on the insulated tank while it was in the vertical assembly fixture (Fig. 6).

5. Installation of Tank in Support Frame.

A lifting lug was attached to the manhole fitting and the tank was supported by an overhead crane while the handling ring was detached. The

structural supports were attached to the tank and the tank was installed into its support frame.

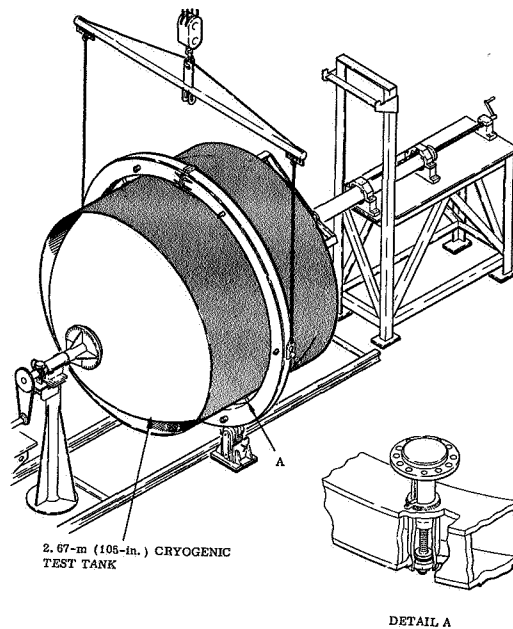


FIGURE 5. REMOVAL OF CRYOGENIC TEST TANK FROM ASSEMBLY FIXTURE

6. Insulation of Piping and Structural Supports and Completion of Purge Jacket.

The insulation was cut back around the four piping penetrations and three structural supports. Precut insulation battens were installed around the piping and structural supports and interleaved into the insulation installed on the tank. Figure 7 shows the insulation cut away from one of the pipes, and Figure 8 shows a completely insulated pipe. After all of the penetrations were insulated, the purge jacket was completed by bonding preformed transition pieces to the purge manifolds and to the main jacket. The completed job is shown in Figure 9.

The installation of NRC-2 insulation was relatively straightforward and easy except for insulation of the penetrations. Interleaving of the insulation is difficult and time consuming, and it is practically impossible to maintain the desired thickness within reasonable tolerances when insulating around discontinuities. One of the main advantages

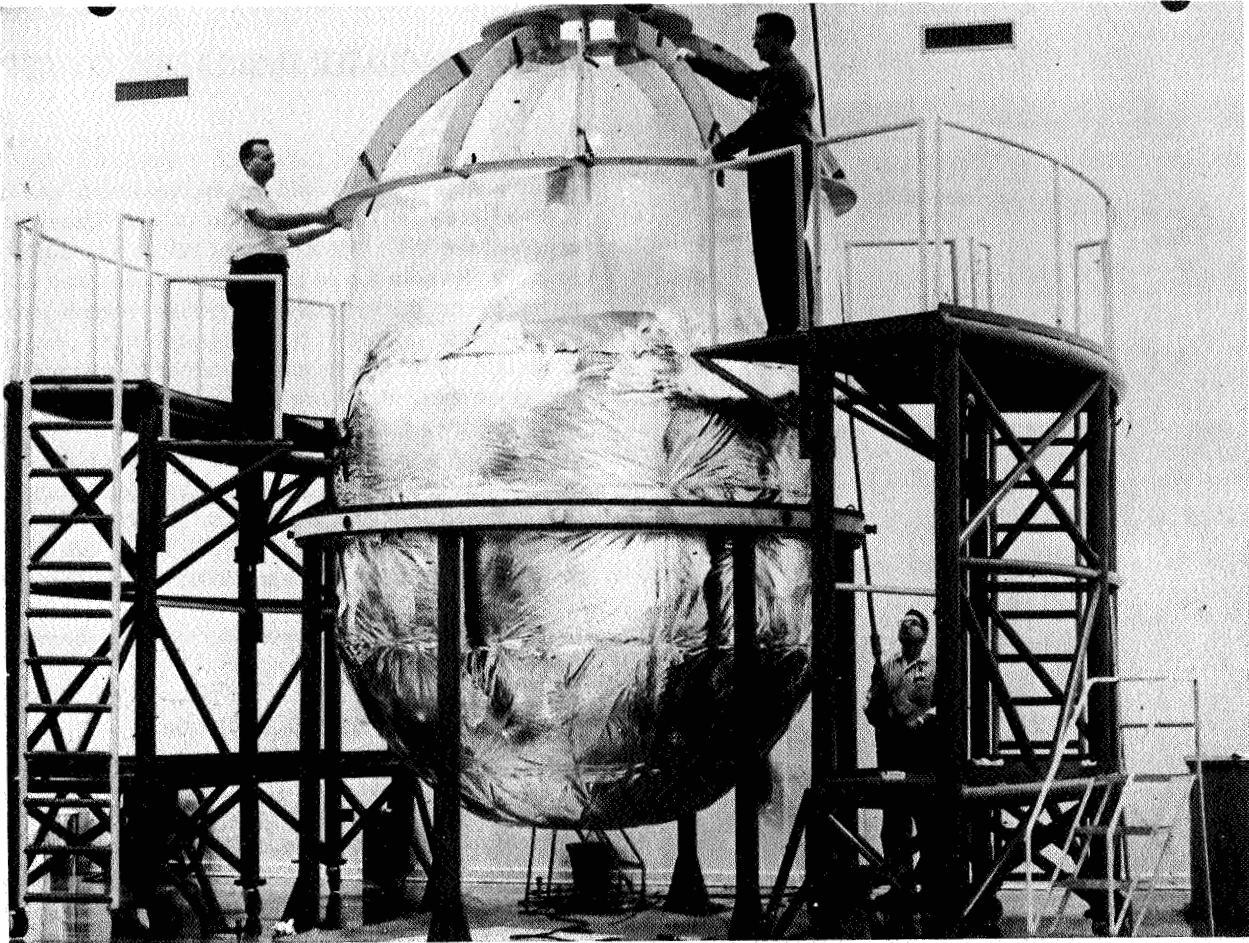


FIGURE 6. INSTALLATION OF PURGE JACKET

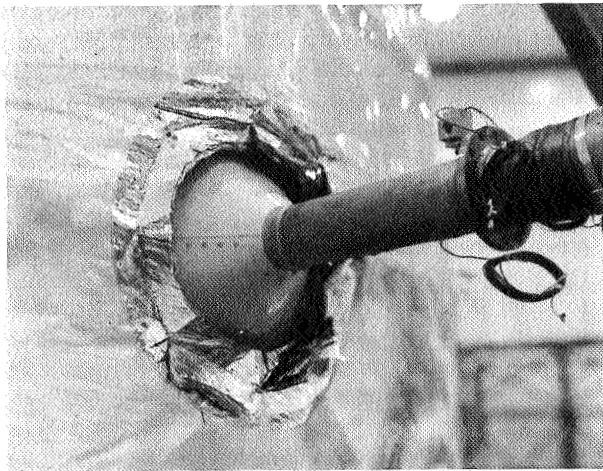


FIGURE 7. PIPING PENETRATION  
BEFORE INSULATION

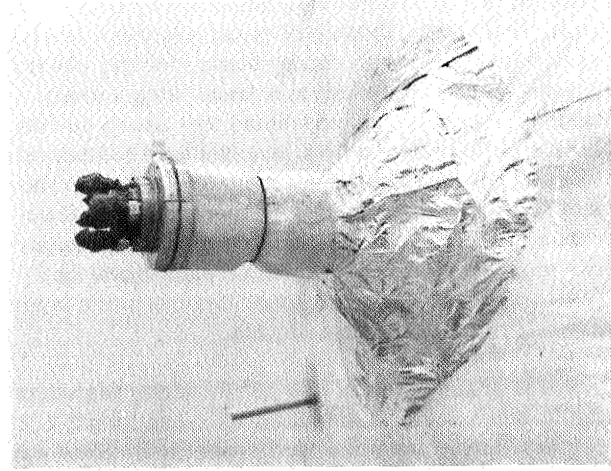


FIGURE 8. PIPING PENETRATION  
AFTER INSULATION

## PRE-EVACUATED INSULATION CONCEPT

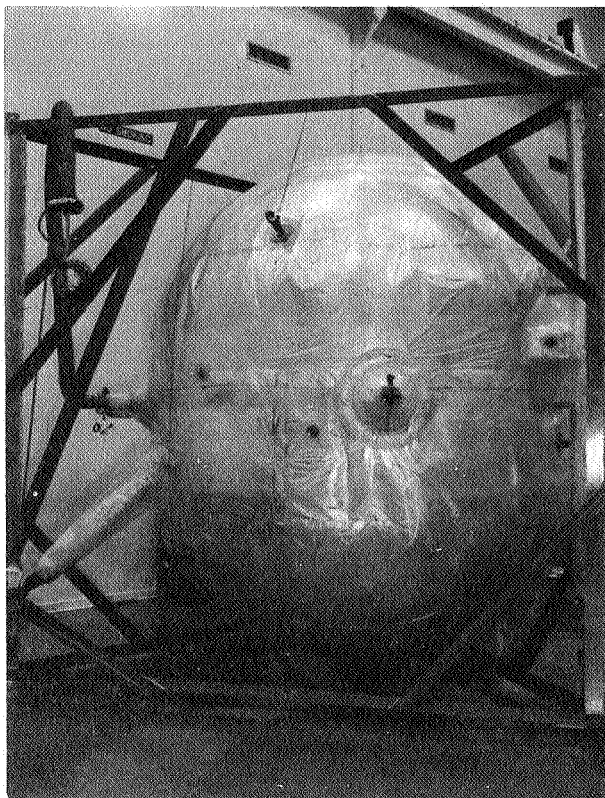


FIGURE 9. COMPLETED HELIUM PURGED INSULATION CONCEPT

of this insulation is its toughness and resistance to handling damage during application. The material should be handled only with clean cotton gloves to prevent degradation of its emissivity by oil secretions from the hands. Cutting of relatively thick layups can be done best with rotary blade electric shears. A few layers may be cut at a time using a sharp knife or scissors. It was found that sharp cutouts should be terminated by a punched hole to prevent tearing. Some problems were experienced in the fabrication and installation of the purge jacket because of the relatively inflexible material. Improved purge jackets were developed on subsequent contracts where zippers and other devices were incorporated to facilitate installation.

The insulated tank was subsequently tested and the hydrogen evaporation loss was less than 2 1/2% per day during the simulated space test. This was satisfactory for the planned mission although the experimental performance was considerably higher than the predicted performance.

A pre-evacuated insulation concept was designed under contract with Linde for application to one of the 2.67-m (105-in.) diameter test tanks. Under this contract the major development effort was directed towards the solution of problems encountered in the initial producibility study. Flexible vacuum jacket development, effect of compression on the recovery of insulation thickness and its effect on thermal performance, methods of improving evacuation of insulation, and insulation structural support were major tasks in the program. The final design called for SI-62 (aluminum foil and glass-fiber paper) insulation encased in a flexible vacuum jacket made from a laminate of 25.4 $\mu$  mylar - 20.3 $\mu$  lead - 25.4 $\mu$  mylar (1 mil mylar - 0.8 mil lead - 1 mil mylar).

The general procedure used to apply the insulation system was as follows:

### 1. Apply Cylindrical Insulation.

The tank was set up in the assembly fixture and the rolls of insulation material were placed on either side for simultaneous wrapping onto the tank as shown in Figure 10. Aluminum foil bands were bonded to the tank and two turns were wrapped on the tank while being held in tension by a band tension machine shown in Figure 11. The air actuated brake on the aluminum foil roll can be adjusted to obtain the desired tension in the bands. These tension bands are wrapped onto the tank simultaneously with the insulation and prevent it from telescoping or sagging. After the tension bands were attached and the tension was properly adjusted, the aluminum foil and glass-fiber paper were taped to the tank with pressure sensitive tape, and the wrapping process was started. Periodically, thickness measurements were made, and the band tension was adjusted as needed to control the density. After the required 70 layers of insulation were installed, the insulation was cut off and taped down. An additional two wraps of the tension bands were made and then bonded in place. During the wrapping process holes were cut in the insulation to allow it to pass over the bimetallic joints. The bimetallic joints (aluminum fitting brazed to 7.62-cm (3-in.) stainless steel tubing) were welded into the tank to eliminate the leakage problem caused by bolted joints. The necessity of cutting these holes was a difficult and time consuming operation. The completed cylindrical wrap is shown in Figure 12, with the fittings installed for attachment of the handling ring.

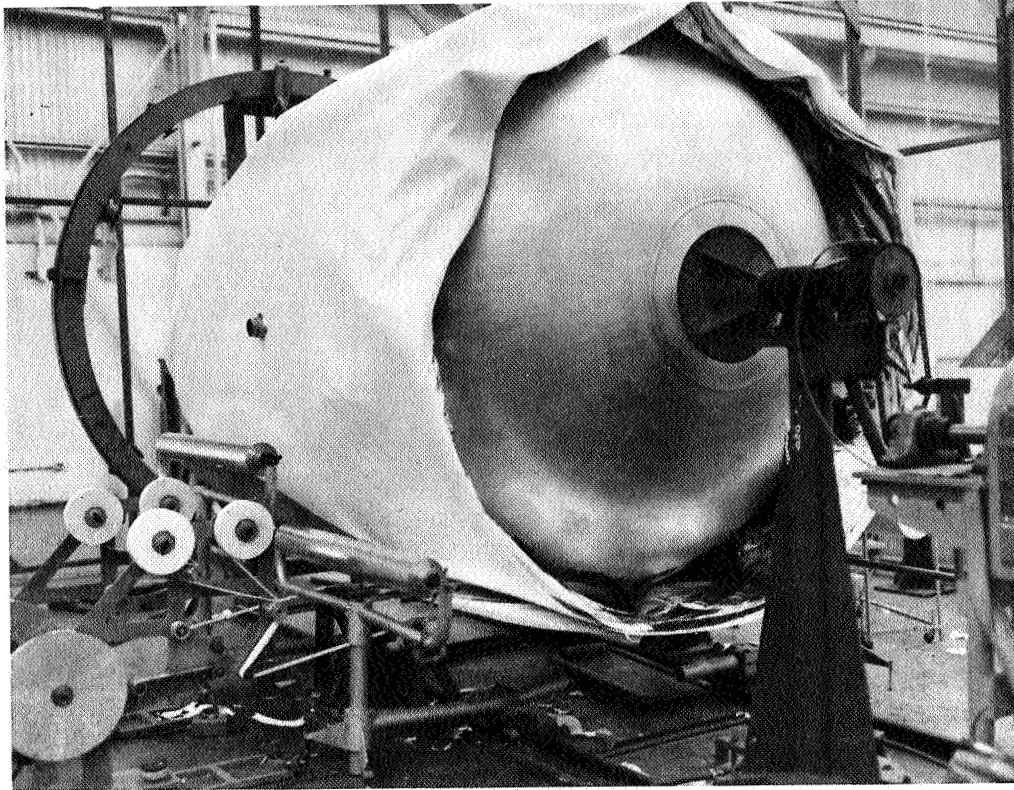


FIGURE 10. WRAPPING OF LINDE SI-62 INSULATION

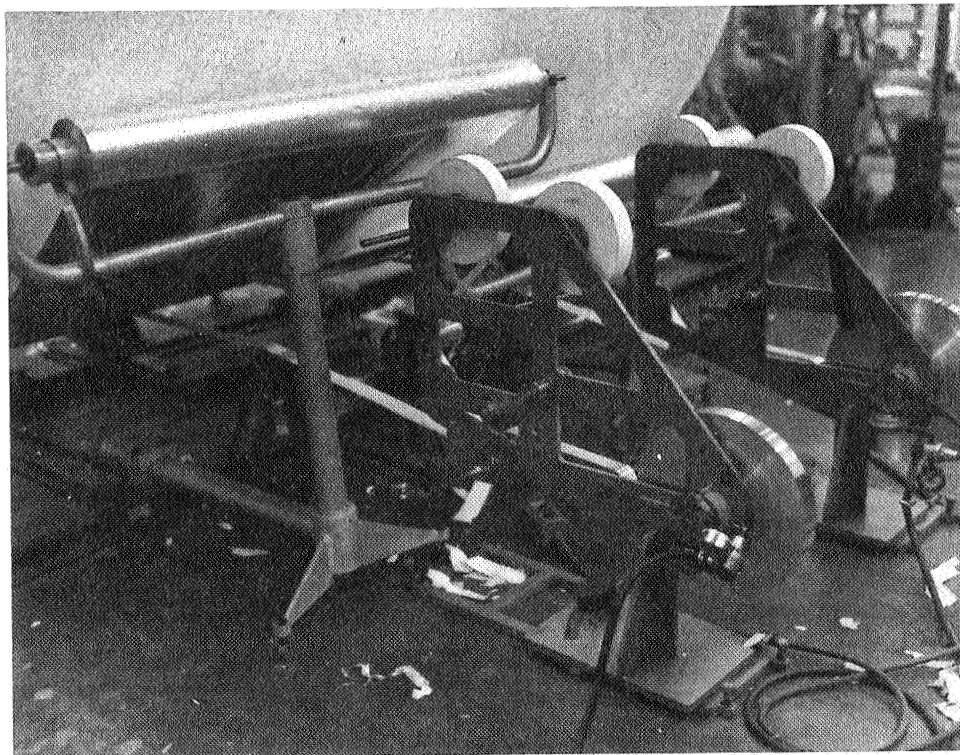


FIGURE 11. BAND TENSION MACHINES

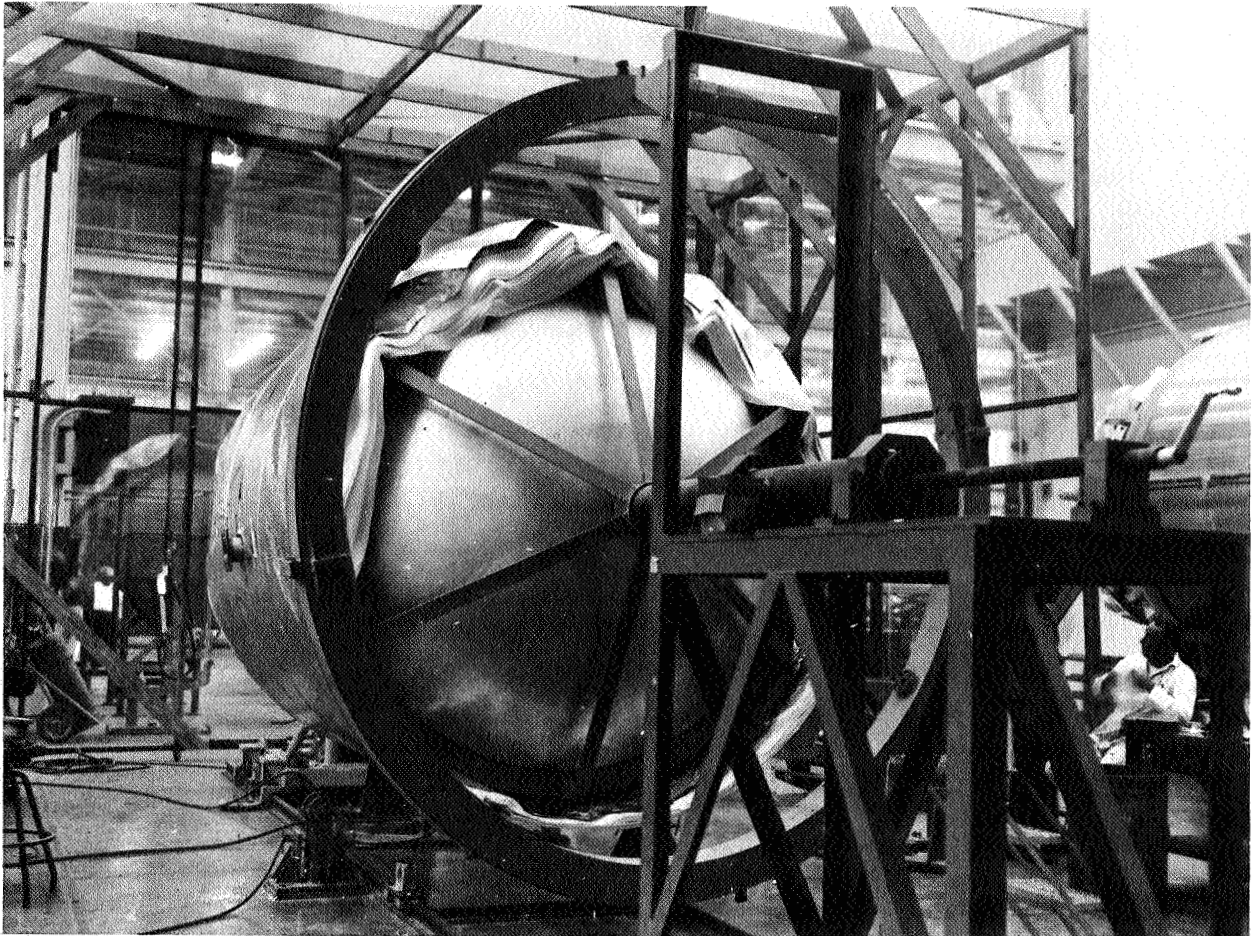


FIGURE 12. COMPLETED CYLINDRICAL WRAP

## 2. Insulation Bulkheads.

The handling ring was attached to the tank to provide support so that the spider ring supporting the rear bulkhead could be withdrawn. Blankets of insulation were wrapped on an auxiliary fixture to provide the material for insulating the bulkheads. Discs 2.44 m (96 in.) in diameter were cut from these blankets and installed a layer at a time on the bulkheads. The discs of insulation were interleaved into the cylindrical wrap and taped in place. As each disc was installed a layer of foil and a layer of glass-fiber paper from the cylindrical wrap were pulled down over the disc and the excess material folded, tucked and taped. Care was taken so that there was no shorting between layers of aluminum foil. This procedure was followed on each end, the only difference being the treatment around the man-hole fitting. The completed insulation on the lower bulkhead is shown in Figure 13.

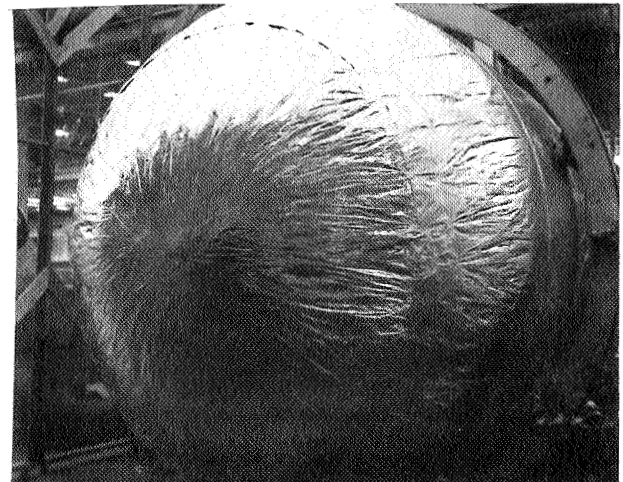


FIGURE 13. COMPLETED INSULATION ON LOWER BULKHEAD

### 3. Insulate Penetrations.

The tank was removed from the assembly fixture and installed in the support frames. The insulation around each penetration was cut back and layers of opacified paper (glass-fiber and aluminum slurry) interleaved as shown in Figure 14. After



FIGURE 14. INTERLEAVING OPACIFIED PAPER AROUND PIPING PENETRATION

the 70 layers were interleaved around the base, the penetration was helically wrapped with aluminum foil and glass-fiber paper as shown in Figure 15.

### 4. Install Flexible Vacuum Jacket.

The vacuum jacket was assembled on the tank using a portable heat sealer. Sheets of the 25.4 $\mu$  mylar - 20.3 $\mu$  lead - 25.4 $\mu$  mylar (1 mil mylar - 0.8 mil lead - 1 mil mylar) laminate were joined to form a cylinder that was in turn joined to vacuum-formed head caps. Sheet metal transition pieces over the penetrations were joined to the flexible jacket by means of a mechanical joint sealed with an O-ring. The completed vacuum jacket shown in Figure 16 was then evacuated to a pressure of about 66.7 N/m<sup>2</sup> (0.5 torr). During the evacuation process, leak tests were performed with a helium mass spectrometer. Most of the leaks were the result of handling damage. The overall permeability of the material was excellent as was the leak tightness of the heat sealed joints.

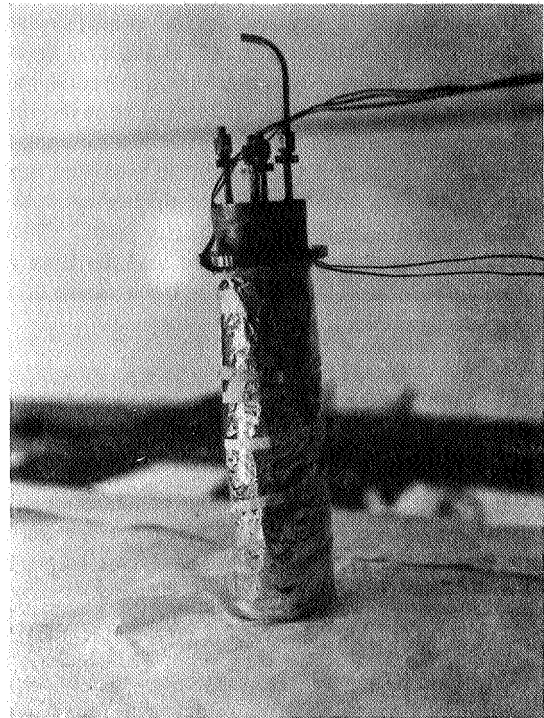


FIGURE 15. HELICALLY WRAPPED INSULATION ON PIPING PENETRATION

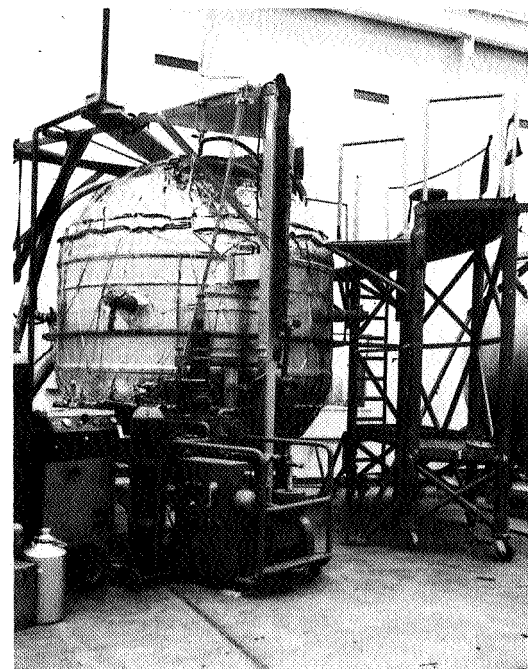


FIGURE 16. COMPLETED PRE-EVACUATED INSULATION CONCEPT

The application techniques employed were effective although improvements are needed in cutting insulation around penetrations. The advantage of fast application by the wrapping technique was nullified by having to cut holes in the insulation during the wrapping process. The requirement for interleaving insulation over bulkheads and around penetrations remained a problem. Flexible vacuum jackets were proven to be within current technology and capable of maintaining a satisfactory vacuum. A satisfactory test of the insulated tank has not been accomplished to date because of problems with a leaking manhole seal and bimetallic joint. These deficiencies have been corrected and the tank was proven to be sound. Plans have been made to test this system within the next few months.

## CONCLUSIONS

It was concluded from these application studies that the current technology is adequate for the application of high performance insulation to flight type tanks for short term space storage of cryogenic fluids.

In comparing the pre-evacuated and helium purged concepts from a manufacturing viewpoint, the helium purged concept is favored. The helium

purged concept was prefabricated to a large extent and required less time for actual application on the tank. This would result in a shorter flow time for an actual flight vehicle. The purge jacket was much less sensitive to physical damage than the vacuum jacket and was therefore more reliable. The poor conductance of compressed multilayer insulation makes evacuation a slow process. The material used in the helium purged concept was easier to handle and less sensitive to damage during application. The applied density of the pre-evacuated concept was more consistent and predictable than the helium purged concept because a spacer was used. Purged concepts with spacers probably could be applied with the same degree of consistency. Both systems can be repaired in the field although evacuation of a pre-evacuated concept would require considerably more time to repair. Quality control for both concepts would require in-process inspection and is largely dependent upon operator skill and motivation.

Additional development work is necessary to further refine the manufacturing process and to better assess the effects of manufacturing methods on thermal performance. Application of high performance insulation to large vessels as the Nuclear Vehicle for long term storage will require development of panel or modular concepts. Investigations are now underway to develop this advanced technology.

## BIBLIOGRAPHY

1. Jones, Robert G.: Purged NRC-2 Super-Insulation Installation on a 105-Inch Diameter Liquid Hydrogen Tank. Manufacturing Development Memorandum, MDM-18-65, November 1965.
2. Aberle, J. L.: Development of Techniques and Hardware for Insulation Wrappings of Cryogenic Containers. Contract NAS8-11041, November 1964.
3. Lindquist, C. R.: Super-Insulation Systems for Cryogenic Test Tank. Contract NAS8-11740, February 1966.
4. Reed, M. E.: The Development of Techniques for Insulation Wrappings of Cryogenic Containers. Contract NAS8-11042.



# DEVELOPMENT OF A COMBINED HIGH PERFORMANCE MULTILAYER INSULATION AND MICROMETEOROID PROTECTION SYSTEM

By

James M. Stuckey

## SUMMARY

The development of a combined high performance multilayer insulation and micrometeoroid protection system for cryogenic tanks in outer space is discussed. The helium purged system consists of an outer micrometeoroid bumper of polyurethane resin impregnated glass cloth and a multilayer insulation of alternate layers of double aluminized Mylar film reflective shields and thin sliced polyurethane foam spacers. The four combined concepts that have been evaluated include two concepts with and two concepts without a special ground-hold insulation section inserted between the multilayer space insulation and the tank wall. In the combined concepts the aluminized Mylar can be applied in ribbon form using a filament winding technique on tanks not much larger than 3.05 m (120 in.) in diameter. For application to larger tanks the insulation concept was panelized. Excluding the bumper, the density of the basic insulation concepts is slightly more than  $32 \text{ kg/m}^3$  ( $2.0 \text{ lb/ft}^3$ ). Thermal tests at high vacuum conditions on the filament wound insulation concept installed on a 76.2-cm (30-in.) diameter tank, in thicknesses varying from 3.0 to 5.1 cm (1.18 to 2.0 in.), showed heat leaks of approximately  $6.92 \times 10^{-5} \text{ W/m} \cdot \text{K}$  ( $4.0 \times 10^{-5} \text{ Btu/hr-ft} \cdot \text{F}$ ). The heat leak for the initial panelized concept was somewhat greater, being approximately  $1.04 \times 10^{-4} \text{ W/m} \cdot \text{K}$  ( $6.0 \times 10^{-5} \text{ Btu/hr-ft} \cdot \text{F}$ ). Tests simulating aerodynamic heating have shown that this concept can be applied externally to cryogenic tanks without requiring a protective shroud. Hypervelocity impact tests have shown that the multilayer insulation has energy adsorption capabilities and will tend to dissipate the energy of micrometeoroids that have been shattered by an outer bumper.

## INTRODUCTION

The possibilities of incorporating the insulation system needed for cryogenic tanks in outer space with the micrometeoroid protection system required for extended space missions were envisioned at this Center. Assistance was solicited from industrial organizations to develop these possibilities, and in June, 1964, program NAS8-11747 was initiated with the Goodyear Aerospace Corporation to accomplish this objective. The following are the present goals of the program:

1. The average equilibrium heat leak under high vacuum conditions shall not exceed  $0.79 \text{ W/m}^2$  ( $0.25 \text{ Btu/ft}^2\text{-hr}$ ) and should be approximately  $0.63 \text{ W/m}^2$  ( $0.20 \text{ Btu/ft}^2\text{-hr}$ ).
2. The mass of the complete system shall be less than  $2.44 \text{ kg/m}^2$  ( $0.5 \text{ lb/ft}^2$ ).
3. The composite concept shall be capable of preventing or instantaneously sealing a penetration of a particle in the mass range of  $10^{-1}$  to  $10^{-5} \text{ g}$  impacting at a velocity of 9150 m/sec (30 000 ft/sec) or greater.
4. When applied externally to a launch or space vehicle, the composite concept shall give reliable service under conditions of prelaunch, launch, and space flight.
5. The composite concept shall be capable of withstanding surface temperature up to  $505^\circ \text{K}$  ( $450^\circ \text{F}$ ) for short times during the aerodynamic heating portion of flight.

6. The composite concept shall be capable of being reliably applied to the external surface of launch vehicles that are 10 m (33 ft) in diameter or larger.

7. The composite concept shall allow reliable application to tanks with irregular surface protruberances such as fuel lines, skirt sections, and instrument tunnels.

2. Aluminized Mylar was selected for the radiation shields to obtain light mass and have low conductivity along the shield.

3. For a spacer material between the multi-layer reflective shields, thin sliced foams are one of the lightest materials that can be used and also possess energy adsorption characteristics.

## MULTILAYER INSULATION SYSTEMS

### COMBINED SYSTEM DESIGN AND MATERIAL SELECTION

The four insulation concepts developed in this program were derived from the following considerations:

1. From hypervelocity impact test data and information in literature, the bumper wall was displaced approximately 5.1 cm (2 in.) from the tank wall to allow adequate spreading and adsorption of the shattered micrometeoroid particles that penetrate the bumper.

Flat plate calorimeter screening tests using liquid hydrogen and high vacuum conditions were employed to select the foam spacer material to be used. Variables investigated were types of foam, foam spacer thickness, sample thickness, and surface pressure (compaction). The results of these tests are graphically summarized in Figure 1. The data show that thermal performance was affected by the type of foam, foam thickness, and pressure on the sample. Several of the foams gave essentially the same results. A red polyurethane foam was selected because of its availability commercially in sliced sheets. This material at a density of 27.2 kg/m<sup>3</sup> (1.7 lb/ft<sup>3</sup>) is available in nominal 0.762-mm (30-mil) thick, 1.22 by 3.66 m (4 by 12 ft) sheets. The broken cells on the surface afford gas passage through the sheet and minimal contact resistance.

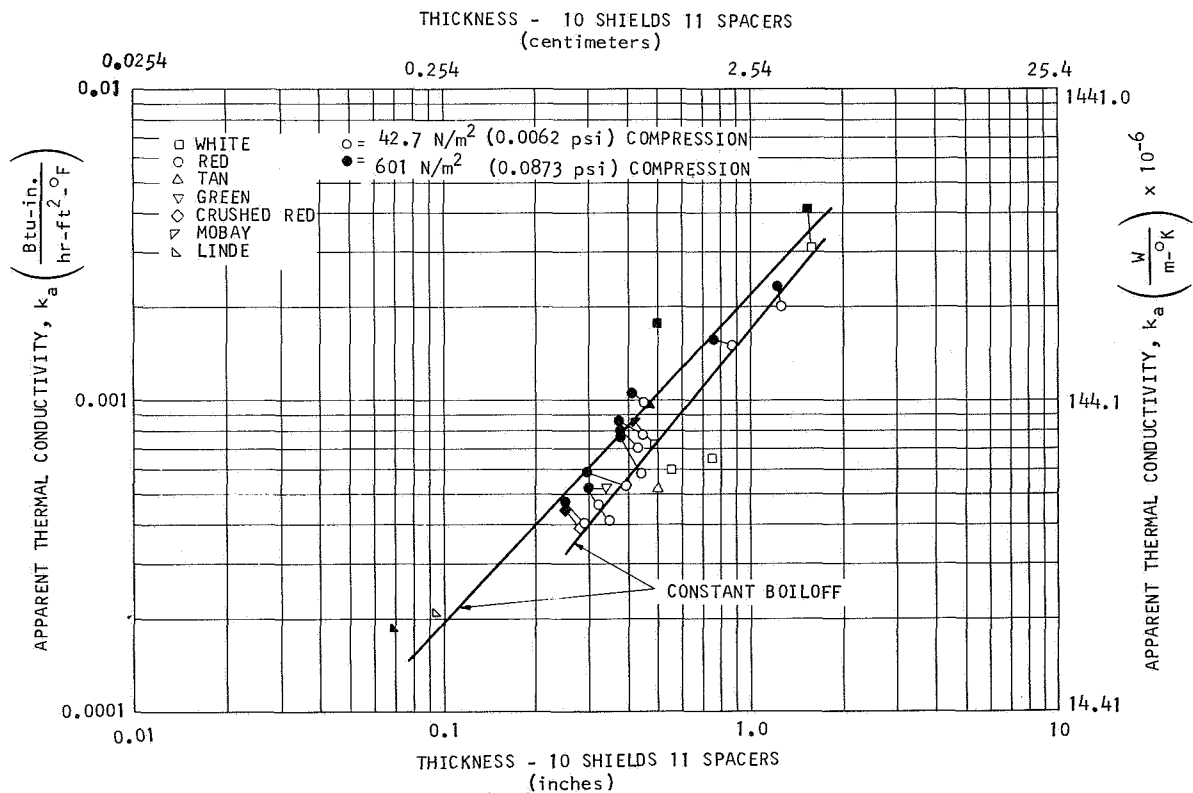


FIGURE 1. FOAM SCREENING ON FLAT PLATE CALORIMETER

INSULATION CONCEPTS INVESTIGATED

The four insulation concepts investigated in this program to date are briefly summarized in Figure 2. For all multilayer systems a dry gas purge is required to protect the aluminized Mylar radiation shields from the degradation effects of moisture. The first concept represents an optimum system for both ground-hold and high vacuum performance. However, there is little or no confidence that a completely leak proof vacuum bag can be consistently fabricated and installed on tanks or that a leak proof vacuum bag will remain in that condition throughout testing until launch. On this basis, sealed-cell Mylar-honeycomb core is bonded directly on the tank for the ground-hold insulation in the second concept. The need for a ground-hold section is based primarily on how close to launch the liquid hydrogen can be replenished. In some cases the liquid hydrogen tanks are topped off shortly before lift-off, thus there is a minimum requirement for a ground-hold section. On this assumption, the ground-hold insulation section was deleted from the third concept. In the fourth concept the third insulation concept was panelized and applied in two approximately 2.54-cm (1.0-in.) thick panels.

INSULATION CONCEPT	GROUND-HOLD SECTION	SPACE SECTION	BUMPER WALL
GAC-1	VACUUM BAG OVER ELEVEN SHIELD-SPACER COMBINATIONS	37 SHIELD-SPACER COMBINATIONS	RESIN IMPREGNATED GLASS CLOTH
GAC-2	SEALED-CELL MYLAR CORE	SAME	SAME
GAC-3	FULL INSULATION THICKNESS IS HELIUM PURGED	48 SHIELD-SPACER COMBINATIONS	SAME
GAC-4	SAME	2 PANELS OF 24 SHIELD-SPACER COMBINATIONS	SAME

FIGURE 2. INSULATION CONCEPTS EVALUATED ON 76.2-cm DIAMETER END-GUARDED CALORIMETER

The first composite insulation concept is described more thoroughly in Figure 3. In this system the lower eleven reflective shield-spacer combinations were encased in a vacuum jacket for the ground-hold insulation. The space insulation is the same as that in the ground-hold section, and consists of alternate layers of double aluminized 6.35- $\mu$  (1/4-mil) Mylar and thin foam spacers. The bumper wall consists of 0.375-mm (15-mil) 181 fiberglass cloth impregnated with approximately 17% polyurethane resin.

At this low resin concentration, gases readily pass through the bumper wall. The calculated mass for this system is approximately 2.28 kg/m<sup>2</sup> (0.468 lb/ft<sup>2</sup>). The third insulation concept is exactly like the first concept except that the vacuum bag has been deleted. On this basis the calculated mass for this system is approximately 1.98 kg/m<sup>2</sup> (0.405 lb/ft<sup>2</sup>). The panelization of the third concept was designated as the fourth insulation concept. In insulation concepts 1, 3, and 4, 48 layers of foam spacer-aluminized Mylar were employed.

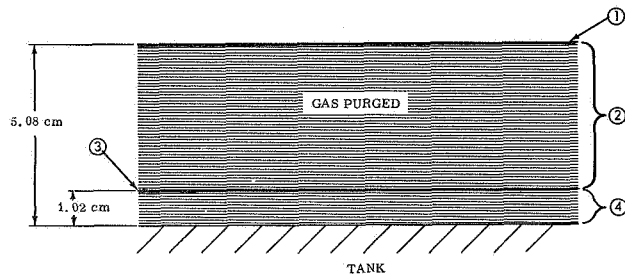


FIGURE 3. COMPOSITE INSULATION SYSTEM GAC-1

Legend for Figure 3:	lb/ft <sup>2</sup>	kg/m <sup>2</sup>
① Micrometeoroid Bumper [0.0381-cm (0.015-in.) fiberglass cloth impregnated with polyurethane resin]	0.100	0.488
② Micrometeorite Spacer and Multilayer Space Insulation 37 Radiation Shields [6.35- $\mu$ (1/4-mil) aluminized Mylar] 37 Insulation Spacers [0.089-cm (0.035-in.) thick polyurethane foam]	0.067	0.327
③ Vacuum Jacket [0.00635-cm (0.0025-in.) MAAM film with nylon backing]	0.168	0.820
④ Sealed Multilayer Insulation 11 Radiation Shields [6.35- $\mu$ (1/4-mil) aluminized Mylar film] 11 Insulation Spacers [0.089-cm (0.35-in.) thick polyurethane foam]	0.020	0.0976
	<u>0.050</u>	<u>0.244</u>
<b>Total Mass</b>	<b>0.468 lb</b>	<b>2.28 kg</b>

The second insulation concept, shown in Figure 4, differs from the first concept only in the ground-hold insulation. In the second concept a 1.02-cm (0.4-in.) thick sealed-cell Mylar-honeycomb substrate replaced the 1.02-cm (0.4-in.) vacuum jacketed multilayer section. This system was heavier with a mass of approximately 2.38 kg/m<sup>2</sup> (0.483 lb/ft<sup>2</sup>).

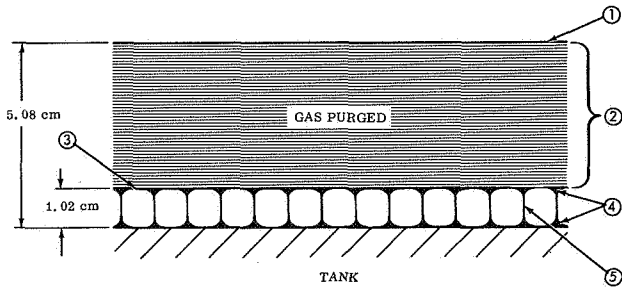


FIGURE 4. COMPOSITE INSULATION SYSTEM GAC-2

Legend for Figure 4:

	lb/ft <sup>2</sup>	kg/m <sup>2</sup>
① Micrometeorite Bumper [0.0381-cm (0.015-in.) fiber-glass cloth impregnated with polyurethane resin]	0.100	0.488
② Micrometeorite Spacer and Multilayer Space Insulation 37 Radiation Shields [6.35-μ (1/4-mil) aluminized Mylar] 37 Insulation Spacers [0.089-cm (0.035-in.) thick polyurethane foam]	0.067	0.327
③ Substrate Seal Layer [0.00635-cm (0.0025-in.) MAAM film]	0.018	0.088
④ Polyurethane Adhesive Bond Lines (2 required)	0.060	0.293
⑤ Core Substrate [1.02-cm (0.40-in.) thick, 0.95-cm (3/8-in.) cell Mylar honeycomb, 34.1 kg/m <sup>3</sup> (2.13 lb/ft <sup>3</sup> ) density]	0.070	0.342
<b>Total Mass</b>	<b>0.483 lb</b>	<b>2.36 kg</b>

APPLICATION OF INSULATION CONCEPTS TO TEST TANK

To evaluate the insulation systems, a 76.2-cm (30-in.) diameter stainless steel double-guarded cylindrical tank was designed and fabricated to serve as a subscale tank for application tests and as a space calorimeter. The 2.03-m (80-in.) long calorimeter is shown in Figure 5. Each of the three sections is equipped with liquid hydrogen fill and vent lines. The center measuring section is 1.22-m (4-ft.) long.

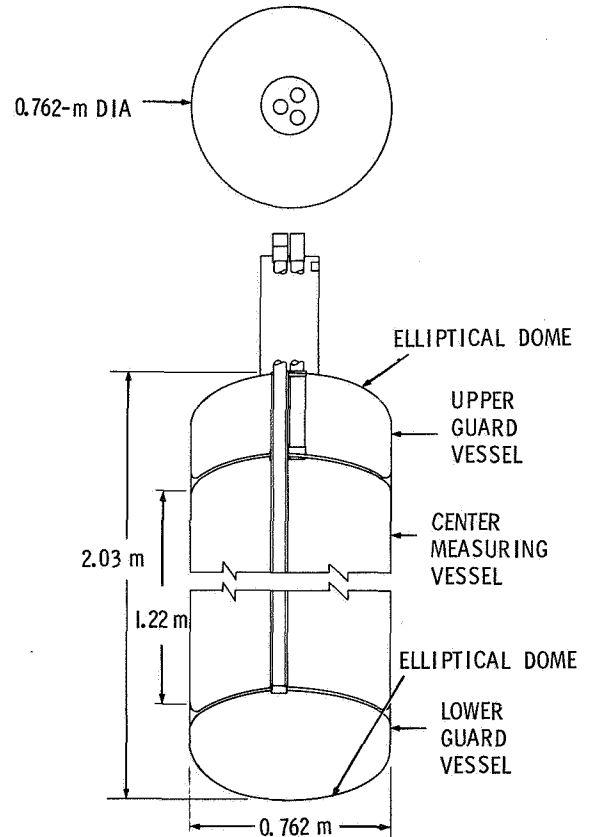


FIGURE 5. 76.2-cm DIAMETER CYLINDRICAL CALORIMETER

To apply the first three insulation concepts, the subscale tank was mounted in a filament winding machine. Installation of the foam spacer is shown in Figure 6. Spot bonding with quick drying adhesive was necessary to hold the foam in place. The foam was gored for application to the domes of the tank. The aluminized Mylar was applied by wrapping with 1.27-cm (1/2-in.) wide tape as shown in Figure 7. In the first insulation concept a vacuum jacket

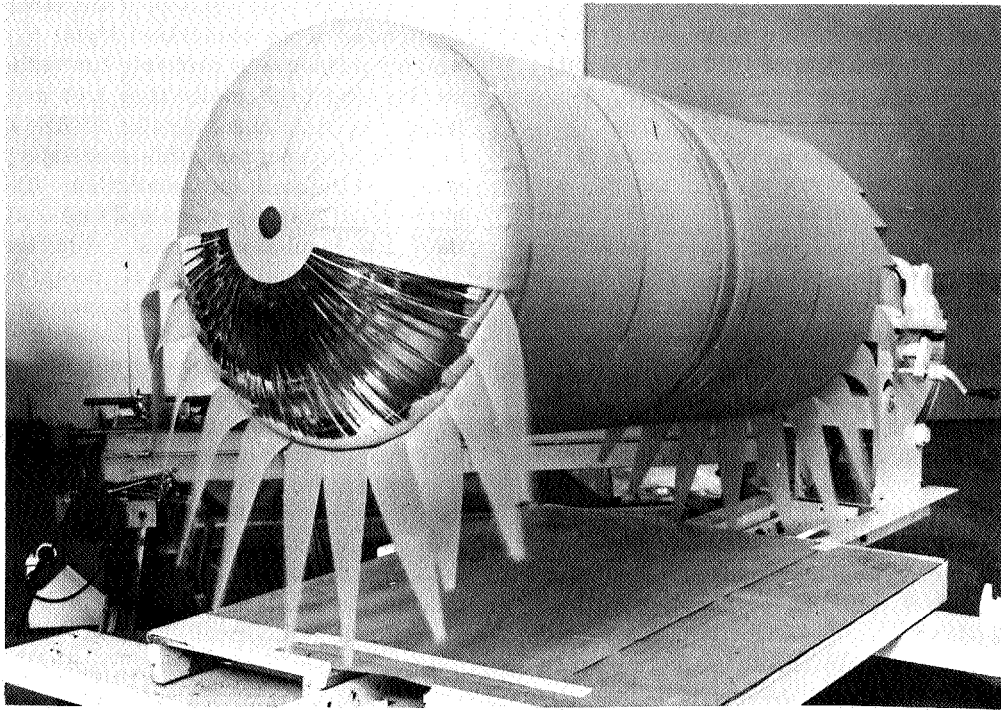


FIGURE 6. INSTALLATION OF FOAM SPACER ON 76.2-cm DIAMETER CALORIMETER

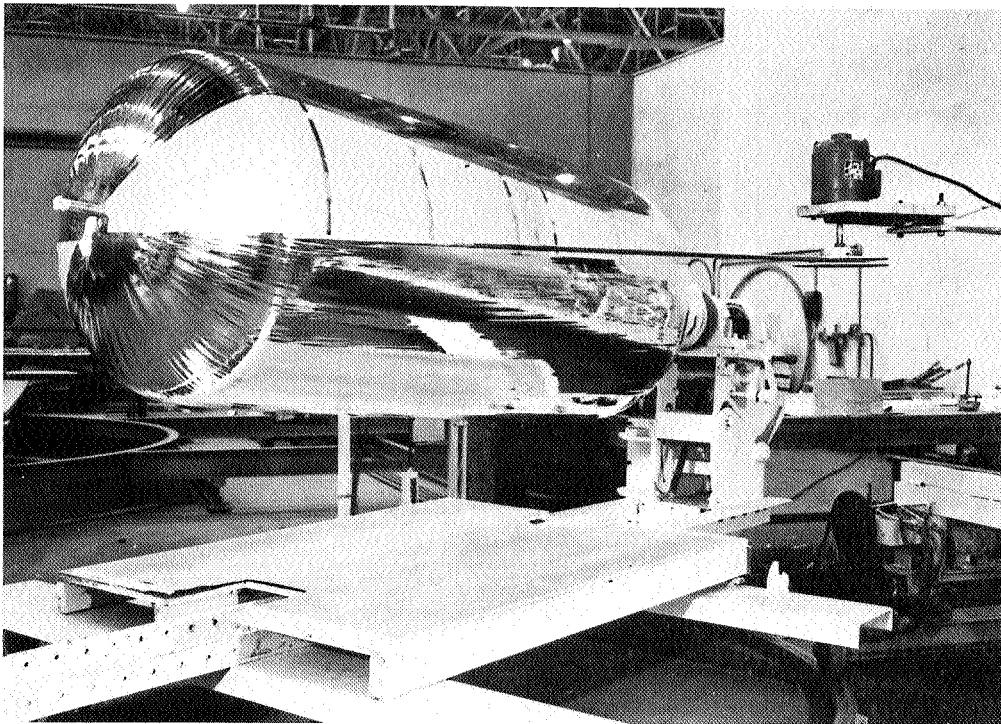


FIGURE 7. WRAP OF ALUMINIZED MYLAR OVER  
FOAM SPACER ON 76.2-cm DIAMETER CALORIMETER

fabricated with nylon back MAAM was installed over the initial 11 layers of Mylar-foam combinations. MAAM is a composite of 12.7- $\mu$  (0.5-mil) Mylar, 8.9- $\mu$  (0.35-mil) aluminum, 8.9- $\mu$  (0.35-mil) aluminum, 12.7- $\mu$  (0.5-mil) Mylar. The evacuation port for the vacuum jacketed section is located on the bottom dome (Fig. 7).

Thirty-seven layers of foam-Mylar combination were applied over the vacuum jacket. The pre-constructed bumper wall was installed as two halves over the space insulation using pressure-sensitive tape to facilitate removal.

In the second insulation concept the ground-hold insulation consisted of a 1.02-cm (0.4-in.) thick, 0.95-cm (3/8-in.) cell Mylar-honeycomb core bonded directly to the tank (Fig. 8). Thirty-seven alternate layers of aluminized Mylar and foam spacers were applied over the ground-hold insulation, and a bumper wall was added as previously described. The third insulation concept was fabricated by applying 48 alternate layers of aluminized Mylar and foam spacers and then attaching the bumper wall.

With present equipment and technology the application of the aluminized Mylar by the filament winding technique is probably limited to tanks not much larger in diameter than 3.05 m (120 in.). For large cryogenic tanks similar in size to those used in the Saturn program, this multilayer concept was panelized to facilitate installation. The panelization of the third insulation concept was designated as the fourth insulation concept. A preformed outer panel of the fourth insulation concept as shown in Figure 9 consisted of 24 alternate layers of aluminized Mylar and foam spacers between an inner and outer grid of glass fiber preimpregnated rovings spaced approximately 2.54 cm (1.0 in.) apart with an edge band picture frame of No. 181 glass cloth impregnated with epoxy resin. Load bearing phenolic washers were bonded to the edge band to serve as attachment points for installation. The bumper wall was included within the grid. The panel was held together by Dacron or nylon drop threads through the insulation; the threads were located approximately every 10.2 cm (4.0 in.) and secured to the grids on both sides.

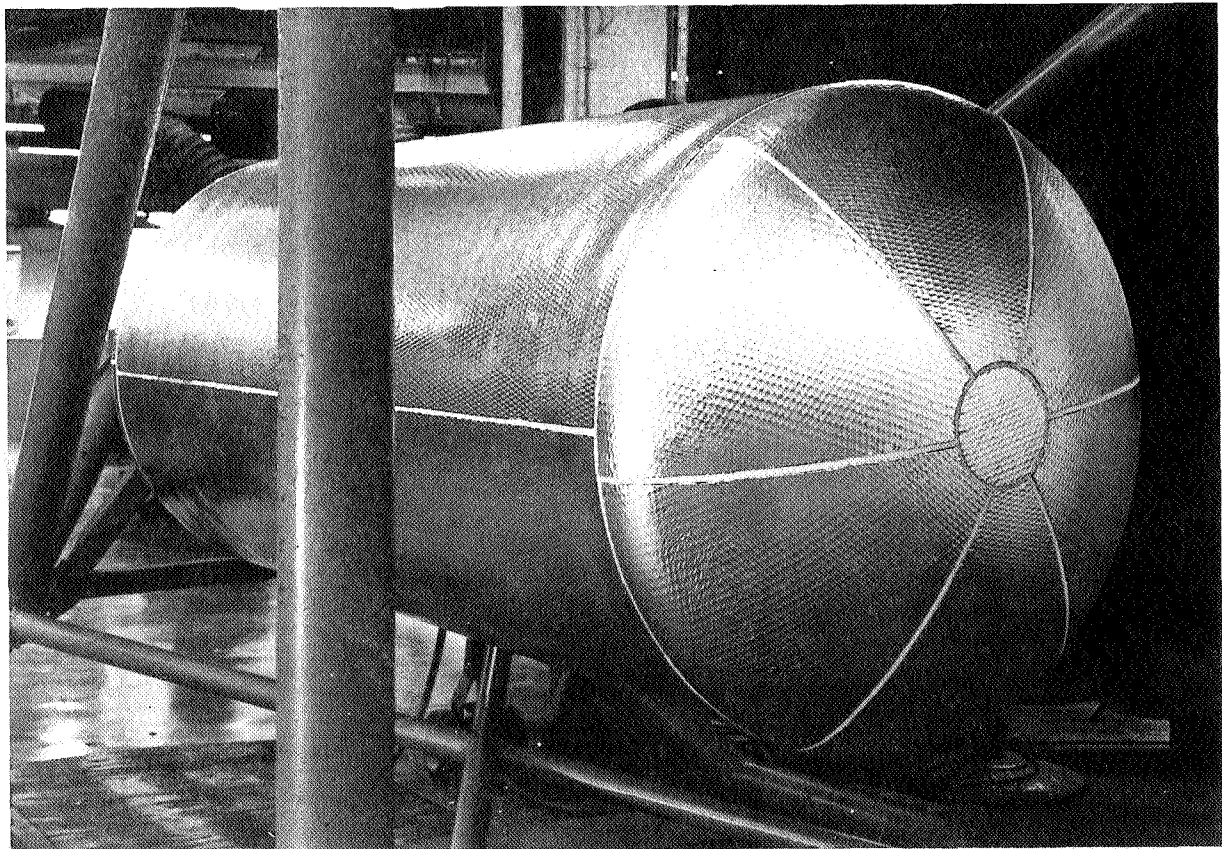


FIGURE 8. SECOND INSULATION CONCEPT: SUBPANEL ON CALORIMETER

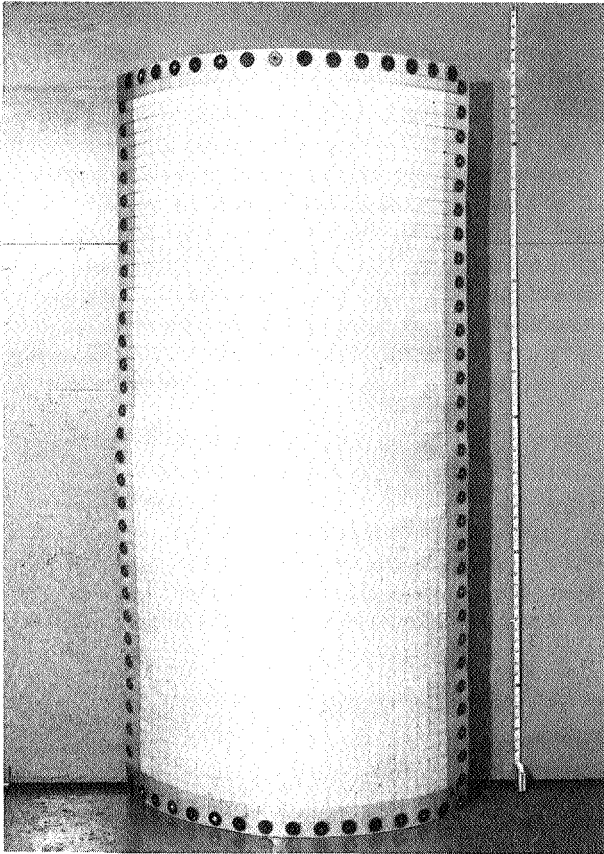


FIGURE 9. PREFORMED OUTER GAC-4 INSULATION PANEL

In the initial attempt at panelization, only the cylindrical section was considered. To save both time and money, the filament wound aluminized Mylar and foam spacers for the third insulation concept were carefully cut so that both dome ends remained intact while removing the cylindrical portion. The cylindrical section was insulated with a set of three inner panels next to the tank, and a set of three outer panels over the inner panels. The outer panels were 10.2 cm (4.0 in.) longer than the inner panels to provide a stepped joint with the domed ends. The insulation panels were supported vertically by a net covering the top dome. The insulation on the bottom dome was held in place by a similar net attached to the panels. The joints of the inner and outer panels were staggered to minimize the heat leaks. The completely insulated tank with the fourth panelized insulation concept is shown in Figure 10. The panels were further supported by lacing them together circumferentially.

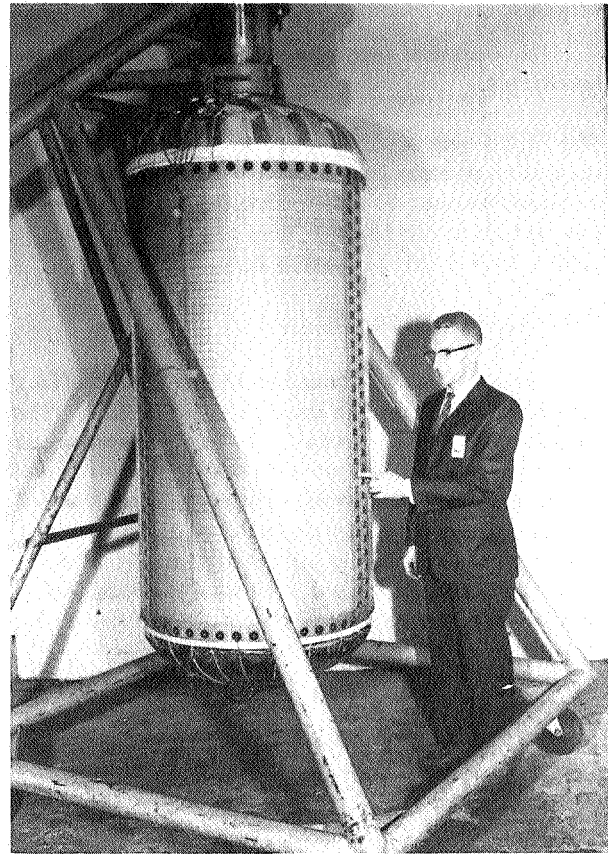


FIGURE 10. INSULATION SYSTEM GAC-4 COMPLETELY INSTALLED ON CALORIMETER

## TESTS ON INSULATION SYSTEMS

### TEST PROCEDURE AND FACILITIES

Insulation composite systems attached to the 76.2-cm (30-in.) diameter cylindrical test tank were evaluated by subjecting the tank filled with liquid hydrogen to the following sequence and minimum conditions:

1. Boiloff measurements under high vacuum conditions.
2. Five liquid hydrogen fill and drain cycles using a helium purge in the multilayer space insulation to simulate ground testing.
3. Simulated aerodynamic heating cycle combined with atmospheric pressure decay.

4. Boiloff measurements under high vacuum conditions.

The liquid hydrogen test facility used to test the insulation system is shown in Figure 11. The vacuum chamber is equipped with a heater to simulate aerodynamic heating, and can be evacuated to  $1.33 \times 10^{-4}$  N/m<sup>2</sup> ( $10^{-6}$  mm Hg).

GROUND-HOLD TESTS

Results of the ground-hold tests for the four insulation concepts are presented in Table I. The data showed that essentially the same thermal performances were obtained with the first, third, and fourth insulation concepts, and approached that of helium. These results together with other data showed that the vacuum jacket used in the first insulation concept leaked, and thus three of the insulation concepts were practically the same.

The second insulation concept differed from the first insulation concept in having a ground-hold insulation section consisting of sealed-cell Mylar-honeycomb core. The performance of this insulation concept with a helium purge reduced the boiloff of hydrogen considerably, and the boiloff was even lower when a dry nitrogen purge was substituted for helium. After the second concept was exposed to 14 ground-hold tests and two simulated aerodynamic heating tests, there was no indication that the sealed-cell Mylar-core ground-hold insulation section had been damaged or adversely affected.

TEMPERATURE, PRESSURE AND BOILOFF DURING SIMULATED ASCENT CYCLE

At the end of a ground-hold test, a simulated aerodynamic heating cycle was performed while evacuating the test chamber. Temperature profiles for simulated ascent cycles for the third and fourth

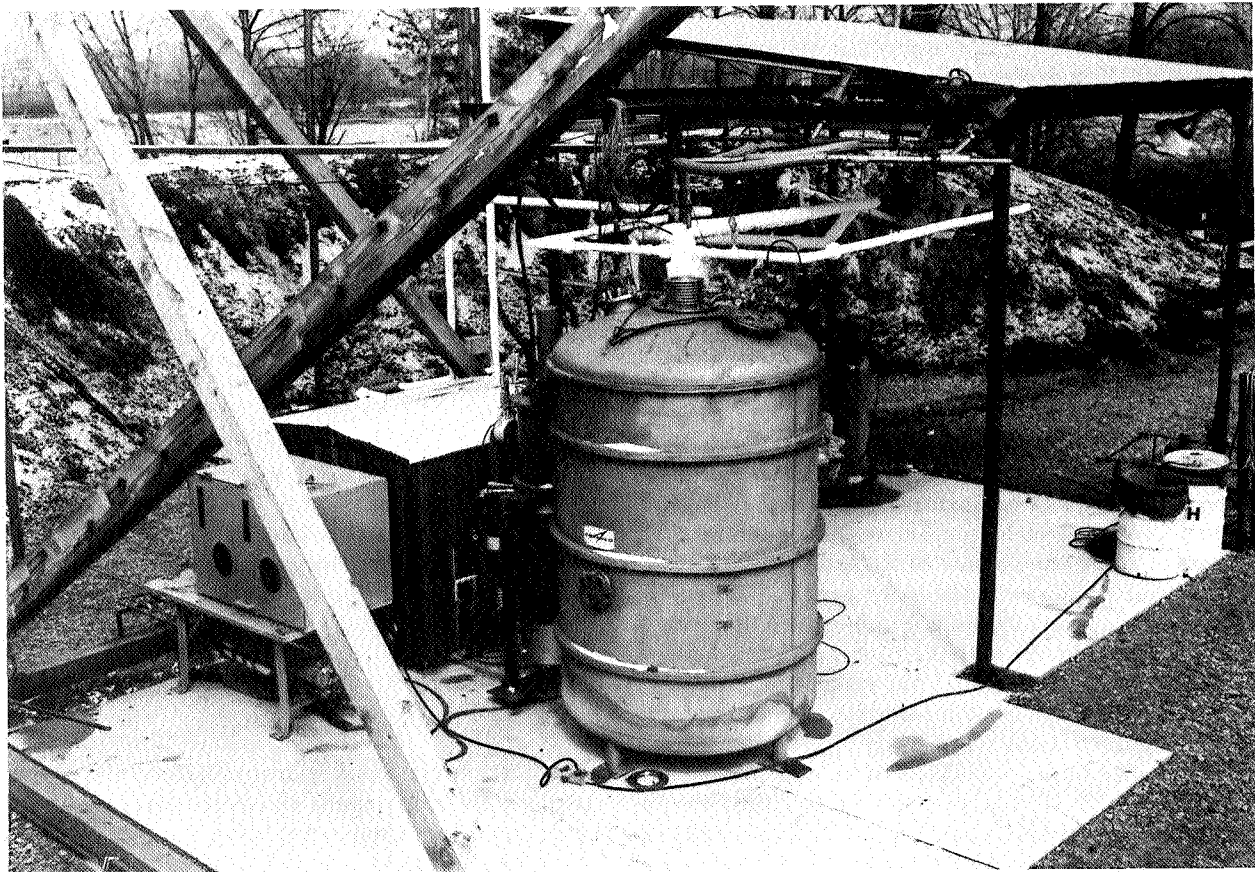


FIGURE 11. LIQUID HYDROGEN TEST FACILITY

TABLE I. THERMAL PERFORMANCE OF HELIUM PURGED INSULATION CONCEPTS

Insulation System	No. of Tests	Purge Gas	Outer Surface Temperature °K (°F)	$\dot{q}$ W/m <sup>2</sup> (Btu/hr-ft <sup>2</sup> )	$k \times 10^{-2}$ W/m <sup>2</sup> ·°K (Btu/hr-ft·°R)
GAC-1	5	He	252 to 231 (-6 to -43)	274 - 322 (87 - 102)	6.40 - 7.44 (3.7 - 4.3)
GAC-2	6	He	253 to 244 (-4 to -22)	208 - 252 (66 - 80)	4.50 - 5.71 (2.6 - 3.3)
	4	N <sub>2</sub>	272 to 280 (30 to 44)	129 - 148 (41 - 47)	2.60 - 2.94 (1.5 - 1.7)
GAC-3	5	He	244 to 238 (-20 to -32)	318 - 341 (101 - 108)	7.26 - 7.79 (4.2 - 4.5)
GAC-4	5	He	236 to 228 (-35 to -50)	372 - 400 (118 - 127)	9.00 - 9.70 (5.2 - 5.6)
	1	He	214 (-75)	304 (96.5)	7.95 (4.6)

insulation concepts are shown in Figure 12. These results show that the tests reached the desired 505°K (450°F) maximum temperature somewhat later than will be encountered in flight, and that the surface did not cool off as fast as expected in space.

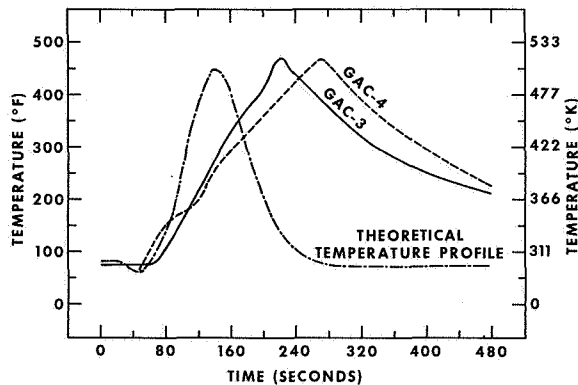


FIGURE 12. TEMPERATURE PROFILES FOR SIMULATED ASCENT CYCLE

Boiloff for the simulated ascent cycles is shown in Figure 13. These tests showed that boiloff of hydrogen decreased markedly within 20 minutes. Pressure profiles during the simulated launch cycle are shown in Figure 14. These results show that a much higher vacuum had been obtained in the test chamber with the third insulation concept than with the fourth insulation concept, indicating that the filament wound concept had better venting characteristics than the panelized concept.

Examination of the insulation systems after the simulated aerodynamic heating cycles to surface temperature of 505°K (450°F) showed that the aluminized Mylar film in the outer 2 or 3 layers had been damaged. This is not considered to be a major problem because aluminized Kapton film can be substituted for the aluminized Mylar film for the outer few layers.

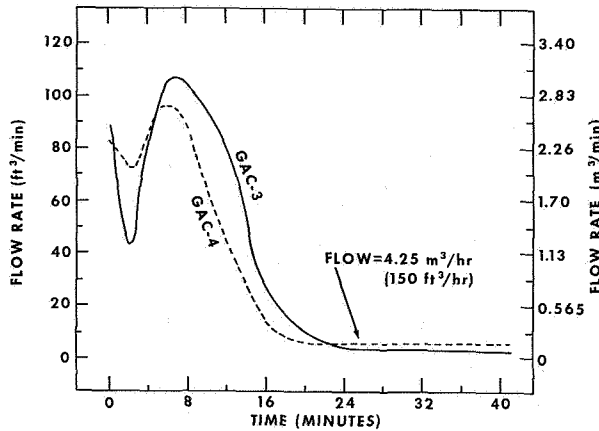


FIGURE 13. BOILOFF PROFILES FOR SIMULATED ASCENT CYCLE

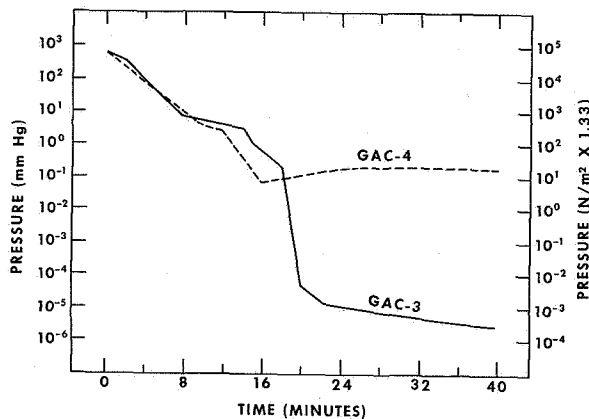


FIGURE 14. VACUUM PUMP-DOWN PROFILES FOR SIMULATED ASCENT CYCLE

INSULATION PERFORMANCE UNDER HIGH VACUUM CONDITIONS

Test results under high vacuum conditions for the first three insulation concepts on the 76.2-cm (30-in.) diameter tank for the center measuring section that is end-guarded are shown in Table II. In all cases the results reported are average values for a 24-hour period. The marked difference in performance between test 1 and 2 on the first insulation concept was attributed to a leak in the vacuum jacket for the ground-hold insulation and the inability to pump out the helium entrapped behind the vacuum jacket in a reasonable period of time.

Since the second insulation concept has a ground-hold insulation section consisting of sealed-cell Mylar core 1.02-cm (0.4-in.) thick, the effective multilayer section was only 4.06-cm (1.6-in.) thick. Under high vacuum conditions, tests have indicated that the Mylar core contributes very little to the thermal effectiveness of the multilayer insulation. Accordingly, only the multilayer section was considered in calculating test results, and on this basis there is general agreement for the results obtained for the first and second insulation concepts. For the fourth test on the second insulation concept, the tank was taken out of the test chamber and the outer 10 layers of the 37 total reflective insulation layers were removed before returning the tank to the test chamber. Space tests on this second insulation concept with only 27 reflective insulation layers showed that again a thermal conductivity value around  $6.05 \times 10^{-5} \text{ W/m} \cdot ^\circ\text{K}$  ( $3.5 \times 10^{-5} \text{ Btu/ft} \cdot \text{hr} \cdot ^\circ\text{F}$ ) was obtained. The thermal conductivities determined for the third insulation concept are essentially the same and are in general agreement with the other data on the first and second insulation concepts.

In Table III test results under high vacuum conditions are shown for the panelized fourth insulation concept. Essentially the same thermal performance was obtained during the first three tests on this insulation concept. The first two tests were run for visual observation of the panels during vacuum pump-down, and the third test followed the simulated aerodynamic heating cycle. It was expected that thermal performance would be degraded by panelization, but not to the extent encountered.

Several factors probably contributed to this greater heat leak, and the leaks caused by the longitudinal joints were suspected to be one of the major contributors because these joints passed directly across the center measuring section. To eliminate this heat leak, 5.1 to 7.6-cm (2 to 3-in.) wide strips of double aluminized Mylar were interleaved in the joints for all 24 layers in the outer panel. Test No. 4 was run on this configuration, and both the heat leak and thermal conductivity were improved some as shown in Table III. Another possible source of heat leak is the circumferential joints. These were not too good, and their proximity to the junctions of the guard tank and to the center measuring tank probably affected the results, but the extent of this effect has not been adequately determined yet.

TABLE II. THERMAL PERFORMANCE UNDER HIGH VACUUM - INSULATION CONCEPTS GAC-1, GAC-2 AND GAC-3

Insulation System	Test No.	Outer Surface Temperature °K (°F)	Multilayer Thickness Centimeters (Inches)	$\dot{q}$ W/m <sup>2</sup> (Btu/hr-ft <sup>2</sup> )	$k \times 10^{-5}$ W/m <sup>2</sup> -°K (Btu/hr-ft <sup>2</sup> -°R)
GAC-1	1	286 (55)	5.08 (2.0)	0.306 (0.097)	5.88 (3.4)
	2	285 (53)	5.08 (2.0)	0.678 (0.215)	13.0 (7.5)
GAC-2	1	289 (60)	4.06 (1.6)	0.505 (0.160)	7.61* (4.4)
	2	292 (65)	4.06 (1.6)	0.407 (0.129)	6.05* (3.5)
	4	284 (50)	3.00 (1.18)	0.501 (0.159)	5.88* (3.4)
GAC-3	1	290 (62)	5.08 (2.0)	0.312 (0.099)	5.88 (3.4)
	2	288 (58)	5.08 (2.0)	0.338 (0.107)	6.40 (3.7)

TABLE III. THERMAL PERFORMANCE UNDER HIGH VACUUM - INSULATION CONCEPT GAC-4

Test No.	Outer Surface °K (°F)	Multilayer Thickness Centimeters (Inches)	$\dot{q}$ W/m <sup>2</sup> (Btu/hr-ft <sup>2</sup> )	$k \times 10^{-5}$ W/m <sup>2</sup> -°K (Btu/hr-ft <sup>2</sup> -°R)
1	279 (42)	4.70 (1.85)	0.615 (0.195)	11.24 (6.5)
2	270 (25)	4.70 (1.85)	0.596 (0.189)	11.24 (6.5)
3	270 (26)	4.70 (1.85)	0.609 (0.193)	11.41 (6.6)
4	282 (48)	4.70 (1.85)	0.502 (0.159)	9.00 (5.2)

### EFFECT OF COMBINED VIBRATION, ACCELERATION AND RAPID EVACUATION

In contract NAS8-18021 with General Dynamics-Convair, monitored by Mr. Hyde of the Propulsion Division of the Propulsion and Vehicle Engineering Laboratory, insulation concepts are being evaluated under the combined effects of vibration, acceleration, and rapid evacuation while being cooled with helium gas. Later the insulation concepts are tested acoustically. The insulation systems are installed on a scale model of a 2.67-m (105-in.) diameter tank, approximately 73.7 cm (29 in.) in diameter and about 61 cm (24 in.) in length. The panelized insulation concept developed in this program has been included in the evaluation program at General Dynamics and one of the test tanks has been insulated with concept No. 4. The panels used to insulate the tank are shown in Figure 15. The fully insulated tank is shown in Figure 16. The insulated tank has been subjected to all four system tests without causing structural damage to the insulation. Cryogenic tests also showed the same thermal performance both before and after the tests, again indicating that combined environments had little or no adverse effects on the insulation.

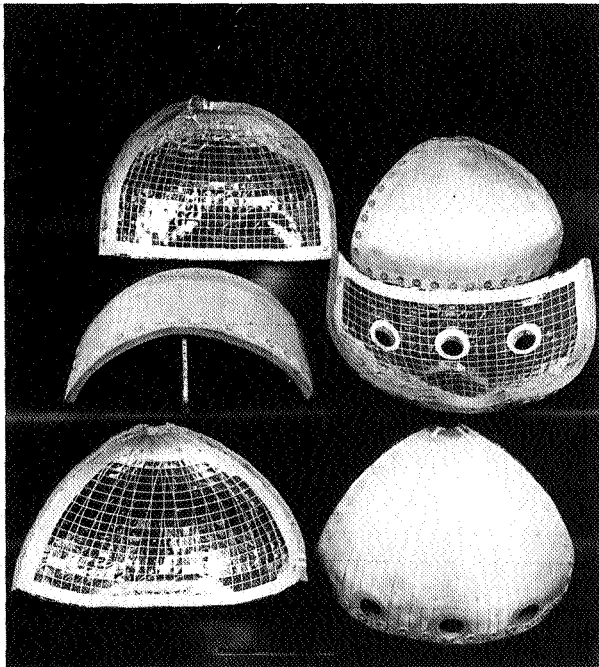


FIGURE 15. GAC-4 PANELS EMPLOYED TO INSULATE 73.7-CM DIAMETER TANK

### HYPERVELOCITY IMPACT TESTS

To evaluate the potential of these insulation concepts for affording protection to cryogenic tanks from penetration by micrometeoroids, extensive hypervelocity impact tests have been carried out at Illinois Institute of Technology at Chicago. In these tests pyrex balls weighing 5, 17, and 71.4 mg traveling at speeds up to 7160 m/sec (23 500 ft/sec) have been used. A typical sample used in these tests is presented in Figure 17. In Figure 18 is shown the effect of impacting the first and second insulation concepts with 17 mg pyrex balls traveling at 6710 to 7010 m/sec (22 000 to 23 000 ft/sec). In both cases debris penetrated completely through the insulation, but did not damage the 0.762-mm (30-mil) aluminum back-up plate. When 71.4 mg pyrex balls were fired at similar samples at speeds up to 6400 to 6710 m/sec (21 000 to 22 000 ft/sec), no significant depth penetration occurred in the back-up plate. When 5 mg pyrex balls were used at speeds up to 7160 m/sec (23 500 ft/sec), debris did not penetrate the insulation completely. To determine how significant a role the multilayer insulation played in preventing damage to the tank wall from the debris resulting from micrometeoroids striking the bumper wall, hypervelocity impact tests were conducted on samples having only a bumper wall spaced at the same 5.1 cm (2.0 in.) from a 0.476-cm (3/16-in.) aluminum witness plate. The effect of impacting the sample with a 17 mg glass projectile traveling about 6710 m/sec (22 000 ft/sec) is shown in Figure 19. In this test significant penetration of the witness plate occurred.

### FUTURE PLANS

Future efforts will be concentrated on the optimization of the panelized insulation concept. Panel and joint design, size, thickness, and ultimate methods of panel fabrication will be studied to optimize thermal performance and to enhance reliable installation on large flight vehicles. Purging and venting studies on the insulation will include the design and application of a purge jacket that not only will contain the purge gas but will reliably vent the gas inside the jacket immediately after launch. Improved methods will be developed for applying the insulation around and to protuberances of cryogenic tanks.

Information on the heat leak through the basic panel, panel joints, and joints around protuberances will be developed as feasible.

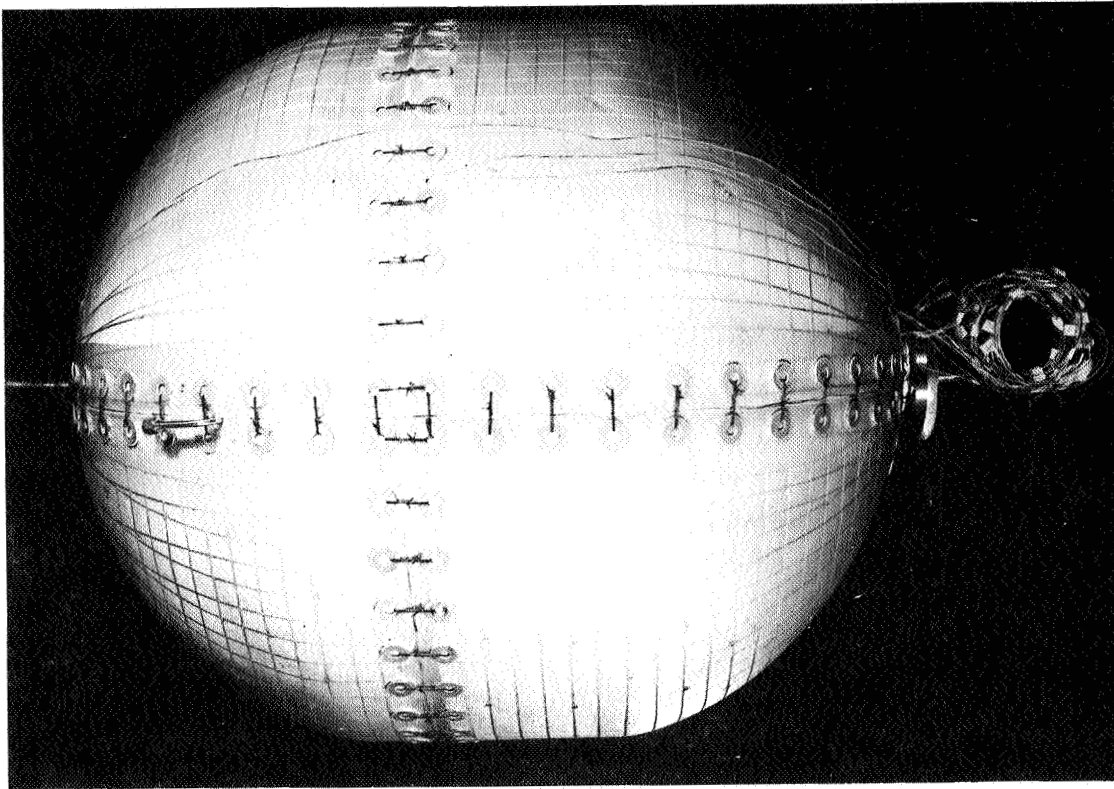
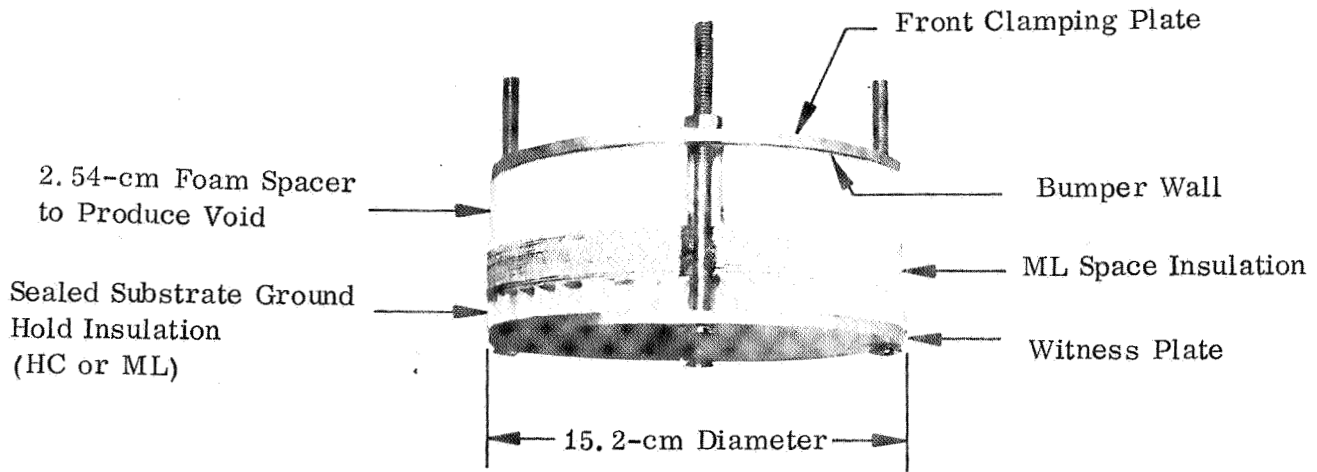


FIGURE 16. GAC-4 INSULATION INSTALLED ON 73.7-cm DIAMETER TANK



ML - Multilayer Foam Spacer Insulation  
HC - Sealed-Cell Mylar Honeycomb

FIGURE 17. SAMPLE FOR HYPERVELOCITY IMPACT TEST

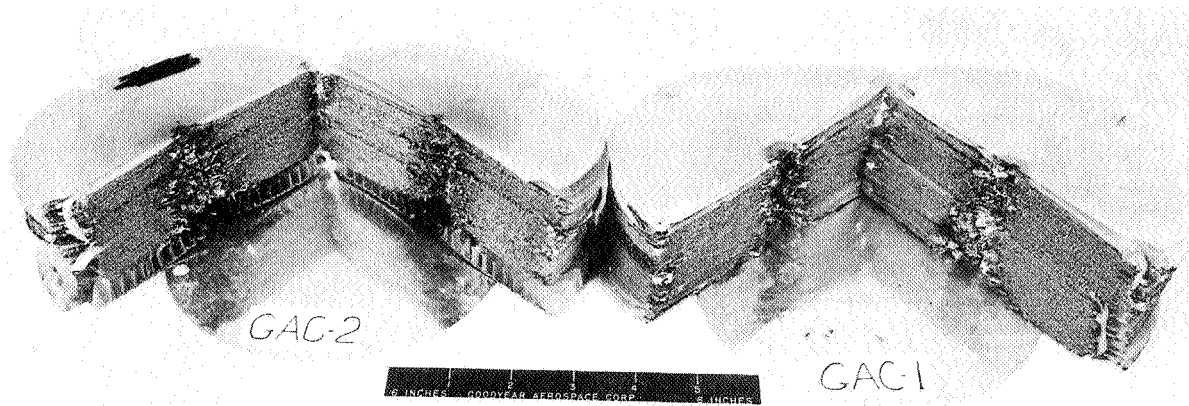


FIGURE 18. HYPERVELOCITY IMPACT TEST ON INSULATION CONCEPTS GAC-1 AND GAC-2

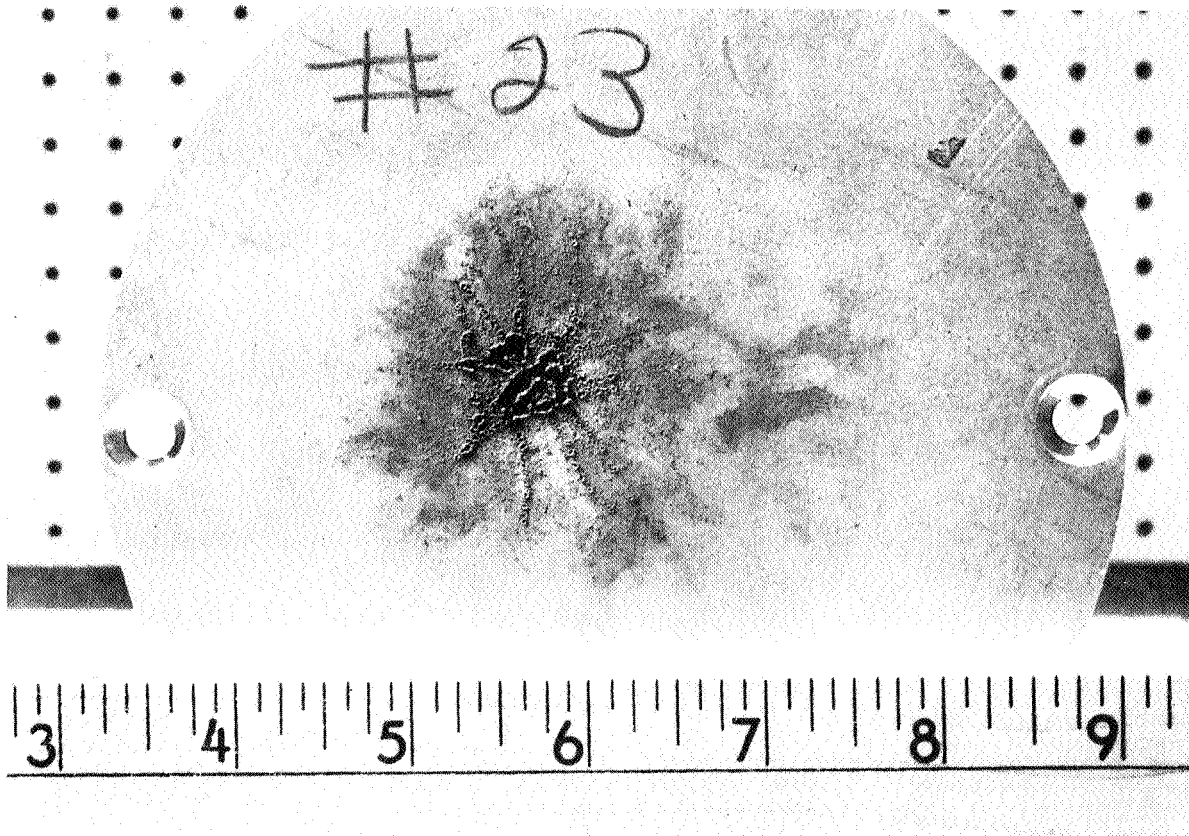


FIGURE 19. HYPERVELOCITY IMPACT TEST ON SAMPLE WITHOUT MULTILAYER INSULATION

Plans are to apply the panelized insulation concept to 2.67-m (105-in.) diameter tanks and perform liquid hydrogen tests under high vacuum conditions to fully evaluate the performance of both the concept and method of application.

The panelized insulation concept is being considered for possible application on the Multiple Docking Adapter (MDA), Orbital Tanker, and other programs.

# NUCLEAR GROUND TEST MODULE INSULATION DEVELOPMENT

By

Raymond L. Gause

## SUMMARY

A description is given of Project Rover and the Nuclear Engine for Rocket Vehicle Applications (NERVA). The Nuclear Ground Test Module (NGTM) program at MSFC is discussed and the relationship between the NGTM program and the NERVA program is established. The criteria for the design of an insulation system for the NGTM are presented. In addition, the NGTM environment and the impact of this environment on the development of an insulation system with the desired properties are discussed. The selection of the candidate materials for the NGTM insulation system is given and the test program for evaluating their suitability for full-size tanks is outlined.

## INTRODUCTION

Ever since their invention by Chinese makers of ceremonial fireworks, rockets have been propelled by the energy liberated by burning chemicals, and this fundamental fact has not been altered by the tremendous strides that have been made in American and Russian rocketry since World War II. Rockets began as fireworks and they are still fireworks. Now, however, after a thousand years this basic truth is about to change as a result of a new breed of rocket engines presently being developed under Project Rover. Project Rover is America's program to develop a nuclear propelled rocket and is jointly sponsored by the Atomic Energy Commission and the National Aeronautics and Space Administration. Currently, nuclear reactors suitable for use as power sources for rocket propulsion are being developed. Larger versions of these reactors will be used in the construction of NERVA (Nuclear Engine for Rocket Vehicle Application), a flight type engine that will be tested at the Nuclear Rocket Development Station (NRDS) at Jackass Flats, Nevada.

To support these NERVA tests at NRDS, the Marshall Space Flight Center presently is involved in an inhouse program to develop the technology

required for the design and fabrication of a nuclear ground test module (NGTM). The dual purpose of the NGTM is to provide the propellant tankage and control systems necessary for the hot firing of the NERVA and to serve as a test article for the development of hardware required for future nuclear flight stages. Because the NERVA will use liquid hydrogen (LH<sub>2</sub>) as a propellant, the NGTM will require a thermal insulation system to limit propellant boiloff. The unique environments in which this insulation system will have to function, the impact of these environments on the selection of insulation materials, and the test program required to develop an insulation system to meet the necessary design requirements will be described in this paper.

## INSULATION SYSTEM DESIGN CRITERIA

In considering the design of an insulation system for the NGTM, the feasibility of developing an insulation which will be suitable for both the ground test module and any future flight vehicle was investigated. To aid in the evaluation of this approach, the design criteria shown in Table I were established.

TABLE I. INSULATION SYSTEM DESIGN CRITERIA

<u>Ground Test Module</u>	<u>Flight Vehicle</u>
Short Term LH <sub>2</sub> Storage	Long Term LH <sub>2</sub> Storage in Space
High Cumulative Radiation Levels	Low Cumulative Radiation Levels
Mass is of Secondary Importance	Minimum Mass Required
Long Term Weathering Protection	Micrometeoroid Protection
High Cumulative Vibration	Short Term Vibration
Considerable Handling	Nominal Handling

An analysis of the criteria in Table I shows that the requirements for the ground test module

are completely different from those for an operational flight stage. The operational stage insulation will not be subjected to the mechanical, thermal, and radiation cycling associated with ground stage static testing. The ground test stage probably will be subjected to many full duration hot firings over many months or possibly years, whereas the flight vehicle will be subjected to only one or possibly two short duration firings. In addition, the operational stage will require the long term storage of liquid hydrogen in space by maintaining the rigid control of LH<sub>2</sub> boiloff. For the ground test module, boiloff considerations are less critical. Therefore, based on these considerations, it was concluded that the development of an insulation system that could be used for both the ground test stage and an operational flight vehicle was not feasible at this time. However, studies in this area are continuing. Thus, the approach taken was first to develop an insulation system that would meet all of the requirements for the NGTM and then use the operational NGTM as a test article for the development of a flight type insulation system.

## THE NGTM ENVIRONMENT

One of the most important considerations in the development of the NGTM insulation system is the environment to which the insulation will be exposed. This environment and the resulting effects on the insulation system must be defined in order to provide a basis for the selection of candidate insulation materials and composites. To arrive at this definition, the operation of the nuclear engine must be examined. Figure 1 shows the configuration of the NERVA, which basically consists of a 5000 MW solid core reactor, a pressure vessel, a liquid hydrogen turbopump assembly, and a nozzle. The engine is designed to produce a nominal thrust of 1.11 MN (250 000 lbf) and a specific impulse in the order of 800 sec for a liquid hydrogen propellant flow rate of 136 kg/sec (300 lb/sec) through the reactor. The NERVA will be larger than any chemical engine presently in use. The reactor core lifetime is expected to be approximately 60 min while operating at 5000 MW. The anticipated neutron flux and gamma dose rates for the engine operating at full power are shown in Figure 2. With the engine located at the test stand and mounted on the GTM, the neutron and gamma radiation levels expected at various points on the GTM are shown in Figure 3. These levels assume no internal engine shield and an operating power level of 5000 MW (a worst case condition). As shown in Figure 3, the maximum

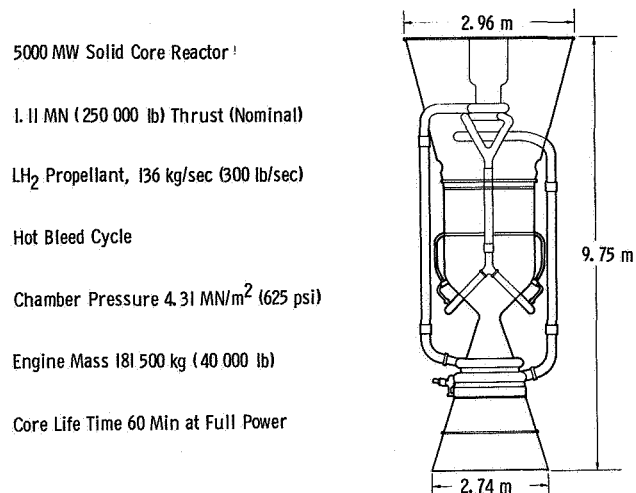


FIGURE 1. THE NERVA ENGINE

neutron and gamma dose rates at the propellant tank bottom (point 2) are expected to be about

$$1.0 \times 10^9 \frac{\text{ergs}}{\text{g(C)} \cdot \text{hr}} \quad \text{and} \quad 2.0 \times 10^9 \frac{\text{ergs}}{\text{g(C)} \cdot \text{hr}},$$

respectively. Based on the current requirement that the NGTM be capable of supporting 30 hours of full power engine operation, the materials selected for use in the vicinity of the tank bottom will have to be capable of retaining their functional integrity after a neutron exposure of  $3.0 \times 10^{10} \frac{\text{ergs}}{\text{g(C)}}$  and a gamma dose of  $6 \times 10^{10} \frac{\text{ergs}}{\text{g(C)}}$ . Because of the uncertainty in these numbers, the radiation effects tests to be described later in this paper will be made to levels greater than these.

The NGTM acoustic level anticipated during an engine firing is about 140 decibels (dB) at a center frequency of 80 Hz. Although it is not expected that this will affect significantly the structural integrity of the insulation, acoustic tests at this level are planned in conjunction with nuclear radiation-cryogenic temperature tests.

Other factors which must be considered as part of the overall NGTM environment include (1) thermal, mechanical, and radiation cycling, (2) the desert weather (sand storms, temperature extremes, etc.), and (3) handling.

It is obvious then that the development of a cryogenic insulation system that will meet the desired performance requirements must include testing in combined environments.

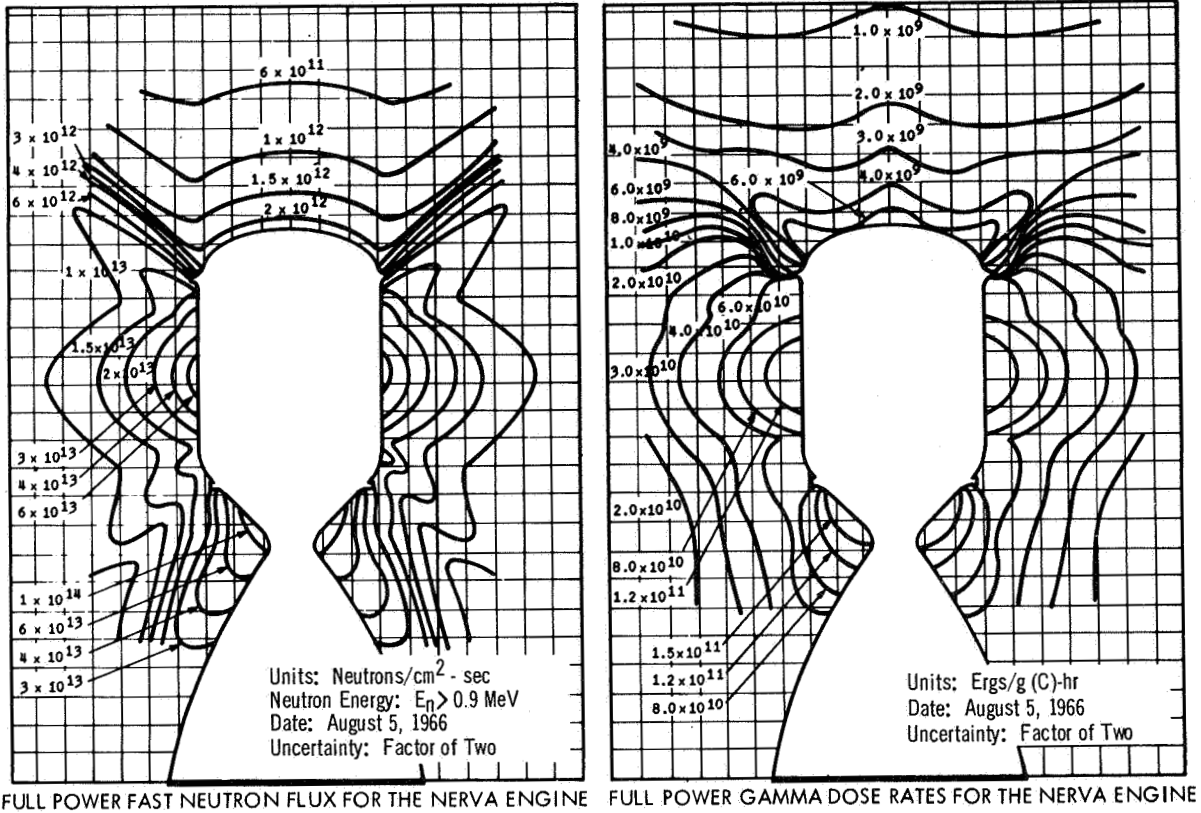


FIGURE 2. RADIATION PROFILES FOR THE 5000 MW NERVA

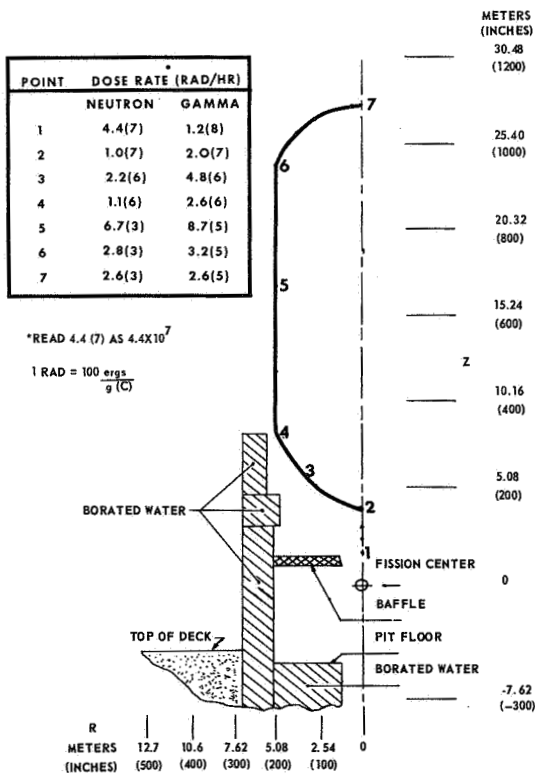


FIGURE 3. NGTM RADIATION ENVIRONMENT

### INSULATION DEVELOPMENT CONSIDERATIONS

Several important factors pertaining to performance, maintenance, and cost must be considered during the development of the NGTM insulation system. First, because of the environment just described, materials to be considered for use must have high radiation resistance, good cryogenic properties, and possess some degree of ruggedness. In addition, it is highly desirable from an economic standpoint to have an insulation system which basically is inexpensive, easily applied, uncomplicated, and requires minimum ground support equipment. After the first hot firing of the NGTM, the module will be radioactive and thus limit personnel access for the performance of maintenance and repair tasks. Only insulation systems suitable for external application to the propellant tank are being considered because an internal system would be difficult if not impossible to repair after the tank becomes activated.

The thermal performance of the insulation also has to be considered. Presently, a maximum LH<sub>2</sub> boiloff rate of 454 kg/hr (1000 lb/hr) under

cold-flow conditions is being used as one of the criteria for the selection of candidate insulation materials. To limit the boiloff to this value, a thermal conductivity-insulation thickness ratio ( $K/X$ ) of approximately 0.06 is required as shown in Figure 4. Of course, during hot firing of the engine, the boiloff will be greater than this because of the heating of the propellant by the absorption of nuclear energy and the increased conductance of heat through the metal thrust structure and other bulkhead appendages. Insulation mass, which is of great importance for flight vehicles, is of secondary importance for the NGTM because it will be used only for ground tests. The factors just described, which are summarized in Table II, are the principal ones that affect the development of the NGTM insulation system.

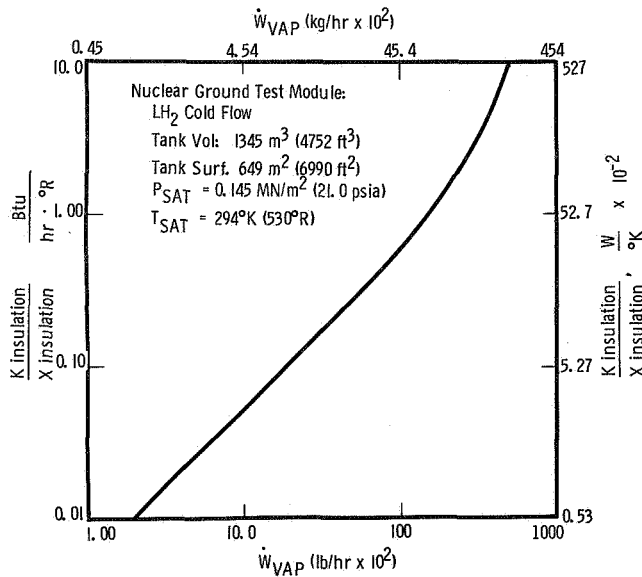


FIGURE 4. NGTM COLD-FLOW LH<sub>2</sub> BOILOFF VS. INSULATION PERFORMANCE

### SELECTION OF CANDIDATE INSULATION MATERIALS

With the preceding information as evaluation criteria, several different insulation schemes were reviewed for use in the NGTM program. Included in these systems were the insulations currently used on the various stages of the Saturn V vehicle and the multilayer superinsulations. Many of these were found to have some of the desired properties; however, most of them were not believed to be durable enough to meet the service

TABLE II. INSULATION DEVELOPMENT CONSIDERATIONS

- A. High Radiation Resistance  
( $\sim 6 \times 10^{10} \frac{\text{ergs}}{\text{g(C)}} \text{ gamma}$ )
- B. Good Cryogenic Properties
- C. Inexpensive
- D. External Application
- E. Uncomplicated
- F. Minimum GSE
- G. Repairable with Minimum Effort
- H. Moderate Thermal Efficiency
- I. Mass Relatively Unimportant

requirements. The superinsulations, like most of the other insulations considered, are very satisfactory from the standpoint of thermal performance but are not desirable based on installation costs, handling, and repair considerations. One insulation which was proposed by the Boeing Company for this application is corkboard. The thermal properties of cork appear to be adequate, the cost is acceptable, cork should not present any major fabrication problems, and cork is durable. To determine how its properties are affected by radiation, a search of the radiation effects literature was made. Bolt and Carroll [1] have summarized the limited information available on the effects of radiation on cork. In 1951, several types of wood, including cork, were exposed in the Canadian NRX reactor [2]; samples exposed showed only slight darkening after a dosage of  $6 \times 10^{11} \frac{\text{ergs}}{\text{g(C)}}$ . In another test, ordinary stopper corks were exposed to a gamma dose of  $5 \times 10^{10} \frac{\text{ergs}}{\text{g(C)}}$ ; the stoppers showed no discoloration or increased brittleness. In 1958, DeZeih [3] exposed cork to  $1 \times 10^{10} \frac{\text{ergs}}{\text{g(C)}}$ , which produced a slight (4%) increase in tensile strength. Flexibility was not impaired and compression and recovery from compression were reduced only about 5%. Another consideration regarding cork insulation is the possible deterioration of the cork binder materials. An evaluation of the binders commonly used showed that they generally are of the thermosetting resin type. Since the phenolic, polyester, and other

thermosetting resins usually have high radiation resistance, the binder is not expected to be a source of failure.

After reviewing the information which was available for corkboard and comparing this information with the previously described evaluation criteria, corkboard was selected as one of the candidate insulation materials. The particular corkboard which appeared to be most appropriate for this program was the Insulcork 7326 Cryogenic Insulation, a new lightweight [112-128 kg/m<sup>3</sup> (7-8 lbs/ft<sup>3</sup>)] corkboard distributed by the Industry Products Division of the Armstrong Cork Company. A conceptual insulation system design based on this material is shown in Figure 5. It consists of four basic elements: the adhesive bond, the corkboard insulation, the internal vapor barriers, and the protective facing cover. A

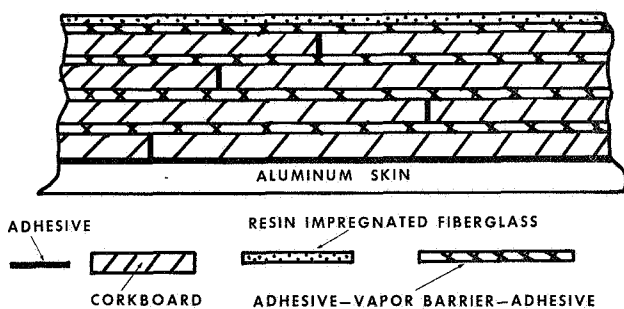


FIGURE 5. LAMINATED CORKBOARD INSULATION SYSTEM

laminated structure was selected because the layers of insulation can be staggered to preclude the existence of any direct thermal paths through the insulation. Internal vapor barriers are used to provide protection against cryopumping of air in the event the outer cover is ruptured. The system is given a high degree of ruggedness by the protective facing cover which consists of two plies of resin impregnated fiberglass. Presently, other materials are being investigated for this application.

Because of the desire to include more than one basic type of insulation in the development program, an additional insulation material was selected. A type of insulation that has many characteristics desirable for the NGTM insulation is the rigid spray foam insulation. The rigid, small, uniform closed-cell structure of the spray foams gives them an inherently low thermal conductivity. In addition,

the foam has extremely low moisture-vapor permeability and a high resistance to water absorption. The structural stability prevents costly heat leaks caused by shrinkage, buckling, or cracking. The application of the foam by spraying provides a convenient method of insulating difficult geometries. Also, repair is simple because the damaged material can be removed easily and replaced by respraying the area. Sealing problems are minimized because the new foam will adhere directly to the undamaged foam. Another major advantage is that the foam can be sprayed directly on the metal, which eliminates the requirement for a separate adhesive bond between the foam and the metal. Foams now are available having low density [nominal 32 kg/m<sup>3</sup> (2.0 lbs/ft<sup>3</sup>)] and high strength. The foam that was selected for testing is from a group of isocyanate-polyol resins commonly known as polyurethanes. They are formed by the reactions of compounds containing two or more active hydroxyl, amino, or carboxyl groups, with diisocyanates. The principal polyols used today are either polyesters or polyethers. The highly branched polyesters give rigid polyurethanes. In the spray foam process, the isocyanate and polyol reactants are mixed with catalysts chosen to accelerate the reaction sufficiently to bring about foaming within seconds. The reactants are pumped to the spray gun by metering pumps adjusted to provide the proper proportions. In the spray gun, the reactants are mixed and then expelled through a nozzle onto the surface being coated in much the same way as paint is sprayed.

A polyurethane type foam was selected because as a chemical class, the polyurethanes are high on the list of radiation resistant elastomers and plastics. From Harrington's studies [4], it may be stated that polyurethane elastomers are capable of giving satisfactory service to at least  $8.7 \times 10^{10} \frac{\text{ergs}}{\text{g}(C)}$ .

The work by Schollenberger, at the B. F. Goodrich Company [5] concluded that limited dynamic application might be practical after an exposure of  $1.7 \times 10^{10} \frac{\text{ergs}}{\text{g}(C)}$  and static applications might be feasible after exposure to  $4.4 \times 10^{11} \frac{\text{ergs}}{\text{g}(C)}$ . Tests

made by the General Dynamics Corporation, Fort Worth Division under contract NAS8-2450 on two different polyurethane foams indicated that they were not significantly affected after an exposure of

$3 \times 10^{10} \frac{\text{ergs}}{\text{g}(C)}$ . Since there are many chemical com-

binations, temperature cures, and additives, some variation in reported results in radiation effects tests are to be expected. However, a possible service

level of  $1 \times 10^{11} \frac{\text{ergs}}{\text{g}(C)}$  seems feasible.

The particular spray foam that was chosen as the second candidate insulation material for this program was the CPR 368 rigid urethane foam manufactured by the CPR Division of the Upjohn Company. It is a flame retardent spray foam designed for either airless or air atomized spray equipment for particular use at low ambient temperature conditions. The nominal density is 32-48 kg/m<sup>3</sup> (2-3 lb/ft<sup>3</sup>) and the thermal conductivity is approximately  $0.01585 \frac{W}{m \cdot ^\circ K} \left( 0.11 \frac{Btu \cdot in.}{ft^2 \cdot ^\circ F \cdot hr} \right)$ . A conceptual insulation system based on this type of insulation is shown in Figure 6. It consists basically of two elements: the spray foam and the seal coat.

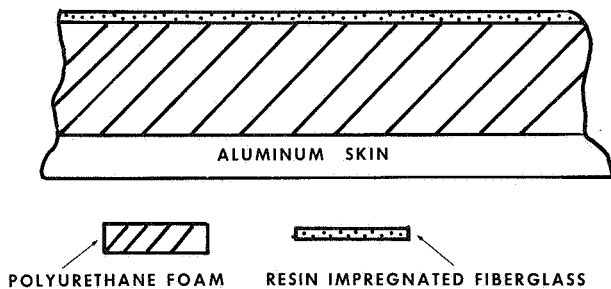


FIGURE 6. POLYURETHANE SPRAY FOAM INSULATION

The foam is sprayed directly on the primed aluminum surface, thereby eliminating the need for adhesive bonding. The desired thickness can be achieved by building successive layers of foam because each layer becomes homogeneous with the previous layers. After the foam is sprayed, it is cured and then the surface is machined to a smooth finish and sealed.

### SELECTION OF CANDIDATE ADHESIVE MATERIALS

The adhesives being considered in this program are for bonding the cryogenic insulation to the propellant tank and for bonding the vapor barrier to the insulation. Generally, adhesives which cure at elevated temperatures and high pressures are less attractive because autoclaves and presses are required, which complicate the installation of the insulation system and increase the cost. Thus, the adhesives selected for this program are those which cure at room temperature and require only contact pressure for proper bonding. Since the adhesive in some areas may be subjected simultaneously to both

cryogenic temperatures and to nuclear radiation during engine operation, an adhesive material is desired whose functional properties are not seriously affected by this environment.

In reviewing the different chemical classes of adhesives, it is noted that the epoxy and phenolic-base adhesives have a higher radiation tolerance, but most of these are cured at elevated temperatures. The epoxy-nylon types are good cryogenic adhesives, but they also have a high temperature cure. However, the polyurethanes have good radiation resistance and can be cured at room temperature. The epoxy-polyamide adhesives, in general, are better in the radiation environment than many other types. Also, some of these cure at room temperature.

The adhesives that were chosen for inclusion in this program are of the polyurethane and epoxy-polyamide types, and all of them may be used under room temperature and contact pressure conditions. Furthermore, they have been used in previous aerospace programs. These adhesives are listed in Table III.

TABLE III. CANDIDATE ADHESIVE MATERIALS

Adhesive	Chemical Class	Manufacturer
Narmco 7343/7139	Polyurethane	Whittaker Corporation
APCO 1219	Polyurethane	Applied Plastics Company
Lefkowied 109/LM-52	Epoxy-Polyamide	Lefingwell Chemical Company
Narmco 3135/7111	Epoxy-Polyamide	Whittaker Corporation

### SELECTION OF CANDIDATE VAPOR BARRIER MATERIALS

The vapor barrier materials are used to cover cryogenic insulations to prevent moisture or air from penetrating the insulation and increasing the thermal conductivity. Therefore, it is important to have a vapor barrier material which possesses low permeability. Vapor barrier materials may be bare plastic films of various thicknesses, films combined as composites, films laminated with such reinforcements as glass cloth or epoxy-fiberglass, and plastic films vapor deposited, spray coated, or bonded with metal films.

Based on a survey of available information on the effects of radiation and cryogenic temperatures on these films, the following materials were selected as being promising candidate vapor barrier materials for the intended application: a polyimide (Kapton); a polyester (Mylar); a polyvinyl fluoride (Tedlar); and a polyurethane-fiberglass cloth.

included for the evaluation of the candidate thermal insulation materials. The first category involves the determination of the physical properties appropriate for each type of material and the various composites. The second is an application test of the two composite insulation systems using a specially fabricated cryogenic insulation test dewar (CITD).

### THE TEST PROGRAM

The insulation test program for the NGTM is composed of four phases: (I) the environmental testing of candidate materials and composites, (II) the environmental testing of insulations installed on model tanks, (III) the investigation of fabrication and installation techniques for large tankage, and (IV) the evaluation of the selected insulation system on full size tanks available from the Saturn V test program. Currently, the work necessary to accomplish the Phase I objectives is underway and the test plan and schedule for Phase II are being finalized. The radiation effects tests required in these phases will be performed under contract NAS8-18024 with the General Dynamics Corporation, Forth Worth Division. In Phase I, two categories of tests are

For the physical property tests, various types of specimens fabricated from the different classes of materials will be subjected to the following test conditions: (1) evaluation in air, (2) evaluation in LH<sub>2</sub>, (3) irradiation in air, and (4) irradiation in LH<sub>2</sub>. Table IV gives the types of tests, the number of specimens for each test, and the test environments. Some of the 150 specimens irradiated in LH<sub>2</sub> will be tested in LH<sub>2</sub> immediately after irradiation and without intervening warmup (in situ tests); the others will be tested at room temperature. The configurations of the lap shear (in situ), double lap shear, and composite flatwise tensile specimens are presented in Figures 7, 8, and 9.

To simulate the actual service conditions (radiation, LH<sub>2</sub> temperature, and acoustic noise) expected for the cryogenic insulation system, an insulation application test using the specially designed

TABLE IV. MATERIAL EVALUATION TESTS, SPECIMENS, AND ENVIRONMENTS

ASTM Test No.	Test Name	Materials Tested	Number of Specimens				TOTAL
			Control		Irradiated		
			Air	LH <sub>2</sub>	Air	LH <sub>2</sub>	
D-1002	Lap Shear	Adhesive	32	32	16	32	112
D-1876	T-peel	Adhesive	16	16	16	16	64
D-882	Thin-Film Tensile	Film Tape	24	24	24	24	96
E96	Thin-Film Permeability	Film Tape	6	6	6	6	24
D-1621	Compression Set	Insulation	8	8	8	8	32
D-1002	Double-Lap Shear	Adhesive Insulation	32	32	32	32	128
C-297	Flatwise Tensile	Adhesive Film Insulation	32	32	32	32	128
TOTAL SPECIMENS			150	150	134	150	584

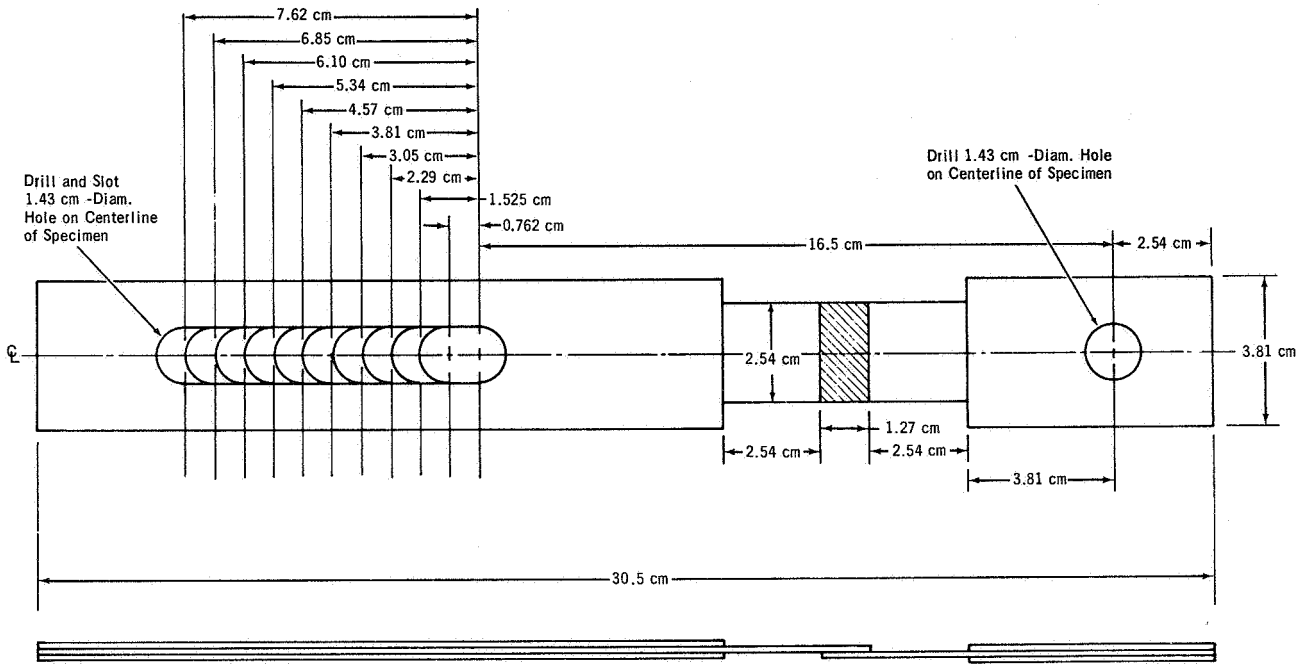


FIGURE 7. TYPICAL LAP SHEAR ADHESIVE SPECIMEN

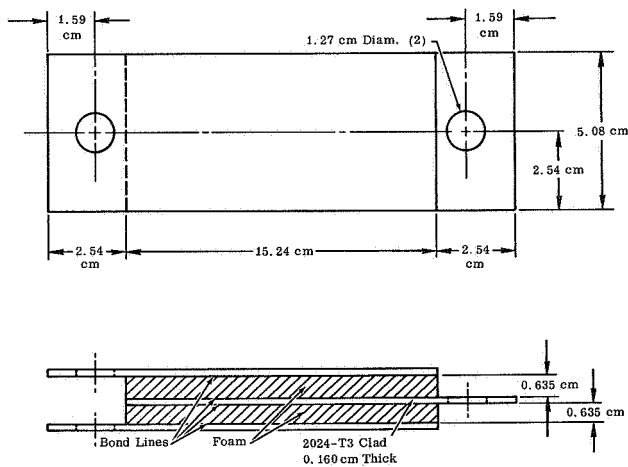


FIGURE 8. COMPOSITE DOUBLE LAP SHEAR TEST SPECIMEN

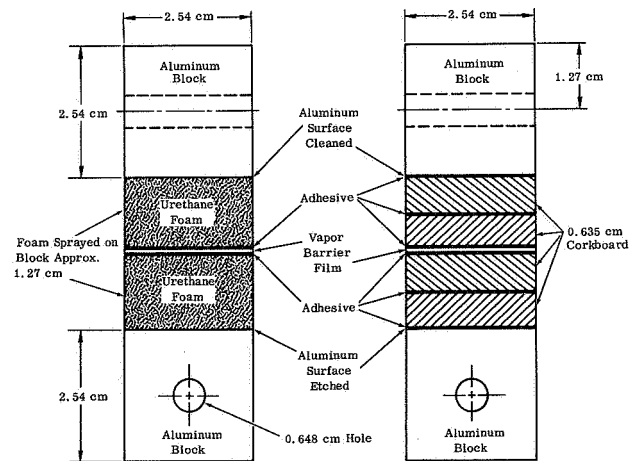


FIGURE 9. TYPICAL COMPOSITE FLATWISE TENSILE SPECIMENS

CITD shown in Figure 10 has been planned. The CITD is a 0.762-m (30-in.) long cubic tank of 1.27-cm (0.50-in.) thick 2219 aluminum with each of the four sides having a 0.635 × 0.635 m (25 × 25 in.) section on the inside surface milled to 0.762 cm (0.30 in.), thus leaving a 6.35-cm (2.5-in.) strip of 1.27 cm (0.50 in.) aluminum around the milled area in each side. The thin center sections correspond to the wall thickness of the NGTM LH<sub>2</sub> tank. This thin section will be used for

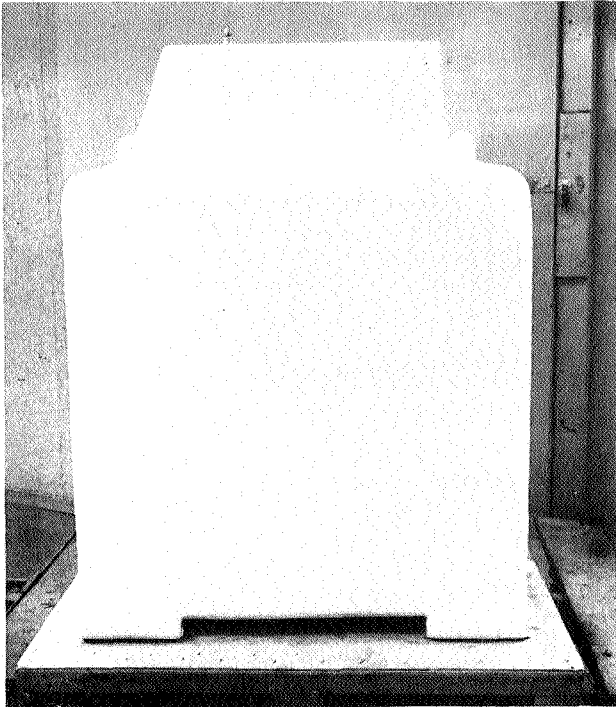


FIGURE 10. CRYOGENIC INSULATION TEST DEWAR

the evaluation of the mechanical and physical stability of the composite insulation during the environmental tests. Both of the previously described candidate insulation systems are installed on the CITD. Two sides were sprayed to a 5.08-cm (2-in.) thickness with CPR 368 foam. The bottom (except for the legs) and the top of the dewar (except for the shroud cover) were also covered with the foam. The remaining two sides were covered with Insulcork 7326 corkboard. One side has four 1.27-cm (0.50-in.) thick cork panels separated by a 0.0127 cm (0.005 in.) Tedlar vapor barrier bonded with Lefkoweld 109/LM52. An adjacent side has the same configuration except that eight 0.635-cm (0.25-in.) thick cork panels were

used. To protect the surface from mechanical damage and to provide an additional vapor seal, the insulation is covered with a layup of two layers of fiberglass cloth impregnated with NARMCO 7343/7139 resin. The cover is painted with a white, epoxy base, thermal control coating. Thermocouples are located in the insulation on two sides to monitor the temperature gradient across the 5.08-cm (2-in.) thickness of each type of insulation.

To perform the tests, the dewar will be irradiated to a gamma dose of approximately  $1 \times 10^{11} \frac{\text{ergs}}{\text{g}(C)}$  while full of LH<sub>2</sub>. During irradiation, the LH<sub>2</sub> level and the temperature profile of the insulation will be continuously monitored. Also, a videotape of the test will be made. After irradiation, the dewar will be drained of LH<sub>2</sub> and moved to an acoustic test facility where the condition of the insulation will be visually inspected before the acoustic exposure is started. If any cracks or other irregularities are visible, they will be photographed before the acoustic exposure. The CITD then will be filled with LN<sub>2</sub> and placed in the acoustic reverberation chamber shown in Figure 11 where it will be exposed to a noise level of 140 dB. After a six-hour exposure, the dewar will be drained of LN<sub>2</sub> and warmed to room temperature for visual inspection of the insulation.

The data obtained from the previously described tests will be used to aid in the selection of insulation materials to be tested in the model tank portion (Phase II) of the overall development program. In Phase II, a 16.65 m<sup>3</sup> (4 400 gal.), 2.74-m (108-in.) diameter tank will be insulated and tested in a radiation, LH<sub>2</sub>, and acoustic environment using the test setup shown in Figure 12. In addition to testing the insulation system in a tank configuration, the model tank will also be used as a test article for the evaluation of various NGTM mechanical components.

## CONCLUSION

In this paper, a brief description has been given of the program being pursued to develop an insulation system having the thermal protection and lifetime required for the satisfactory operation of the Nuclear Ground Test Module. The environment to which the insulation will be exposed is a severe one, but not an insurmountable one, and the results of the test program should provide an excellent NGTM insulation system as well as providing many answers to the solution for an insulation system for a nuclear stage on a flight vehicle.

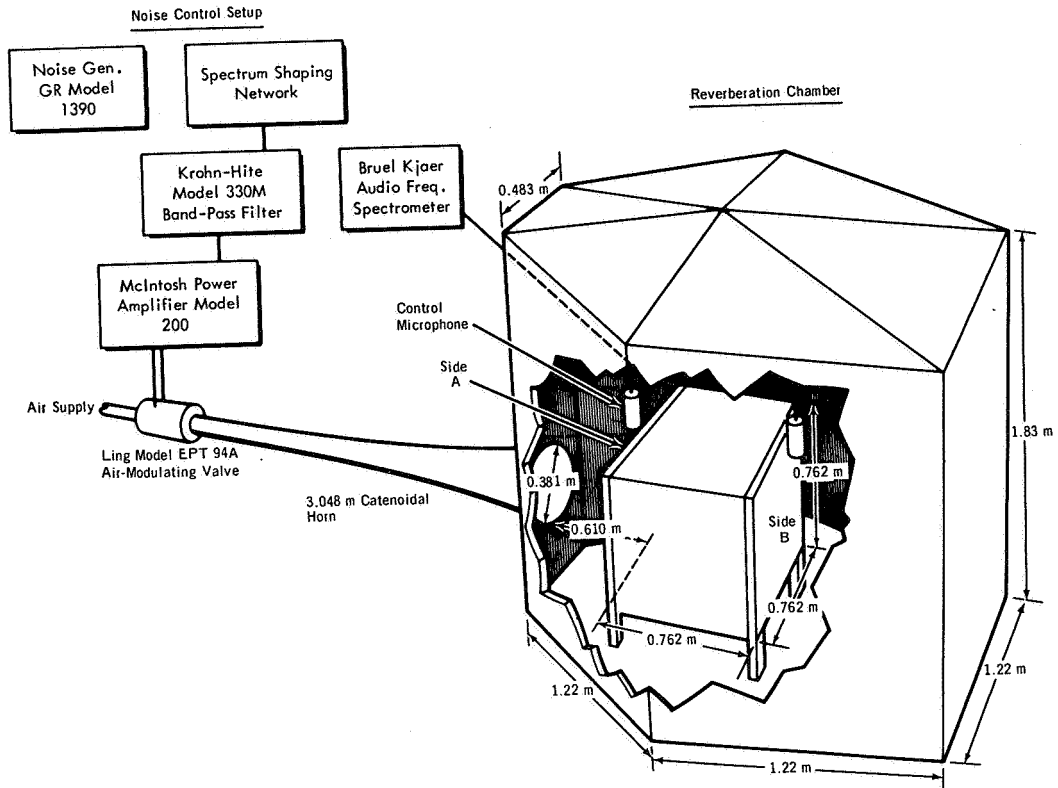


FIGURE 11. ACOUSTIC NOISE SETUP

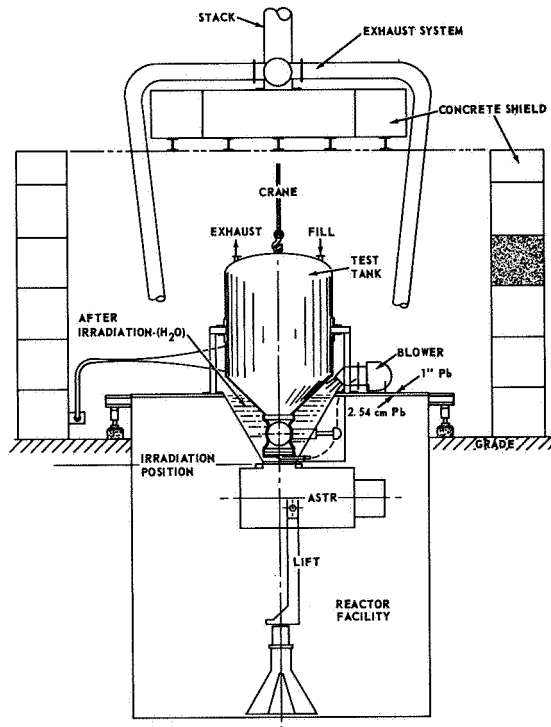


FIGURE 12. SCHEMATIC OF MODEL TANK TEST SETUP (ELEVATION)

## REFERENCES

1. Bolt, R. O. ; and Carroll, J. G. : Radiation Effects on Organic Materials. Academic Press, New York, 1963.
2. Yoshida, N. ; and Horsman, J. C. : Summary of Engineering Materials Irradiated in NRX Reactor. Canadian Report NEI-4, February 1951.
3. DeZeih, C. J. : Effects of Nuclear Radiation on Cork, Leather, and Elastomers. Third Semiannual Radiation Effects Symposium, Paper no. 62, vol. 5, Lockheed - Georgia Company, October 28-30, 1958.
4. Harrington, Robert: Elastomers for Use in Radiation Fields (Part II). Rubber Age, vol. 82, Dec. 1957, pp. 461-470.
5. Schollenberger, C. S., et al. : Polyurethane Gamma Radiation Resistance. Research Center Final Report 6S-72419, B. F. Goodrich Co., June 1, 1959.



# ASSESSMENT OF THE STATUS OF CRYOGENIC INSULATION DEVELOPMENT

By

Charles. C. Wood

Marshall Space Flight Center is attempting to develop insulation technology to achieve cryogenic propellant storage for durations from several days to one year or more for future space missions. A portion of this insulation development activity is reported in previous sections of this publication. The insulation concepts for long-duration missions differ significantly from insulation concepts used on the hydrogen tanks of the present generation of launch vehicles that have mission durations varying from a few minutes to several hours.

The vehicle system that requires the storage of large quantities of cryogenics for long durations and that is best defined at this time is the Modular Nuclear Vehicle, which is being evaluated for manned interplanetary travel. This vehicle configuration will be used in this paper for comparative purposes and is depicted in Figure 1. It has a hydrogen tank

capacity of 104 000 kg (230 000 lb) and a tank diameter of approximately 10.1 m (33 ft). Details of the studies that defined this vehicle are reported by Lockheed [1]. These studies established that the maximum acceptable sum of the hydrogen tank insulation mass and the mass lost by evaporation of propellant was 8% of the mass of propellants at lift-off. The standard used throughout the study to represent insulation performance was the so-called "performance index," the product of insulation density and thermal conductivity. The selected value for the study was  $2.77 \times 10^{-3} \frac{W - kg}{m^4 - ^\circ K}$  ( $10 \times 10^{-5} \frac{Btu - lbm}{hr - ft^4 - ^\circ R}$ ). The lowest known value of this parameter obtained in calorimeter tests under idealized conditions is  $1.11 \times 10^{-3} \frac{W - kg}{m^4 - ^\circ K}$  ( $4 \times 10^{-5} \frac{Btu - lbm}{hr - ft^4 - ^\circ R}$ ). An equivalent value of  $5.53 \times 10^{-3} \frac{W - kg}{m^4 - ^\circ K}$  ( $2 \times 10^{-4} \frac{Btu - lbm}{hr - ft^4 - ^\circ R}$ ), considered typical of thermal performance obtained for similar programs, was obtained on the practical flight-configuration 2.67-m (105-in.) diameter tank that was discussed by Mr. E. H. Hyde. Therefore, for a vehicle configuration represented by the Modular Nuclear Vehicle, an acceptable insulation system requires a factor of two improvement in thermal performance relative to the 2.67-m (105-in.) diameter propellant tank insulation system. Insulation system performance can be improved by two basic means: reduction of insulation density and reduction of thermal conductivity. Minute hydrogen gas leaks within the insulation system and other factors reported by Mr. E. H. Hyde were responsible for major differences between the thermal performance in the applied condition and the thermal performance obtained in calorimeter testing. The major problems that occurred during large-scale testing have been solved on the component level. It is anticipated that the solutions to these problems can be successfully applied to large-scale tanks and that insulation thermal performance in the applied condition will satisfy the requirements for the Modular Nuclear Vehicle missions of interplanetary travel. Other technologies that are essential, or can assist in meeting these requirements, will be discussed in ensuing paragraphs.

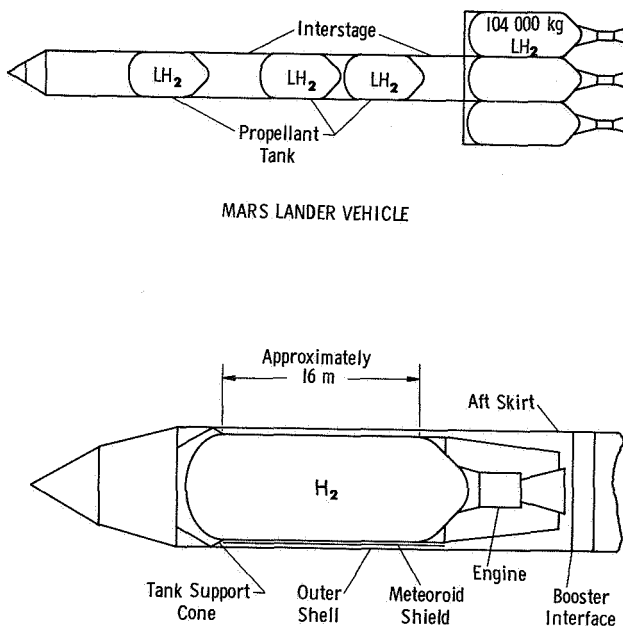


FIGURE 1. MODULAR NUCLEAR VEHICLE CONFIGURATION

Figure 2 summarizes insulation technology development efforts for space application occurring between 1960 and 1967, and lists project requirements for the time frame 1967 through 1970. The

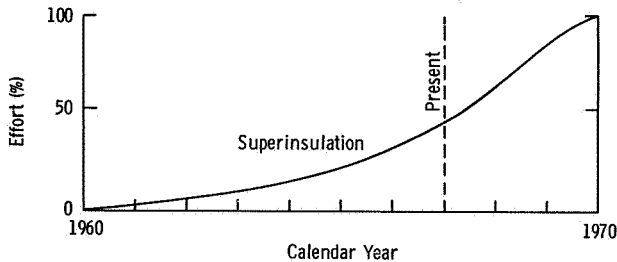


FIGURE 2. ESTIMATION OF EXPENDED AND REQUIRED EFFORT FOR HIGH PERFORMANCE INSULATION DEVELOPMENT FOR SPACE FLIGHT APPLICATION

data are presented in terms of the required total effort to advance insulation technology for space vehicle application from inception to the demonstration of an acceptable system capable of meeting the specified thermal goals. This figure shows that approximately 50% of the required effort for advancing insulation technology has been expended. The increased effort shown to occur between 1967 and 1970 reflects the detailed design and thermal analysis activities required for application of insulation to large flight-configuration containers. Coincident with this accelerated effort is the anticipated rapid improvement in attainable thermal performance of insulation systems because the very latest in available technology will be used in the establishment of new configurations and major efforts will be directed toward unsolved problems.

The storage of cryogenics in space for long durations involves technologies other than insulation, such as fluid behavior and propellant tank venting in a reduced or zero gravity environment, determination of the thermal environment, and other modes for reducing propellant loss such as reliquefaction of evaporated propellant, other states of stored propellant (slush or triple point liquid), and improvised methods for shielding the vehicle from solar energy (shadow shields). Figure 3 illustrates the potential for reduction of propellant loss of two such modes: slush propellants and solar shields. These data are for a Mars braking stage of a manned interplanetary vehicle that has been insulated with sufficient high performance insulation so that

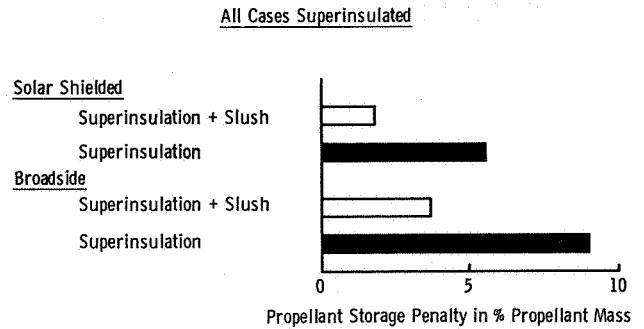


FIGURE 3. SOLAR SHIELD AND PROPELLANT STATE INFLUENCES ON PROPELLANT STORAGE PENALTY FOR A NUCLEAR MANNED MARS BRAKING STAGE

the mass of the insulation system plus the evaporated propellant loss is 8% of the mass of the lift-off propellant. The combined effect of shadow shields and slush hydrogen theoretically reduced the 8% stage penalty to 2%, greatly enhancing the propellant storage capability. The advancement of technology in the areas of slush hydrogen, shadow shields, propellant tank venting, fluid behavior in reduced and zero gravity, etc., is currently underway at MSFC. Other NASA centers, government agencies, and private industries are also contributing to the advancement of the required technology.

Figure 4 summarizes the future MSFC plans for advancing insulation technology for space vehicles requiring long-term storage of cryogenics.

- Develop High Performance Insulation System For Long Term Storage
  - Meet Modular Nuclear Vehicle Performance Goals
- Considering All Practical Flight Vehicle Problems
- He Purge System
  - Rapid Ascent (Pressure, Acceleration)
  - Outgassing - Preconditioning
  - Low Heat Leak Attachments
  - Piping - Tank Support Penetrations
  - Manufacturing - Reproducibility - Density Control
- Efforts To Develop A Lower Insulation Thermal Conductivity And Density Product For High Performance Insulation

FIGURE 4. FUTURE PLANS FOR HIGH PERFORMANCE INSULATION DEVELOPMENT

The major effort is a combined MSFC and contractor program using the Modular Nuclear Vehicle as a base line vehicle configuration whenever possible. During the next year, insulation concepts will be selected and insulation systems will be designed and evaluated from a thermal and fluid mechanics standpoint. A segment of the insulation system will be manufactured and preliminary tests performed using cryogenics only as required to verify the insulation evacuation. Complete thermal testing

will be conducted later contingent upon successful completion of the present scheduled program. The goal of a parallel effort is the development of a basic insulation concept having a significantly lower thermal conductivity and density product. The advanced insulation material will be substituted for the materials used initially in the major study. Insulation concepts with the density thermal conductivity product equal to one-half the values of those currently in use appear possible.

## REFERENCE

1. Modular Nuclear Vehicle Study, Phase II. Lockheed Missiles and Space Company, Sunnyvale, California, Contract NAS8-20007, 1967.